MASTERARBEIT | MASTER'S THESIS

Titel | Title

Antibiotic resistance of preterm infants' gut microbiota

verfasst von | submitted by

Ekaterina Zolotareva BSc

angestrebter akademischer Grad | in partial fulfilment of the requirements for the degree of

Master of Science (MSc)

Wien | Vienna, 2026

Studienkennzahl lt. Studienblatt | Degree programme code as it appears on the student record sheet:	UA 066 830
Studienrichtung lt. Studienblatt | Degree programme as it appears on the student record sheet:	Masterstudium Molecular Microbiology, Microbial Ecology and Immunobiology
Betreut von | Supervisor:	Univ.-Prof. David Berry Privatdoz. PhD

Acknowledgments

First of all, I would like to thank Professor Dr. David Berry for giving me the opportunity to carry out my master's thesis project in his research group. I am very grateful for his constant availability whenever difficulties or questions came up during the project, as well as for his prompt and helpful responses to my emails. This year has been a very valuable experience for me, both scientifically and professionally, and it also helped me grow in terms of communication, organization, and confidence.

I would also like to warmly thank my direct supervisor, Mia, for her time, knowledge, and support throughout this year. I am especially grateful for the coffee breaks, the therapeutic conversations, and for believing in me when I needed it most.

Special thanks go to Anna for her kindness and willingness to help with any lab-related questions, especially everything related to anaerobic experiments and working with anaerobic tents.

I would also like to thank the whole GUT group for the great working atmosphere, their kindness, and the relaxed group meetings with many interesting and inspiring discussions.

A very special thank you goes to my girls, Sasha, Ana, Amina and Dinely, for their emotional support, for keeping me sane, and for not letting me fall into depression or burn out completely. You truly helped me more than you realize.

I am deeply grateful to my parents, Andrei and Tatiana, and my sister, Lena, for supporting me throughout all the long years of my university studies, both in Russia and in Austria. Thank you for supporting my decision to study biology and, more importantly, for supporting my choices.

I am also very grateful to my boyfriend, Maksim, and to my close friends, Kristina and Alti, for bringing me back to life whenever I became too absorbed in myself and in science.

Finally, I would like to thank myself for not giving up, for following my heart and staying in science, for not being afraid to move to another country, and for getting through this journey despite all its challenges, with my nervous system almost intact.

Table of content

Abstract

Preterm infants frequently receive broad-spectrum antibiotics during hospitalization in neonatal intensive care units (NICUs), which can disrupt the development of the gut microbiome and lead to an increase of antibiotic resistance. In this study, bacterial strains isolated from stool samples of preterm infants were analysed to investigate phenotypic antibiotic resistance and potential cross-protection during co-cultivation. Whole-genome sequencing data were screened for antibiotic resistance genes (ARGs) and phenotypic analysis was performed by minimal inhibitory concentration (MIC) assays under aerobic and anaerobic conditions.

Phenotypic resistance generally corresponded to genomic predictions, for both β-lactam and aminoglycoside antibiotics, although heterogeneous behaviour and variability between replicates were occasionally observed. Gentamicin susceptibility was strongly influenced by oxygen availability, with increased resistance observed under anaerobic conditions. Co-cultivation experiments revealed possible cross-protection effects in several bacterial combinations, although interpretation was limited by technical variability, potential minimal contamination and unexpected growth of susceptible strains in some instances.

Overall, the study demonstrated that antibiotic resistance in gut-associated bacteria depends not only on ARG presence, but also on environmental conditions and interspecies interactions. These findings highlight the importance of studying antibiotic resistance in both monoculture and co-culture systems to better understand microbiome dynamics in preterm infants.

Zusammenfassung

Frühgeborene erhalten häufig während ihres Aufenthalts auf neonatologischen Intensivstationen (NICUs) Breitbandantibiotika, was die Entwicklung des Darmmikrobioms stören und zu einer Zunahme von Antibiotikaresistenzen führen kann. In dieser Masterarbeit wurden Bakterienstämme analysiert, die aus Stuhlproben von Frühgeborenen isoliert wurden, um die phänotypische Antibiotikaresistenz und mögliche Kreuzschutzeffekte während der Co-Kultivierung zu untersuchen. Daten der vollständigen Genomsequenzierung (WGS) wurden auf Antibiotikaresistenzgene (ARGs) untersucht, und die phänotypische Analyse wurde mittels Tests zur minimalen Hemmkonzentration (MIC) unter aeroben und anaeroben Bedingungen durchgeführt.

Die phänotypische Resistenz entsprach im Allgemeinen den genomischen Vorhersagen, sowohl für β-Lactam- als auch Aminoglykosid-Antibiotika, obwohl gelegentlich heterogenes Verhalten und Variabilität zwischen biologischen Replikaten beobachtet wurden. Die Empfindlichkeit gegenüber Gentamicin wurde stark durch die Sauerstoffverfügbarkeit beeinflusst, wobei bei den anaeroben Bedingungen eine erhöhte Resistenz festgestellt wurde. Co-Kultivierungsexperimente zeigten in einigen Bakterienkombinationen mögliche Kreuzschutzeffekte, obwohl die Interpretation durch technische Variabilität, potenzielle minimale Kontaminationen und unerwartetes Wachstum empfindlicher Stämme eigeschränkt war.

Zusammenfassend zeigte diese Arbeit, dass die Antibiotikaresistenz bei darmassoziierten Bakterien nicht nur vom Vorhandensein des ARGs abhängig ist, sondern auch von Umweltbedingungen und Interaktionen von unterschiedlichen Arten beeinflusst wird. Diese Ergebnisse verdeutlichen die Bedeutung der Untersuchung von Antibiotikaresistenz sowohl in Monokulturen als auch in komplexen Co-Kulturen zu untersuchen, um die Dynamik des Mikrobioms bei Frühgeborenen besser zu verstehen.

Introduction

Infant gut microbiome

The gut microbiome is a complex and dynamic community of microorganisms, consisting of bacteria, archaea, fungi, and viruses, which colonize the intestinal lumen and play an essential role in host metabolism, functioning of the immune system and regulation of various physiological processes (Moriel, N., et al., 2025; Rao, C., et al. 2021). In recent years it has been shown that gut microbiome is involved in cross-system interactions, particularly in early life, including the gut-brain axis (Sanidad, K., et al, 2020; Beghetti, I., et al, 2023).

The composition of the infant's gut microbiome is shaped by a variety of factors, including gestational age, mode of delivery, type of feeding, and medical interventions/manipulations (Thänert, R., et at, 2024). In healthy term infants, delivered vaginally and breastfed, the gut microbiome is dominated mainly by Bifidobacterium spp. and other beneficial anaerobic microorganisms (Saturio, S., et al, 2021). Their growth is supported by human milk oligosaccharides (HMOs) and this microbiota profile is considered a "healthy" early gut microbiome (Chong, C., et al, 2018). The colonization of the gut begins immediately after birth and progresses from facultative anaerobes to strict anaerobes during the first weeks of life (Arrieta, M., et al, 2014; Arboleya, S., et al, 2012).

Preterm birth refers to birth before 37th gestational week, and the extremely preterm infants are born before 28th gestational week and typically weigh under 1 kg (Cao et al., et al 2022; Mph, Adams-Chapman I., et al 2018). Preterm birth is the leading cause of mortality among newborns, infants and children under 5 years, and is associated with necrotizing enterocolitis (NEC), early- and late-onset neonatal sepsis (EOS, LOS) and long-term neurodevelopmental disorders (Ahmed, A., et al 2024; Healy, D., et al 2021; Beghetti et al., 2023; Seki et al., 2021, Baranowski, J., 2019, Flannery, D., et al, 2021).

The third trimester of pregnancy (starting from 27th gestational week) is particularly important for the development of the central nervous system, during which active formation of synaptic connections and branching of dendrites occur, supporting future cognitive functions (Wang, Y., et al, 2023; Seki et al., 2021). Based on this, extremely preterm infants represent a particularly vulnerable group at high risk of perinatal white matter lesions, including germinal matrix intraventricular haemorrhage (GMH-IVN), periventricular leukomalacia (PVL) and diffuse white matter lesions (Lee, 2017).

The establishment of gut microbiome in preterm infants takes place under significantly altered conditions. Their gastrointestinal tract and immune systems are functionally immature, which

reduces their barrier functions and resistance to infections (Korpela, K., et al. 2018; Arboleya, S., et al. 2015). Furthermore, such infants are often admitted to neonatal intensive care units (NICUs), where they undergo multiple medical interventions, including antibiotic therapy, catheterization and respiratory support (Thänert, R., et al, 2024). This disrupts normal gut colonization, resulting in a predominance of opportunistic pathogens such as *Escherichia coli, Clostridium, Staphylococcus*, *Streptococcus,* and *Klebsiella* species (Moriel, N., et al., 2025; Chen, Y., et al., 2020).

Those patterns lead to the development of dysbiosis. Dysbiosis is an imbalance of gut microbial community, which may contribute to pathological outcomes and the development of various diseases, including inflammatory bowel disease, autoimmune disorders, and neuropsychiatric disorders (Mitrea, L., et al., 2022; Weiss, G., et al, 2017). In this context, antibiotic therapy plays an important role as one of the most significant factors affecting the gut microbiome composition in preterm infants (Thänert R., et al., 2024). Extremely preterm neonates are routinely administered broad-spectrum antibiotics in the early postnatal period, which is considered a key driver of disrupted microbial colonization (Arboleya, S., et al. 2015). Alongside the mode of delivery and the hospital environment, the intensive use of antibiotics is associated with a reduction in microbial diversity and a shift in the composition of the microbiota towards opportunistic and antibiotic-resistant strains (Seki, D., et al., 2021; Gasparrini, A., et al., 2016; Gibson, M., et al., 2016).

The microbiome disruption associated with antibiotics extends beyond local changes and may exert a systemic influence via the gut-brain axis (Wang, Y., et al., 2023). It has been shown that dysbiotic states, including the dominance of specific bacterial taxa, are associated with alterations in the immune response and impairments in central nervous system maturation, in particular with suppression of electrocortical activity and the development of white matter lesions (Seki, D., et al., 2021). According to Seki et al. colonization by pathogenic strains, especially *Klebsiella pneumoniae*, may trigger a pro-inflammatory immune response (elevated γδ T cells, more inflammatory mediators, fewer neuroprotective factors) and suppress cortical maturation (Seki, D., et al., 2021). Further studies also demonstrate that specific characteristics of the gut microbiota in extremely preterm infants correlate with adverse neurophysiological outcomes, confirming the role of the microbiota as a mediator between external influences and neurodevelopment (Seki, D., et al., 2024).

Despite the recognition of antibiotics as an important modifying factor, direct causal links between antibiotic therapy and specific health outcomes remain unclear. The absence of

definitive data suggests the complex, multifactorial nature of the interaction between antibiotics, the microbiota and early-life development (C. Chong et al., 2018).

Therefore, it is likely that a combination of factors, including time of delivery, medical care characteristics, mode of delivery, feeding method and antibiotic therapy, shapes the gut microbiome profile in preterm infants and may impact their long-term health (S. Arboleya et al., 2012; K. Korpela et al., 2018). Especially, antibiotic administration should be considered as a key factor influencing the microbiome disruption (Robert Thänert et al., 2024).

Antimicrobial treatment in NICUs

Antibiotic treatment is often necessary in NICUs, where preterm infants undergo invasive procedures such as central venous catheterization and mechanical ventilation that serve as sources of microbial exposure (Simeoli, R., et al., 2022; Ramasethu, J., 2017). These intensive-care conditions, combined with prematurity, shape an intestinal ecosystem characterized by delayed colonization with typical commensals (e.g. *Bifidobacteria, Bacteroides*) and an increased abundance of potentially pathogenic taxa such as *Enterobacteriaceae, Enterococcus, Staphylococcus* and *Clostridia* (Morreale, C., et al., 2023; Chen, Y., et al., 2020). Therefore, the preterm gut microbiome is less diverse, more unstable and shows greater interindividual variability than that of term infants (Mulinge, M., et al., 2023).

Overlaying antibiotics on this already imbalanced community has a marked effect on microbiota structure. Systematic review data show that the use of antibiotics in NICUs for preterm infants consistently leads to a reduction in bacterial diversity by increasing Enterobacteriaceae, and depleting symbiotic *Bifidobacterium* spp., while enriching antibiotic resistance genes (ARGs) in *Enterococcus, Staphylococcus, Klebsiella, Acinetobacter, Pseudomonas* and other *Enterobacteriaceae,* many of which are typical nosocomial pathogens (Mulinge, M., et al., 2023, Gibson, M., et al, 2016). Longitudinal work further shows that diversity decreases during intravenous antibiotic treatment and then recovers at a lower rate than in minimally antibiotic-exposed infants, while *Enterobacteriaceae* increase, indicating a sustained shift toward a dysbiotic and resistance-enriched microbiome (Hutchinson, R., et al., 2022).

These effects may be amplified by the unique pharmacology of preterm infants. Compared with term infants and older children, preterms exhibit immature gastric, renal, hepatic and intestinal function, that leads to substantial variability in antibiotic absorption, distribution, metabolism and excretion (Butranova, O., et al., 2023). Many antibiotics used in this population

are off-label because robust pharmacokinetic data are lacking, complicating optimal dosing and increasing risk of both under- and overexposure (Simeoli, R., et al., 2022). Together this physiological immaturity and empirical antibiotic use create a setting in which dysbiosis, colonization by multidrug-resistant organisms and expansion of ARGs can easily occur, underscoring the need to understand and carefully manage antibiotic-driven microbiome and resistome development in the preterm gut (Morreale, C., et al., 2023; Simeoli, R., et al, 2022). Previous work conducted within our research group involved the analysis of stool samples from 30 preterm infants hospitalized at the Medical University of Vienna (David Seki et al., 2024). These samples were used to determine the composition and functional potential of the premature gut microbiota. Metagenomic sequencing revealed the presence of antibiotic resistance genes (ARGs) in a subset of bacterial genomes (13 out of 25). From these samples, various bacterial strains were successfully isolated, including both facultative and strictly anaerobic species.

Gut bacteria carrying ARGs are frequently detected in preterm infants in NICUs, and thorough laboratory testing is required to determine whether these genotypic characteristics lead to phenotypic resistance (Mulinge, M., et al., 2023; Chen, Y., et al., 2020). This is commonly assessed by minimal inhibitory concentration (MIC) assays performed under aerobic and anaerobic conditions using broth microdilutions (Gajdács, M., et al, 2017). Obtained MIC values are subsequently interpreted according to the European Committee on Antimicrobial Susceptibility Testing (EUCAST) clinical breakpoints and epidemiological cut-off values (ECOFFs) to classify isolates as susceptible or resistant (Kowalska-Krochmal, B., et al., 2021; EUCAST SOP 10.2, 2021).

Antibiotics and antibiotic resistance

Based on previous research and other studies, three most administrated antibiotics in neonatal care were selected for MIC testing:

Ampicillin (a β-lactam), routinely administered during the first days of life.

Piperacillin (a β-lactam), tested both alone and in combination with **Tazobactam**, a β-lactamase inhibitor.

Gentamicin (an aminoglycoside), frequently used as a first-line agent in combination with β-lactams for the treatment of early-onset sepsis (Simeoli, R., et al, 2022).

Ampicillin is a broad-spectrum β-lactam antibiotic widely used in clinical practice, particularly in neonatology and in the treatment of neonatal sepsis. It is commonly included in

recommended empirical therapy for newborns together with benzylpenicillin or amoxicillin and aminoglycosides (Butranova, O., et al 2023). Despite widespread use of ampicillin, the pharmacokinetics and safety profile of ampicillin in neonates remain poorly characterized (Simeoli R, et al, 2022). Belonging to the aminopenicillin subgroup of β-lactam antibiotics ampicillin acts by inhibiting bacterial cell wall synthesis through interaction with penicillin-binding-proteins (PBPs), which are essential enzymes involved in peptidoglycan formation. Inhibition of PBPs disrupts cell wall synthesis, resulting in osmotic instability and bacterial cell death, leading to the bactericidal mode of action (Türkyılmaz, O., et al, 2026). Resistance to ampicillin is increasingly observed among both commensal and pathogenic bacteria. The primary mechanism of resistance is the production of β-lactamases, enzymes capable of hydrolysing the β-lactam ring and thereby inactivating antibiotic (Türkyılmaz, O., et al, 2026). Within Gram-negative bacteria plasmid encoded β-lactamases such as TEM, SHV and CTX-M are particularly common (Yassara, S., et al, 2025), while chromosomally encoded OXY β-lactamases are characteristic for *Klebsiella* species (Yang, J., 2021). In *Staphylococci* resistance to penicillins is frequently mediated by the *blaZ* β-lactamase gene, however mutations within this operon may result in reduced or absent enzyme activity, potentially explaining phenotypic susceptibility despite the presence of operon in the genome (Kilani, A., et al. 2024; Rocha, G., et al, 2022)

Piperacillin, a semisynthetic penicillin derived from ampicillin, demonstrates improved efficacy against Gram-negative pathogens, especially when used in combination with tazobactam, a β-lactamase inhibitor. Tazobactam acts by binding to and inactivating β-lactamases responsible for hydrolysing the β-lactam ring, thereby recovering the antibacterial activity of piperacillin against β-lactamase-producing bacteria (Yang, F., et al, 2022; Payne, D., et al, 1994). As a result, the piperacillin/tazobactam combination extends the spectrum of activity to include β-lactamase-producing, penicillin-resistant bacteria such as *Escherichia coli*, *Klebsiella* spp., and *Bacteroides*, and is often used in NICUs for empiric treatment of moderate-to-severe infections (Pineda, L., et al, 2015; Butranova, O., et al 2023). However, within the *Klebsiella oxytoca* complex, chromosomally encoded class A OXY β-lactamases can substantially reduce the efficacy of piperacillin/tazobactam (Campos-Madueno, E., et al, 2023).

Gentamicin, an aminoglycoside antibiotic, is widely used in neonatal care for its efficacy against Gram-negative bacteria and is often co-administered with β-lactams to broaden antimicrobial coverage. Its pharmacokinetics are highly variable in neonates and influenced by

gestational and postnatal age, renal function, and body water content (Simeoli, R., et al, 2022; Butranova, O., et al 2023). Gentamicin exerts its bactericidal effect by inhibiting bacterial protein synthesis. The antibiotic passes through the cell membrane via an oxygen-dependent active transport mechanism, explaining the limited effectiveness of aminoglycosides against anaerobic bacteria (Chaves. B., et al, 2023). Aminoglycosides bind to the 16S rRNA of the 30S ribosomal subunit inhibiting translation (Zárate, S., et al, 2018). Despite their effectiveness, resistance to aminoglycosides is increasingly observed. The most common resistance mechanisms involve aminoglycoside-modifying enzymes, including acetyltransferases, nucleotidyltransferases and phosphotransferases, which chemically modify the antibiotic and reduce its ability to bind to the ribosome (Zárate, S., et al, 2018; Dec, M., et al, 2017). For example, in *Enterococcus faecalis*, high-level gentamicin resistance is frequently associated with the bifunctional enzyme Aac(6')-Aph(2"), that is often encoded on mobile genetic elements and allows horizontal gene transfer between bacterial populations (Sparo, M., et al, 2011). Interestingly, intrinsic resistance to aminoglycosides has been described in several *Lactobacillus* spp. Many of them demonstrate high MIC values for gentamicin, kanamycin, streptomycin and other aminoglycosides despite the lack of aminoglycoside resistance genes. This intrinsic resistance is thought to be associated with the absence of cytochrome-mediated transport systems required for antibiotic's uptake (Nøhr-Meldgaard, K., et al, 2023; Campedelli, I., et al, 2019; Abriouel, H., et al, 2015).

Antibiotic resistance can emerge very rapidly with clinically relevant resistance levels achieved within 2 months of antibiotic treatment in most Gram-negative pathogens in laboratory experiments (Daruka, L., et al, 2025). Many resistance genes are already widely distributed in nature and clinical settings (Bottery, M., et al, 2020).

Cross-protection: from pure cultures to environmental interactions

The gut microbiome is a complex multispecies community, where antibiotic susceptibility is formed not only at the level of individual bacterial strains, but also as a community's feature. Antibiotic resistance should be considered as an emergent property of the community, because interspecies interactions can affect the response to antibiotic treatment (Bottery, M., et al, 2020). In polymicrobial infections, antibiotic treatment can have the opposite effect to what is seen in monoculture: strains that are normally sensitive to antibiotic may grow, while strains that are usually more tolerant can be inhibited, because interactions within the microbial community can alter how individual strains respond to the antibiotic (Bottery, M., et al, 2020).

García-Santamarina S. et al have shown that, in model synthetic community of gut bacteria, communal behaviours (cross-protection and cross-sensibilization) occurred in 26% of all tested drug-community interactions (García-Santamarina, S., et al, 2024).

A classic example of a cross-protection mechanism is β-lactam degradation by resistant bacteria. For example, commensal *Bacteroides* secrete β-lactamases within outer membrane vesicles (OMVs) and protect *Salmonella Typhimurium* and *Bifidobacterium* breve from a lethal dose of cefotaxime, a third-generation cephalosporine antibiotic (Stentz, R., et al, 2014). Similarly, β-lactamase-producing *Bacteroides* increase MIC of ceftriaxone for susceptible *E. coli* (Stiefel, U., et al, 2015). In droplet microreactors resistant strains producing β-lactamase create a "cross-protection window", where susceptible strains survive with cefotaxime concentration 100 times higher than their MIC (Zhao, X., et al, 2023). Biofilm models have shown that resistant cells can locally protect nearby susceptible cells from antibiotic exposure, and that this cross-protection becomes more effective in communities with mutualistic interactions, where spatial mixing between resistant and susceptible strains is increased (Estrela, S., et al, 2018). Protection mechanisms do not always require direct contact of bacteria. β-lactamase producing *E. coli* protects susceptible *Salmonella* strains in the presence of ampicillin without any physical contact (Perlin, M., et al, 2009). In addition to extracellular degradation of antibiotic, intracellular detoxification may also result in cross-protection. For instance, resistant *Streptococcus pneumoniae* produces chloramphenicol acetyltransferase, which irreversibly affects the antibiotic within the cell, thereby decreasing its extracellular concentration and protecting nearby susceptible strains (Sorg, R., et al, 2016). Furthermore, spatial structure of the community is critical: modelling and experiments have shown that mixed mutualistic biofilms increase cross-protection, while competitive communities lead to segregation and limit benefits for susceptible species (Estrela, S., et al, 2018; Xu, F., et al, 2024).

Resistance can also be increased by action of signal molecules. In *Pseudomonas putida* expression of efflux-pump TtgGHI is induced by indole, produced by *E. coli*. This increases *P. putida* resistance to ampicillin in co-culture (Molina-Santiago, C., et al 2014). A review about non-genetic mechanisms highlights that indole, polyamines, ammonia and other small molecules can increase or decrease resistance level of neighbouring bacteria by acting as "infochemicals" (El-Halfawy, O., et al, 2012).

Bacterial responses to antibiotics may be also influenced by long-range chemical interference. For example, volatile ammonia released by stationary-phase partner populations can also

confer cross-protection, boosting antibiotic resistance in physically separated *E. coli* by increasing intracellular polyamine levels and altering membrane permeability (Bernier, S., et al., 2011).

In addition, cross-feeding can markedly alter bacterial tolerance to antibiotics. In engineered and clinically relevant communities, dependence on metabolite-sharing partners can make otherwise resistant strains susceptible to lower antibiotic concentrations, a "weakest link" effect in which community tolerance is determined by the least tolerant member. At the same time, resistant partners may provide cross-protection by enzymatically degrading antibiotics in the medium (Adamowicz, E., et al., 2018).

In summary, in polymicrobial infections interspecies interactions can significantly change antibiotic resistance. It was shown that clinical isolates may protect each other in a community from clinically relevant antibiotics (De Vos, M., et al, 2017). Commensal β-lactamase-producing *Bacteroides* and other members of the gut microbiome can reduce disruptive effects of β-lactams and provide microbiome resilience, but may simultaneously support pathogen survival and contribute to the proliferation of antimicrobial resistance (Bhattarai, S., et al, 2024).

Overall, current knowledge demonstrates that antibiotic exposure in early life influences not only individual bacterial strains, but also the structure and interactions within the gut microbial community. Although the use of broad-spectrum antibiotics in neonatal care is often necessary, it creates strong selective pressure for antibiotic-resistant bacteria and may contribute to long-term microbiome disruption in preterm infants. Additionally, bacterial interactions such as cross-protection can change bacterial response to antibiotics, highlighting the importance of investigating resistance not only in monocultures, but also in co-culture systems. Therefore, understanding the microbiological consequences of antibiotic therapy is important for improving neonatal treatment strategies, limiting colonization by resistant pathogens, and supporting the development of a healthy gut microbiome.

The aims of this study were: 1) to investigate the phenotypic expression of antibiotic resistance in individual bacterial strains encoding antibiotic resistance genes using minimal inhibitory concentration assay, and 2) to assess potential cross-protection during co-cultivation of two bacterial strains in the presence of antibiotics. We hypothesized that bacterial strains carrying ARGs would demonstrate phenotypic resistance in monoculture conditions and that co-cultivation of resistant and susceptible strains could lead to cross-protection effects.

Materials

Bacterial isolates

Species	Strain
K. pneumoniae	40.9B
	2.3A
K. michiganensis	8.3A
E. coli	13.3C
	14.3B
S. epidermidis	LH_NM_637
	8.2A
E. faecalis	5.5A
L. fermentum	10.2E
L. plantarum	37.6A
B. bifidum	WS111
B. breve	WS23
B. infantis	WS13
B. pseudocatenulatum	WS19

Table 1. List of bacterial isolates used in this study

These isolates were obtained from stool samples of preterm infants hospitalized at the Medical University of Vienna. Both facultative and strictly anaerobic strains were cultured.

During the strain characterization colony forming units per millilitre (CFU/mL) were determined (Table 2). As CFL/mL values were within a similar range for all strains, optical density measurements of the starting cultures were used to ensure equal cell concentrations between samples.

Strain	CFU/mL
K. pneumoniae 40.9B	$2{,}66 * 10^9$
K. pneumoniae 2.3A	$2{,}33 * 10^9$
K. michiganensis 8.3A	$1{,}83 * 10^9$
E. coli 13.3C	$2{,}79 * 10^9$
E. coli 14.3B	$1{,}9 * 10^9$
S. epidermidis LH_NM_637	$1{,}61 * 10^9$
S. epidermidis 8.2A	$1{,}86 * 10^9$
E. faecalis 5.5A	$1{,}52 * 10^9$

L. fermentum 10.2E	$2{,}47 * 10^{10}$
L. plantarum 37.6A	$1{,}67 * 10^{9}$
B. bifidum WS111	$1{,}33 * 10^{8}$
B. breve WS23	$1{,}08 * 10^{9}$
B. infantis WS13	$9{,}65 * 10^{7}$
B. pseudocatenulatum WS19	$2{,}5 * 10^{10}$

Table 2. Colony-forming units per millilitre (CFU/mL) of bacterial isolates.

Sequencing data

Whole-genome sequencing of the bacterial isolates was conducted previously and provided. Genome annotation was used to identify the presence of antibiotic resistance genes (ARGs), which guided the selection of antibiotics for phenotypic validation.

Antibiotics

The following antibiotics and inhibitors were tested:

- Ampicillin ("Sigma-Aldrich", A9518): stock solution 100 mg/mL in ddH2O, stored at -20°C.
- Gentamicin ("Sigma-Aldrich", G1914): stock solution 10 mg/mL in ddH2O, stored at -20°C.
- Piperacillin ("Sigma-Aldrich", PHR1805): stock solution 100 mg/mL in DMSO, stored at -80°C.
- Tazobactam ("Merck", PHR1686): stock solution 50 mg/mL in DMSO, stored at -80°C.

Antibiotic concentrations for MIC assays (two-fold dilution series) based of EUCAST database (EUCAST, n.d.):

Antibiotic	**Concentration in µg/mL**	**Strains**
Ampicillin	2 – 256	All tested strains
Piperacillin	1 – 128	All tested strains
Gentamicin	0,5 – 64	*K. pneumoniae 40.9B* *K. pneumoniae 2.3A* *K. michiganensis 8.3A* *E. coli 13.3C* *E. coli 14.3B*

		S. epidemidis LH_NM_637 *B. bifidum WS111* *B. breve WS23* *B. infantis WS13* *B. pseudocatenulatum WS19*
Gentamicin	2 – 256	*E. faecalis 5.5A* *S. epidermidis 8.2A* *L. plantarum 37.6A* *L. fermentum 10.2E*

Table 3. Antibiotics concentration used in this study.

Growth Media

- Mueller Hinton Broth – MHB – ("Sigma-Aldrich", 97580) (EUCAST, 2022)
- Mueller Hinton Agar - MHA - plates ("Sigma-Aldrich", 90922) (EUCAST, 2022)
- MRS (De Man, Rogosa, Sharpe) Broth – medium for Lactobacilli – ("Carl Roth", X925)
- 50/50 MH-MRS mix prepared as 1:1 MHB and MRS
- 90/10 MH-MRS mix prepared as 9:1 MHB and MRS
- Brain Heart Infusion – BHI – („Oxoid ", CM1135)

Primers:

Strain-specific primers designed:

Strain	**Number ID**	**Name**	**Sequence**
E. coli 13.3C	29	E_Coli_13.3C_fw3	GCCAGAAAGTTCACGAGGATAG
	30	E_Coli_13.3C_rev3	GCCGCGAGAAAGAAGAGAAA
E. coli 14.3B	7	E_Coli_14.3B_fw2	CCGGCCTACAAAGTCGTATAA
	8	E_Coli_14.3B_rev2	GAGACTGATGACAAGCGTAAGA
K. pneumoniae 40.9B	17	K_pne_40.9B_fw1	GTGACGTTCACCGAGGATTT
	18	K_pne_40.9B_rev1	TGGAACCATTTCGGCTTCTC
K. pneumoniae 2.3A	35	K_pne_2.3A_fw3	GAACTGGACGGTGCCTTAAT
	36	K_pne_2.3A_rev3	CCGTGGCTATTGTTGTAGGTAG
K. michiganensis 8.3A	25	K_mich_8.3A_fw1	GCCATCGTCATGGTGATCTT
	26	K_mich_8.3A_rev1	CGTCACTATCGCCCAGTAAAC
S. epidermidis 8.2A	39	Staph_8.2A_fw1	CAGAAGAAGTGGGCGGAATAA

	40	Staph_8.2A_rev1	GTCCTCCAAGCGAAACATAGA

Table 4. Strain-specific primers designed for this study.

Methods

Anaerobic cultivation

Anaerobic cultivation was performed in a controlled atmosphere chamber containing 10% CO2, 5% H2, and 85% N2. All manipulations of anaerobic cultures were conducted under these conditions. All equipment and media were placed in anaerobic chamber at least 24 hours before each experiment to ensure an anaerobic environment.

Antimicrobial susceptibility testing: Minimal Inhibitory Concentration (MIC) assay

Susceptibility testing to determine the minimum inhibitory concentration (MIC) of ampicillin, piperacillin, and gentamicin was carried out by broth microdilution in Mueller Hinton Broth (MHB). MIC is the lowest concentration of an antibacterial agent expressed in mg/L (μg/mL) which, under strictly controlled in vitro conditions, completely prevents visible growth of the test strain of an organism (EUCAST Definitive Document, 1998). Overnight bacterial cultures grown in MHB were diluted to an optical density at 600 nm (OD_{600}) of 0.002. 100μL of the diluted culture was added to 96-well plates containing 100μL of MHB with serial two-fold dilutions of each antibiotic (Table 3). The concentration of tazobactam was kept constant at 4 μg/mL. Plates were incubated at 37°C under static conditions for 20-22 hours. Bacterial growth in each well was analysed both by visual inspection and by measuring OD_{600} using a TECAN Spark Plate reader (EUCAST, 2021). Measurements were corrected by subtracting background absorbance from blank wells, containing only MHB medium.

Growth analysis

Bacterial growth dynamics were monitored by measuring OD_{600} using a TECAN Spark Plate reader under aerobic conditions and a plate reader placed in anaerobic tents with controlled atmosphere for anaerobic conditions at 37°C. Prior to each measurement, plates were shaken for 3 seconds. Optical density was recorded every 20-30 minutes over a period of 24-36 hours. Data were normalized and analysed using R software.

Co-culturing

To determine potential cross-protection effects, co-culture experiments were performed using antibiotic resistant and susceptible strains in the presence and absence of antibiotics. As an initial experimental setup for studying potential cross-protection, facultative anaerobic bacteria were selected and experiments were conducted under aerobic conditions. The combination of strains used are summarized in Tables 5-7. To ensure comparability with MIC assays, experimental conditions were aligned accordingly.

Overnight cultures grown in MHB were diluted to an OD_{600} of 0.002 for monocultures and 0.001 for co-cultures. On 96-well plate, for monocultures 100 µL of bacterial suspension was added to 100 µL of medium, whereas for co-cultures 50 µL of each strain were combined and added to 100 µL of medium. Antibiotic conditions included: 1) no antibiotic, 2) highest concentration at which resistant strain grew reliably in MIC assays, 3) MIC value of the susceptible strain, and 4) four times the MIC (4x MIC). 96-well plate was incubated for 20-22 hours at 37°C.

Bacterial growth was observed via OD600 measurements and visual inspection using a TECAN Spark plate reader, with background correction using blank wells. Following incubation, cells were harvested by centrifugation (13.500 rpm for 3 minutes), and pellets were stored at -20°C for downstream analysis.

Strain	Resistance	Anaerobe/facultative	Gram staining (+/-)
E. coli 14.3B	Ampicillin	Facultative	-
E. coli 13.3C	-	Facultative	-
K. pneumoniae 40.9B	Ampicillin	Facultative	-
E. coli 13.3C	-	Facultative	-
K. pneumoniae 2.3A	Ampicillin	Facultative	-
E. coli 13.3C	-	Facultative	-
K. michiganensis 8.3A	Ampicillin	Facultative	-
E. coli 13.3C	-	Facultative	-

Table 5. Combinations for potential cross-protection from ampicillin

Strain	Resistance	Anaerobe/facultative	Gram staining (+/-)
E. coli 13.3C	-	Facultative	-
K. michiganensis 8.3A	Piperacillin + Tazobactam	Facultative	-

E. coli 14.3B	-	Facultative	-
K. michiganensis 8.3A	Piperacillin + Tazobactam	Facultative	-
K. pneumoniae 40.9B	-	Facultative	-
K. michiganensis 8.3A	Piperacillin + Tazobactam	Facultative	-
K. pneumoniae 2.3A	-	Facultative	-
K. michiganensis 8.3A	Piperacillin + Tazobactam	Facultative	-

Table 6. Combinations for potential cross-protection from piperacillin with tazobactam

Strain	Resistance	Anaerobe/facultative	Gram staining (+/-)
E. coli 13.3C	-	Facultative	-
S. epidermidis 8.2A	Gentamicin	Facultative	-
E. coli 14.3B	-	Facultative	-
S. epidermidis 8.2A	Gentamicin	Facultative	-
K. pneumoniae 40.9B	-	Facultative	-
S. epidermidis 8.2A	Gentamicin	Facultative	-
K. pneumoniae 2.3A	-	Facultative	-
S. epidermidis 8.2A	Gentamicin	Facultative	-
K. michiganensis 8.3A	-	Facultative	-
S. epidermidis 8.2A	Gentamicin	Facultative	-

Table 7. Combinations for potential cross-protection from gentamicin

DNA extraction

Genomic DNA was extracted using the "innuPREP DNA Mini Kit 2.0" from IST Innuscreen GmbH according to the manufacture's protocol "Protocol for DNA Isolation from bacterial cell cultures" with modifications. Incubation times with lysozyme (10 mg/mL) and with lysis solution (CBV) supplemented with Proteinase K (20 mg/mL) were extended to 45 minutes to improve cell lysis efficiency. For samples containing Gram-positive bacteria, an additional step of three freeze-thaw cycles was introduced following resuspension of the pellet in TE buffer.

Each cycle consisted of freezing on dry ice and thawing at 37°C for 5 minutes to enhance disruption of the peptidoglycan layer. DNA concentration was measured using the Qubit™ 1X dsDNA HS Assay Kits.

Digital PCR (dPCR)

Digital PCR (dPCR) was performed to differentiate between bacterial strains in co-culture samples. Strain-specific primers were designed and validated through conventional PCR and dPCR assays to confirm their specificity and to optimize annealing temperature (Fig. S1).

dPCR was carried out using the QIAcuity One system (Qiagen) with Nanoplate 8.5K 96-well format. EvaGreen fluorescent dye was used for detection of amplification products. Each reaction had a total volume of 12 μL, including 2 μL of template DNA (0.01 ng/μL). The thermal cycling protocol was as follows: initial denaturation at 95°C for 3 minutes; 35 cycles of denaturation at 95°C for 30 seconds, annealing at 59°C for 30 seconds, and elongation at 72°C for 1 min; followed by a final stabilization step at 40°C for 5 minutes. Fluorescence was measured in the green channel with an exposure time of 300 ms and a gain of 3.

Results

Based on the whole-genome sequencing data, genome annotation revealed the presence of multiple antibiotic-resistance genes (ARGs) within our sample collection. Initial screening was performed using the bioinformatic tool ABRicate (Seemann T., 2016) against the NCBI database (Feldgarden, M., et al., 2021), providing a comprehensive overview of ARGs across all antibiotic classes (Fig. 1). From this dataset, β-lactams and aminoglycosides were selected as the primary focus of this study, as they are most frequently used in premature infants (Seki, D., et al., 2024) (Fig. 2). In addition, the genomes were further analysed using the Comprehensive Antibiotic Resistance Database (CARD), which is specifically designed for antibiotic resistance genes (Alcock, B., et al., 2023). This allowed for a more detailed characterization of ARGs, including not only specific resistance determinants but also broader resistance-associated genes such as multidrug efflux pump systems (Fig. 3).

Analysis of aminoglycoside-associated ARGs revealed both specific resistance genes and more general resistance mechanisms. Among the identified ARGs were *aph(3'')-Ib, aph(6)-Id, ant(3'')-IIa, ant(4')-Ib,* and *aac(6')-Ie-aph(2'')-Ia,* which encode aminoglycoside-modifying enzymes that reduce antibiotic activity through enzymatic modification. In addition, several multidrug efflux systems (*mdtABC, arcD*) and their associated regulatory elements (*baeRS, cpxA, tolC*) were detected. However, the CARD database generally reports resistance at the level of the aminoglycoside class and does not always indicate which specific aminoglycosides are affected. Therefore, the presence of aminoglycoside-associated ARGs cannot be directly interpreted as resistance to gentamicin, making phenotype prediction based only on genomic data difficult.

A similar pattern was observed for β-lactam-associated ARGs. In addition to several regulatory genes involved in stress responses (*marA*) and antibiotic resistance regulation (*evgS, evgA, gadW, gadX, CRP*) and multidrug efflux systems (*mdtEF, acrABEF*), numerous β-lactamase genes were identified. Importantly, these β-lactamases differ in their substrate specificity. For example, AmpC-type β-lactamases are primarily associated with resistance to cephalosporins, whereas SHV-type enzymes have been linked to resistance to cephalosporins, carbapenems,

and penams. Therefore, the presence of a β-lactamase gene alone does not necessarily predict resistance to the β-lactam antibiotics investigated in this study.

Overall, the *in silico* analysis revealed that resistance-associated genes were concentrated primarily in members of the *Enterobacteriaceae, Staphylococcus*, and *Enterococcus* groups, whereas no ARGs associated with aminoglycosides or β-lactams were detected in the beneficial bacteria (*Bifidobacterium* and *Lactobacillus* spp.). These findings highlight the complexity of predicting phenotypic resistance from genomic data alone and demonstrate the need for experimental validation using susceptibility testing.

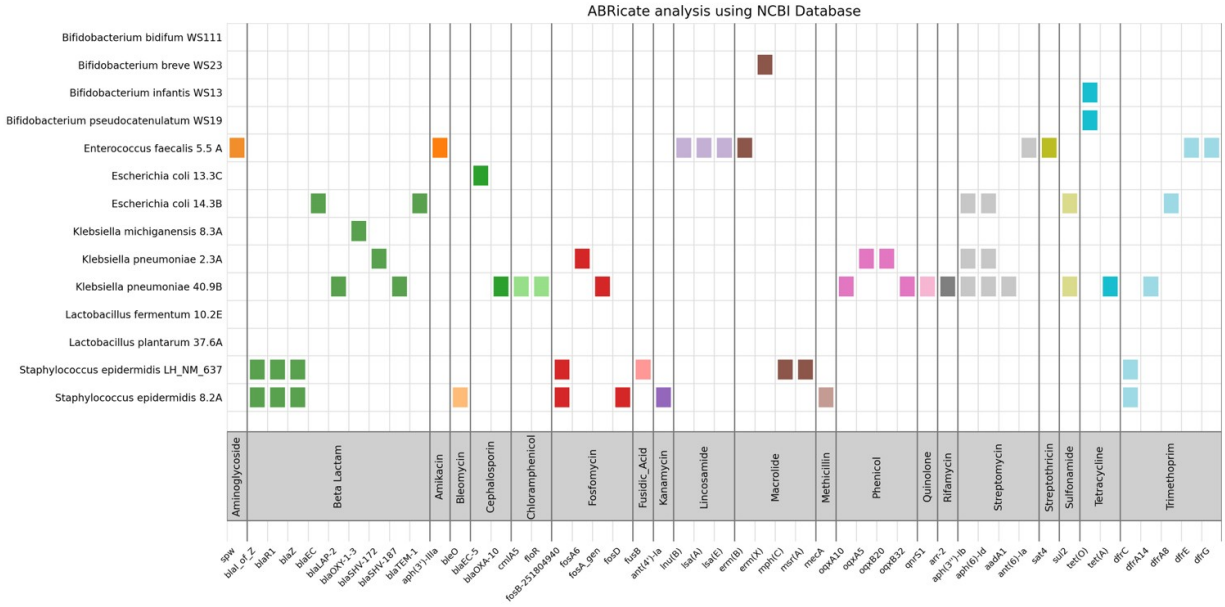

Fig. 1. ABRicate analysis against the NCBI database. Fourteen strains of interest were analysed for the potential presence of ARGs.

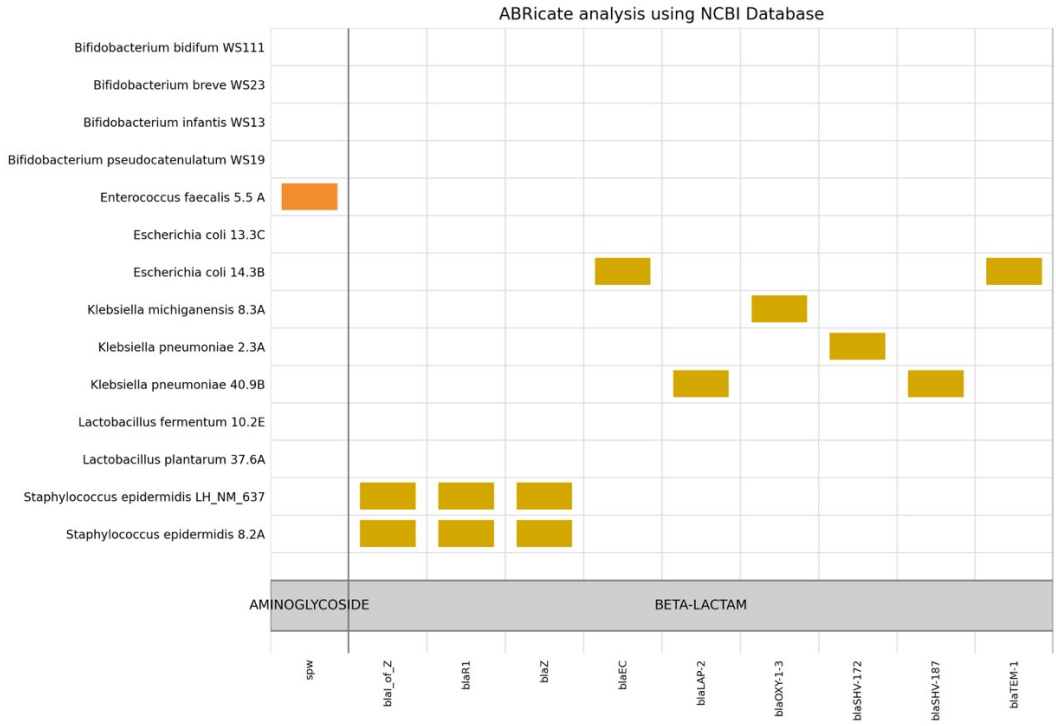

Fig. 2. ABRicate analysis against the NCBI database filtered for β-lactams and aminoglycosides. Fourteen strains of interest were analysed for potential ARGs.

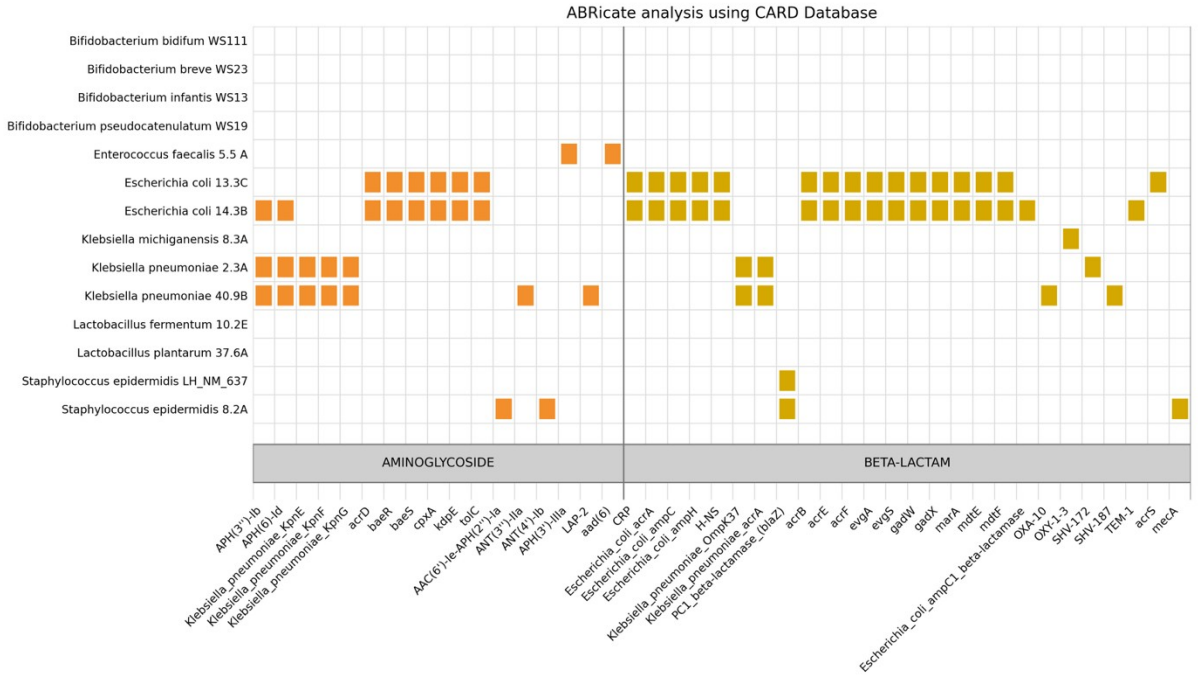

Fig. 3. ABRicate analysis against the CARD database filtered for β-lactams and aminoglycosides. Fourteen strains of interest were analysed for potential ARGs.

Minimal inhibitory concentration assays

To assess the phenotypic expression of resistance predicted by genome-based analyses, we conducted minimal inhibitory concentration (MIC) assays for selected bacterial isolates.
It should be noted that optical density values presented in the results are not intended to provide a quantitative comparison of bacterial growth. Instead, the analysis focuses exclusively on the presence or absence of bacterial growth, with a primary focus on conditions where no growth was observed ($OD_{600} = 0$), corresponding to complete inhibition. Differences in growth levels between biological and technical replicates were not interpreted, as the experimental setup was not designed to compare relative growth performance, but rather to determine inhibitory thresholds.

MIC of β-lactam antibiotics: ampicillin and piperacillin

Escherichia coli 13.3C:

Genome sequencing revealed the presence of *blaEC-5*, which encodes a β-lactamase associated with resistance to cephalosporins. However, this enzyme does not typically confer resistance to standard β-lactams such as ampicillin or piperacillin. Consistent with this, the strain showed full susceptibility to ampicillin (Fig. 4), piperacillin (Fig. 6), and piperacillin/tazobactam (Fig. 7) in MIC assays (no detectable growth across the tested concentrations). According to EUCAST wild-type breakpoints for *E. coli*, the ECOFF values are 8 µg/mL for ampicillin, 8 µg/mL for piperacillin, and 8 µg/mL for piperacillin/tazobactam (EUCAST, last accessed 01.05.2026). Additionally, MIC assay with ampicillin performed under anaerobic conditions revealed the same results, that *E. coli 13.3C* remains susceptible (Fig. 5). However, it is important to note a heterogeneous pattern among technical replicates, as some showed growth at different ampicillin concentrations under anaerobic conditions. This heterogeneous behaviour of the bacterial was previously described in the literature (Bixby, M., et al., 2024). Overall, the majority of MIC values observed for this strain were below these thresholds, confirming susceptibility of the strain.

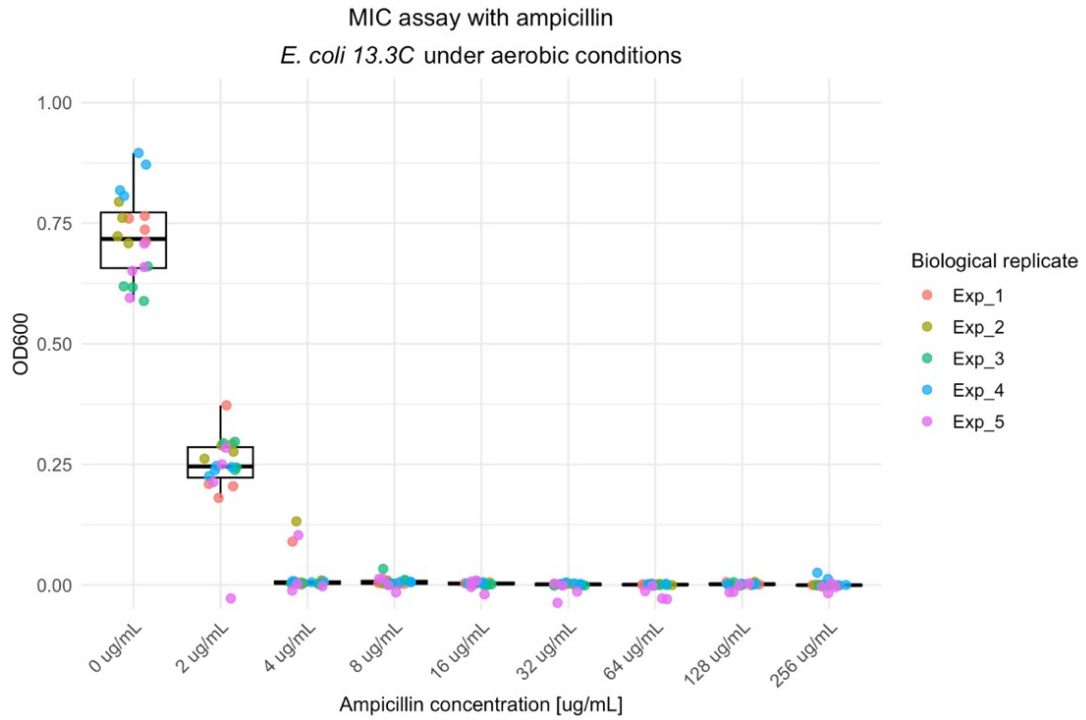

Fig. 4. MIC assay of E. coli 13.3C with ampicillin under aerobic conditions. Each color represents a biological replicate, including four technical replicates. The MIC was determined to be 8 μg/mL.

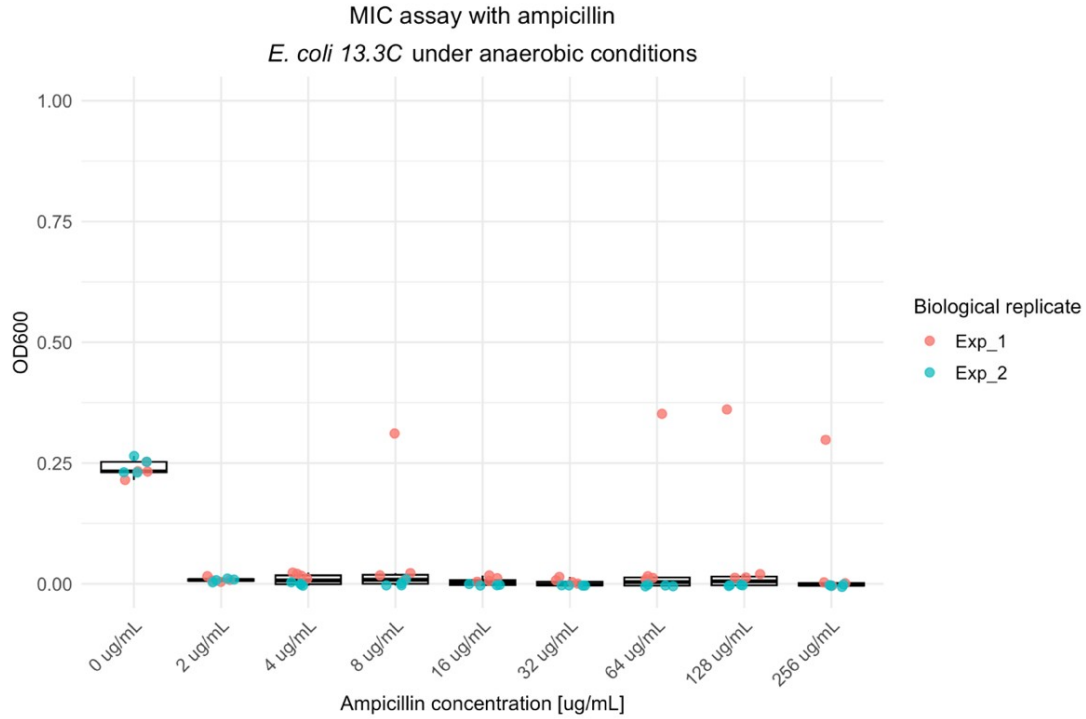

Fig. 5. MIC assay of E. coli 13.3C with ampicillin under anaerobic conditions. Each color represents one biological replicate, including four technical replicates. The MIC was determined to be 2 μg/mL ampicillin. Some outliers can be observed with concentrations 8, 64, 128, and 256 μg/mL, likely indicating a heterogeneous growth pattern within the biological replicate under anaerobic conditions.

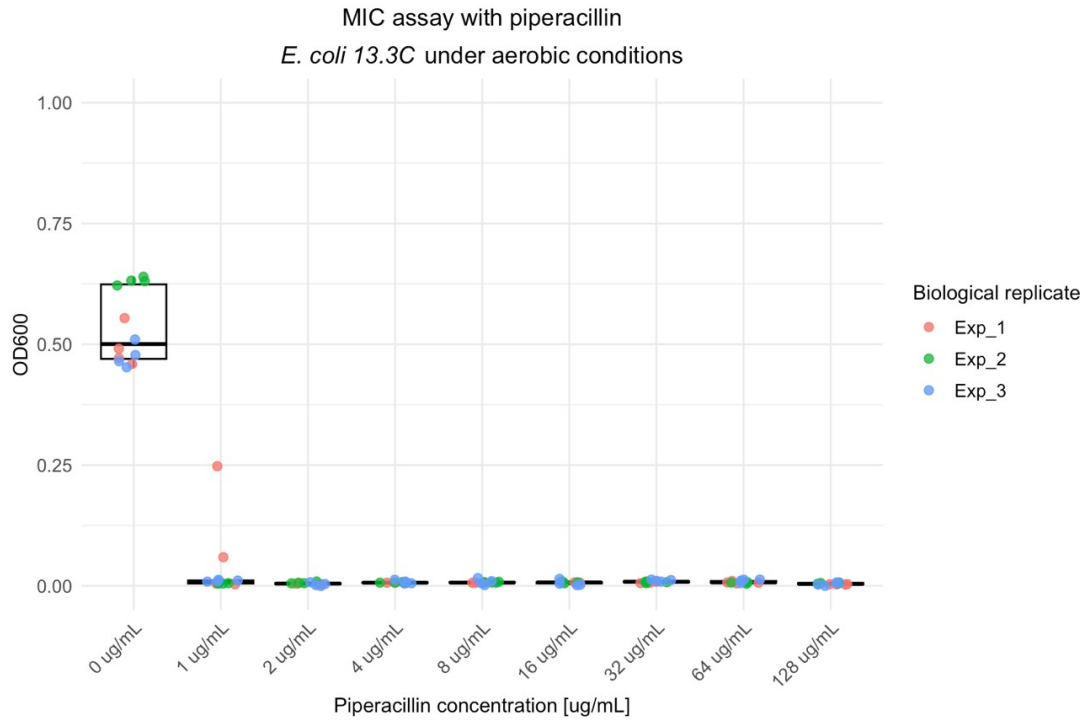

Fig. 6. MIC assay of E. coli 13.3C with piperacillin under aerobic conditions. Each color represents one biological replicate, including four technical replicates. The MIC was determined to be 2 μg/mL.

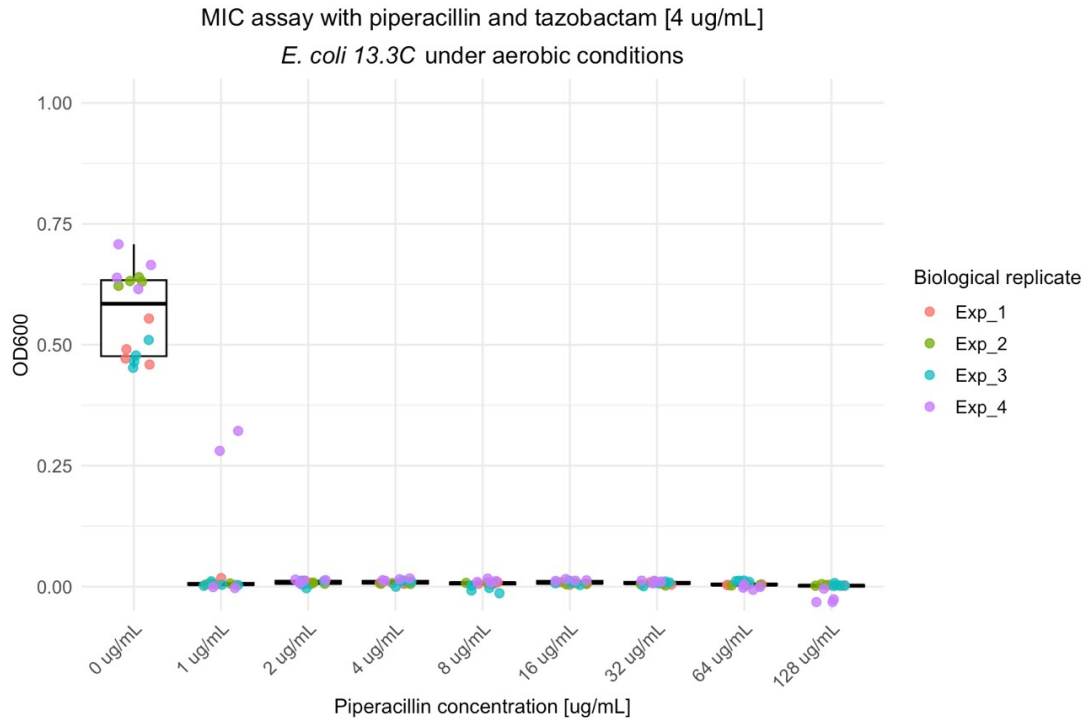

Fig. 7. MIC assay of E. coli 13.3C with piperacillin under aerobic conditions in the presence of tazobactam at a constant concentration of 4 μg/mL. Each color represents one biological replicate, including four technical replicates. The MIC was determined to be 2 μg/mL.

Escherichia coli 14.3B:

This strain encoded both *blaEC* (class C β-lactamase) and *blaTEM-1* (class A broad-spectrum β-lactamase), indicating resistance to multiple β-lactams. In phenotypic assays, the strain demonstrated resistance to ampicillin (under both aerobic and anaerobic conditions) and piperacillin (Figs. 8-10), showing growth even at the highest concentrations tested. However, it remained fully susceptible to piperacillin in the presence of tazobactam, with complete growth inhibition observed in all replicates, highlighting the effective inhibition of β-lactamases by tazobactam (Fig. 11). These results align with our *in silico* predictions for *E. coli 14.3B* based on whole-genome sequencing (Figs. 1-3).

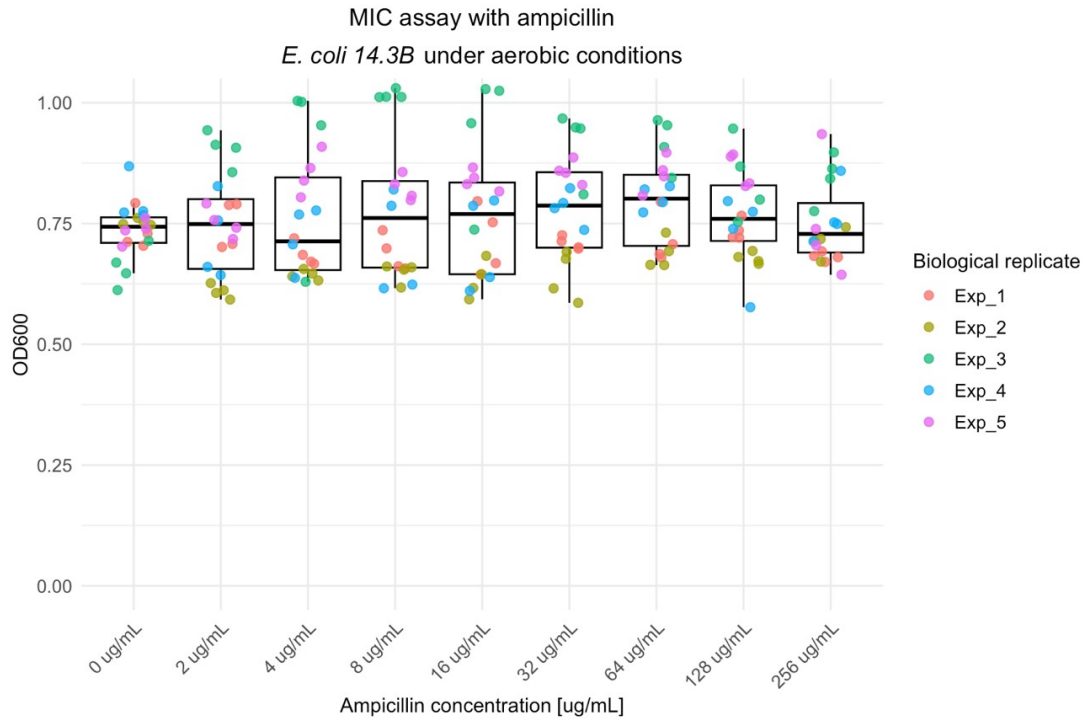

Fig. 8. MIC assay of E. coli 14.3B with ampicillin under aerobic conditions. Each color represents one biological replicate, including four technical replicates. The strain was completely resistant to ampicillin.

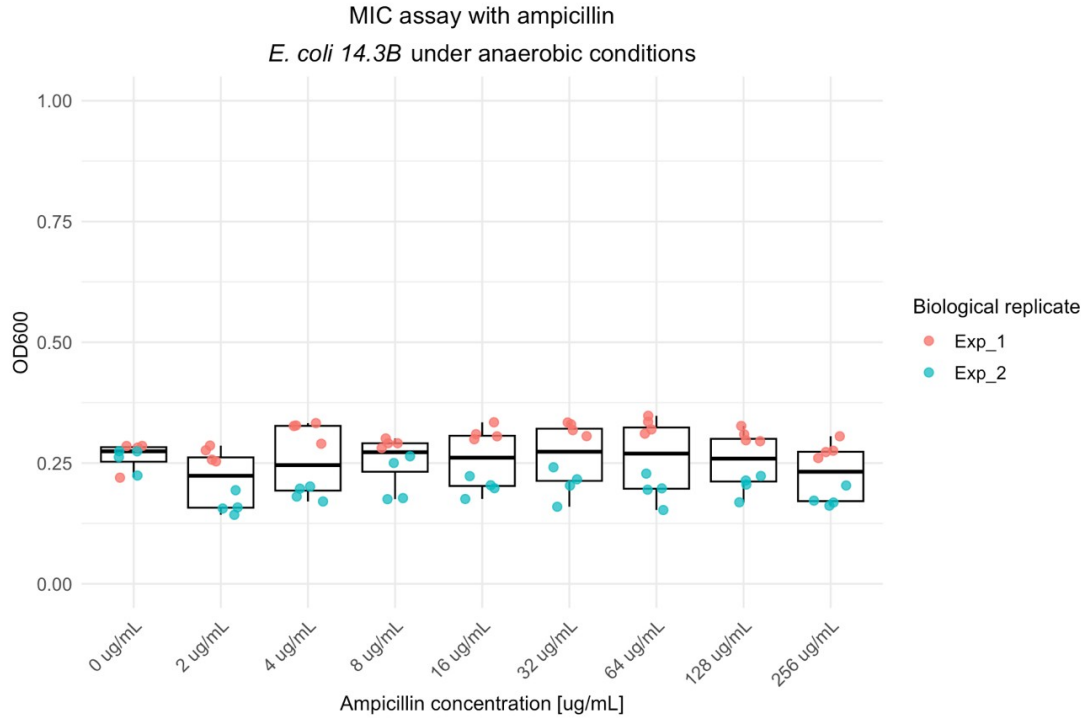

Fig. 9. MIC assay of E. coli 14.3B with ampicillin under anaerobic conditions. Each color represents one biological replicate, including four technical replicates. The strain was completely resistant to ampicillin.

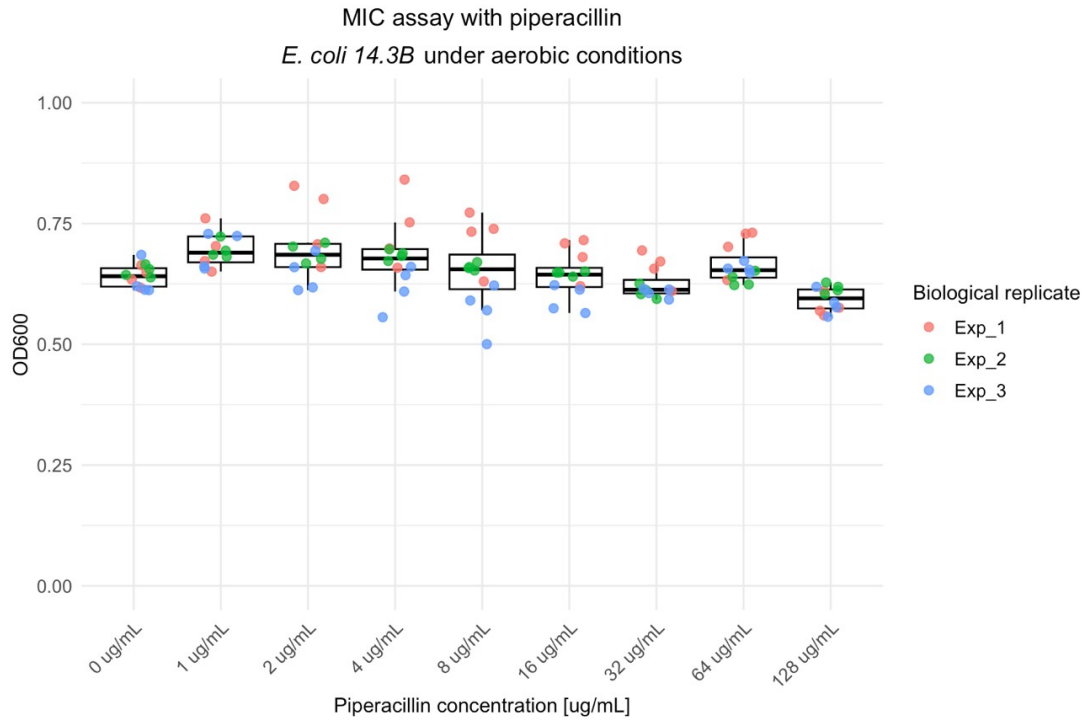

Fig. 10. MIC assay of E. coli 14.3B with piperacillin under aerobic conditions. Each color represents one biological replicate, including four technical replicates. The strain was completely resistant to piperacillin.

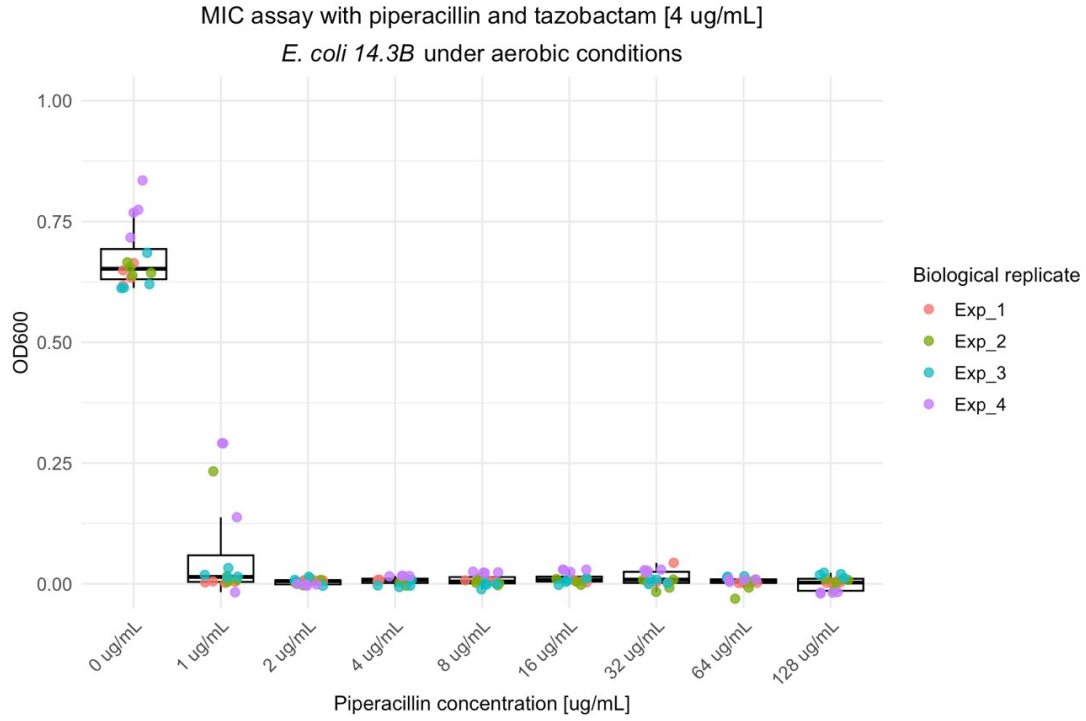

Fig. 11. MIC assay of E. coli 14.3B with piperacillin under aerobic conditions in the presence of tazobactam at a constant concentration of 4 μg/mL. Each color represents one biological replicate, including four technical replicates. The MIC was determined to be 2 μg/mL.

Klebsiella pneumoniae 40.9B:

In silico analysis revealed that this strain carries *blaSHV-187, blaLAP-2,* and *blaOXA-10*, all encoding β-lactamases associated with resistance to various β-lactam antibiotics. As expected, the strain showed complete resistance to ampicillin (growth at all concentrations under both aerobic and anaerobic conditions) and partial resistance to piperacillin, with MIC values ranging from 64 µg/mL (Figs. 12-14). The addition of tazobactam markedly reduced MIC values to 2–4 µg/mL. Notably, anomalous growth patterns were observed in some technical replicates (Fig. 15), where bacterial growth was inhibited at 4 µg/mL but resumed at higher concentrations (e.g., 8 µg/mL). These regrowth events were confirmed upon repeated testing, and the regrown isolates were preserved for subsequent sequencing analysis. This phenomenon has been described in the literature and may reflect the so called Eagle's effect, a paradoxical response in which β-lactamase-producing bacteria survive and grow at higher antibiotic concentrations that would normally be inhibitory (Kowalska-Krochmal, B., et al., 2021). Also, according to Han M. et al., the hyperproduction of SHV could be associated with increased resistance to piperacillin/tazobactam (Han, M., et al., 2020). To determine the underlying cause of this unexpected growth, further experiments are needed.

According to EUCAST, *K. pneumoniae* wild-type strains have no defined ECOFF for ampicillin, while the ECOFF for piperacillin/tazobactam 8 µg/mL is, the observed MIC values

exceeded the ECOFF for piperacillin but remained below the ECOFF for the combination with tazobactam.

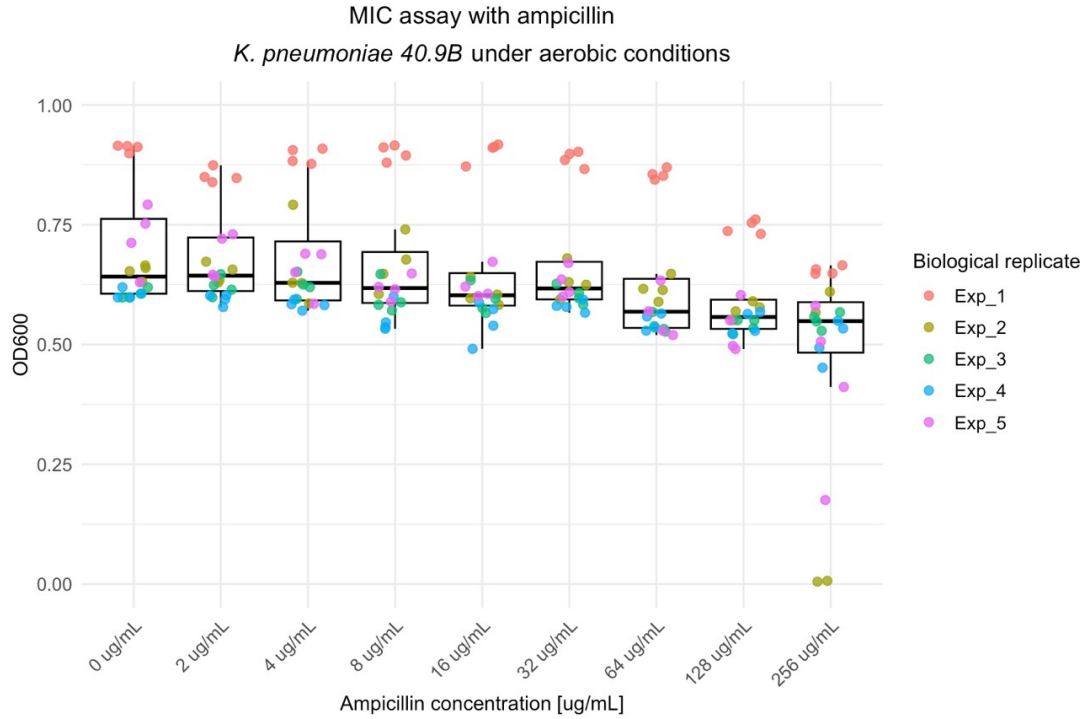

Fig. 12. MIC assay of K. pneumoniae 40.9B with ampicillin under aerobic conditions. Each color represents one biological replicate with 4 technical replicates. The strain was completely resistant to ampicillin.

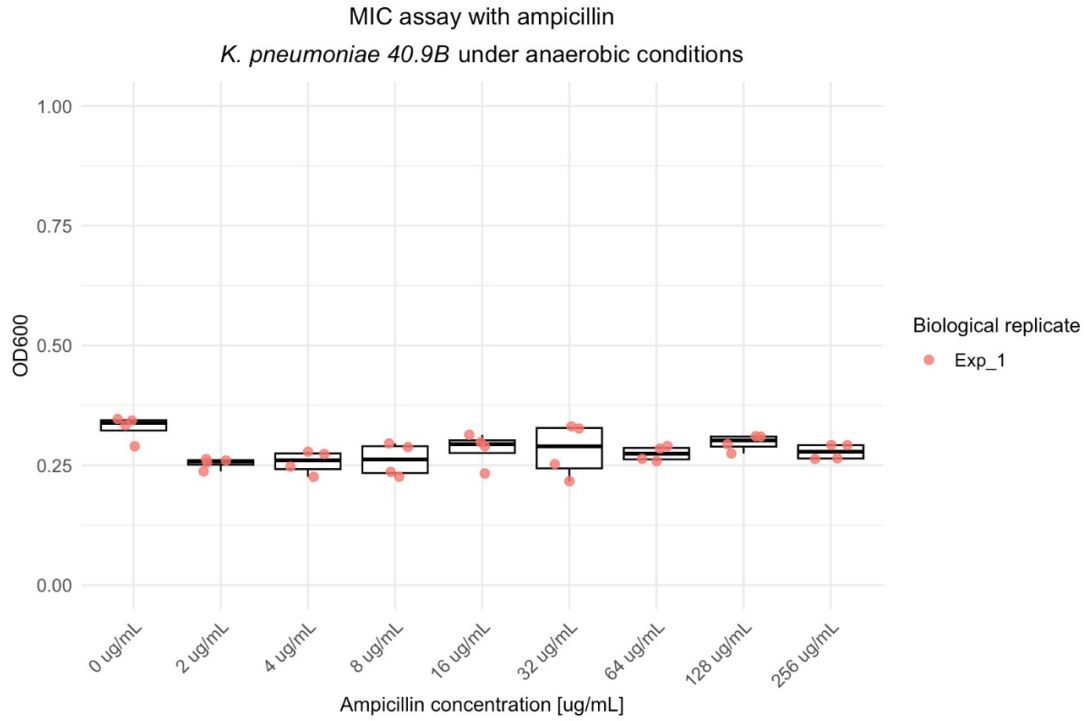

Fig. 13. MIC assay of K. pneumoniae 40.9B with ampicillin under anaerobic conditions. Individual data points represent one technical replicate. The strain was completely resistant to ampicillin.

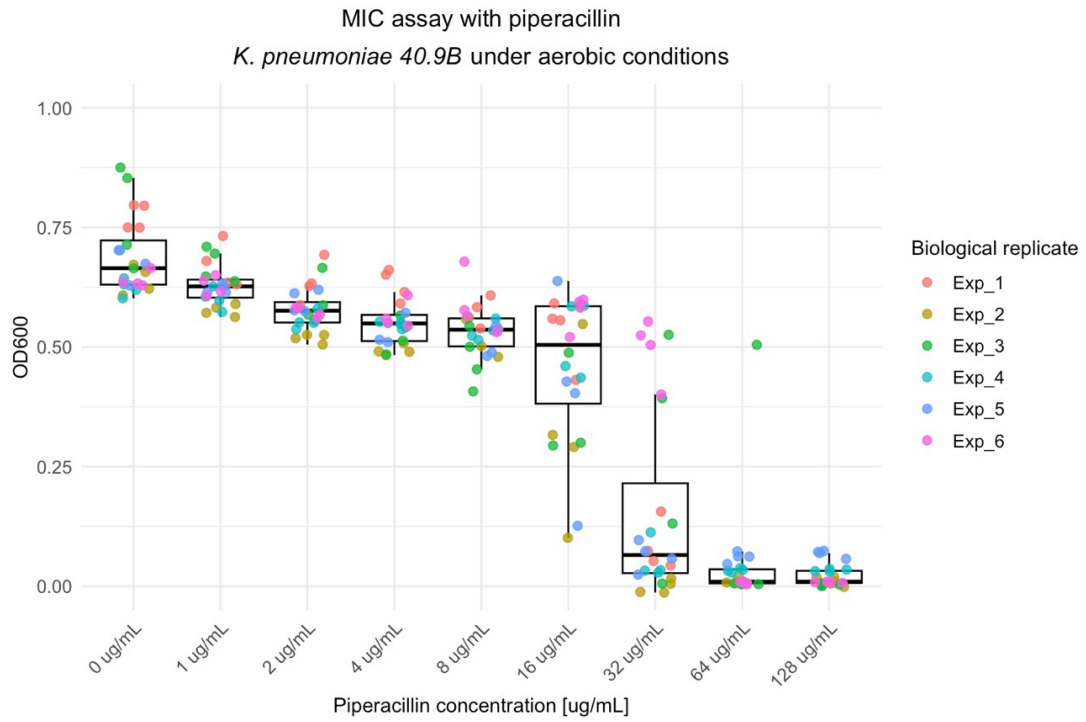

Fig. 14. MIC assay of K. pneumoniae 40.9B with piperacillin under aerobic conditions. Each color represents one biological replicate with four technical replicates. The MIC was determined to be 64 μg/mL.

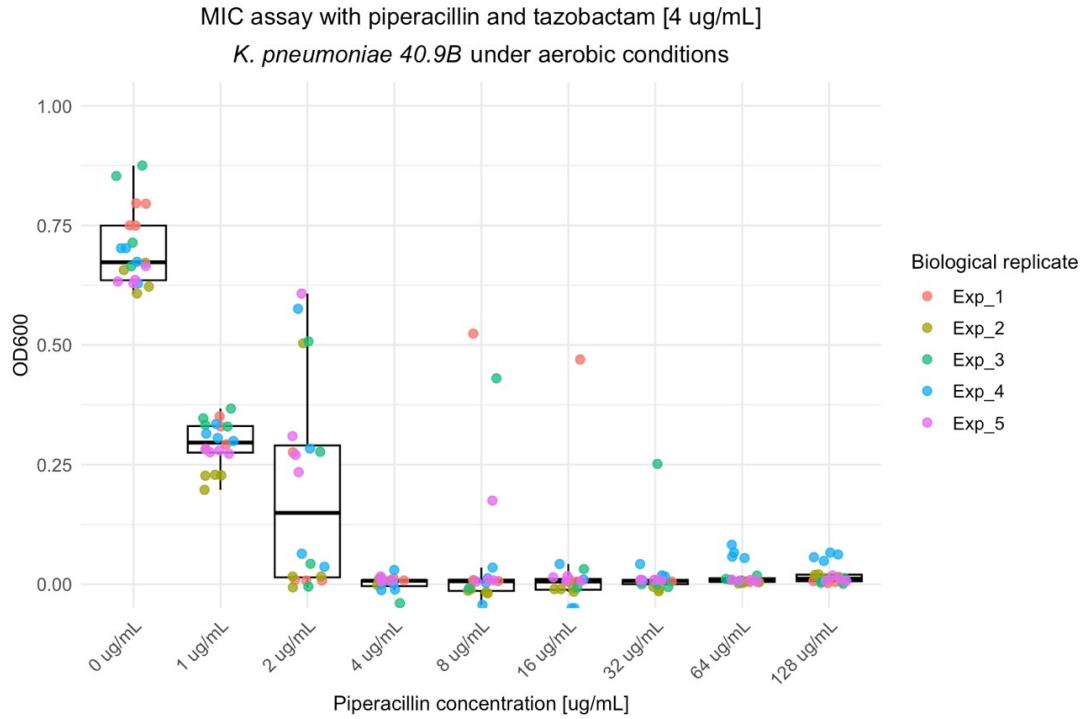

Fig. 15. MIC assay of K. pneumoniae 40.9B with piperacillin under aerobic conditions in the presence of tazobactam at a constant concentration of 4 μg/mL. Each color represents one biological replicate, including four technical replicates. The MIC was determined to be 4 μg/mL. Some outliers can be observed at concentrations of 8, 16, and 32 μg/mL, likely indicating a heterogeneous growth pattern between biological replicates.

Klebsiella pneumoniae 2.3A:

In silico analysis predicted resistance to β-lactams due to the presence of the *blaSHV-172* gene encoding a class A β-lactamase. However, susceptibility to piperacillin/tazobactam was expected, as tazobactam inhibits SHV-172 activity (Payne, D., et al., 1994). MIC assays confirmed resistance to ampicillin (MIC = 128 µg/mL) under aerobic conditions (Figs. 16), while under anaerobic conditions the MIC value increased to 256 µg/mL (Fig. 17). Resistance to piperacillin (MIC = 16 µg/mL) was also detected (Fig. 18), whereas piperacillin/tazobactam showed a MIC of 1–2 µg/mL (Fig. 19).

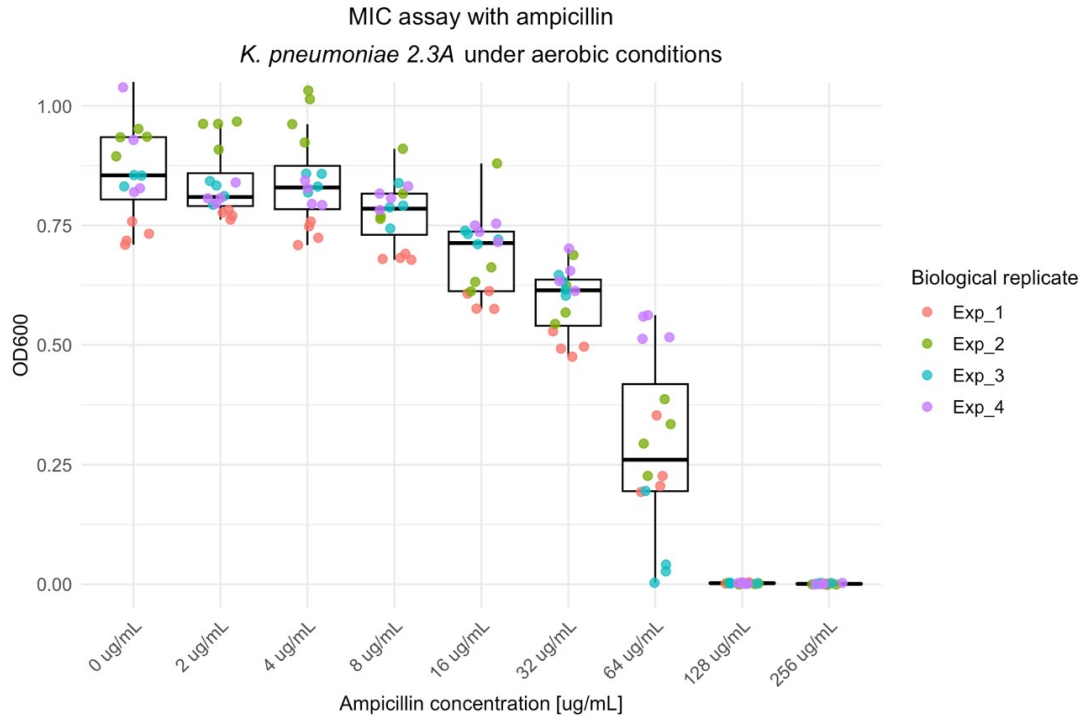

Fig. 16. MIC assay of K. pneumoniae 2.3A with ampicillin under aerobic conditions. Each color represents one biological replicate, including four technical replicates. The MIC was determined to be 128 µg/mL.

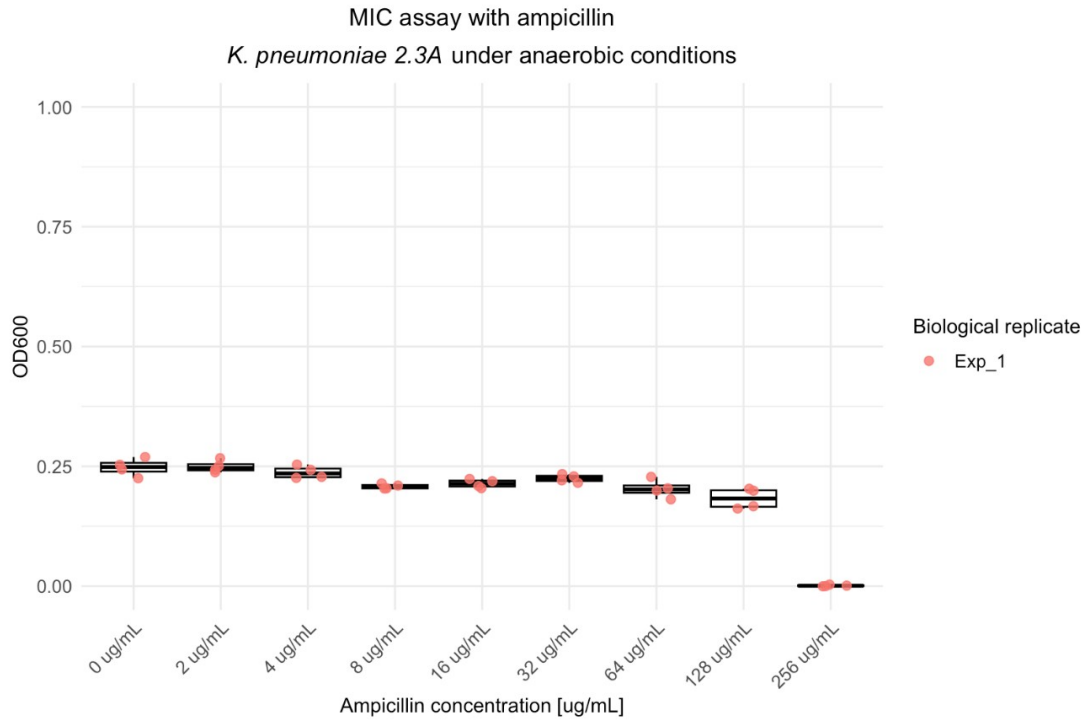

Fig. 17. MIC assay of K. pneumoniae 2.3A with ampicillin under anaerobic conditions. Each color represents one biological replicate, including four technical replicates. The MIC was determined to be 256 μg/mL.

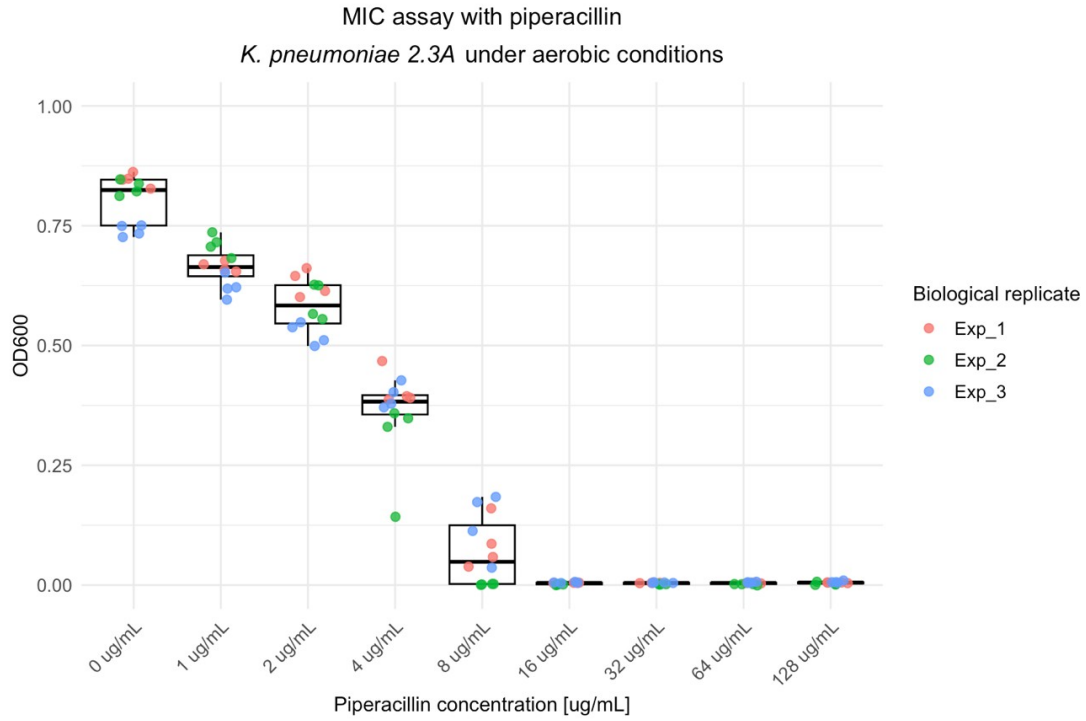

Fig. 18. MIC assay of K. pneumoniae 2.3A with piperacillin under aerobic conditions. Each color represents one biological replicate, including four technical replicates. The MIC was determined at 16 μg/mL.

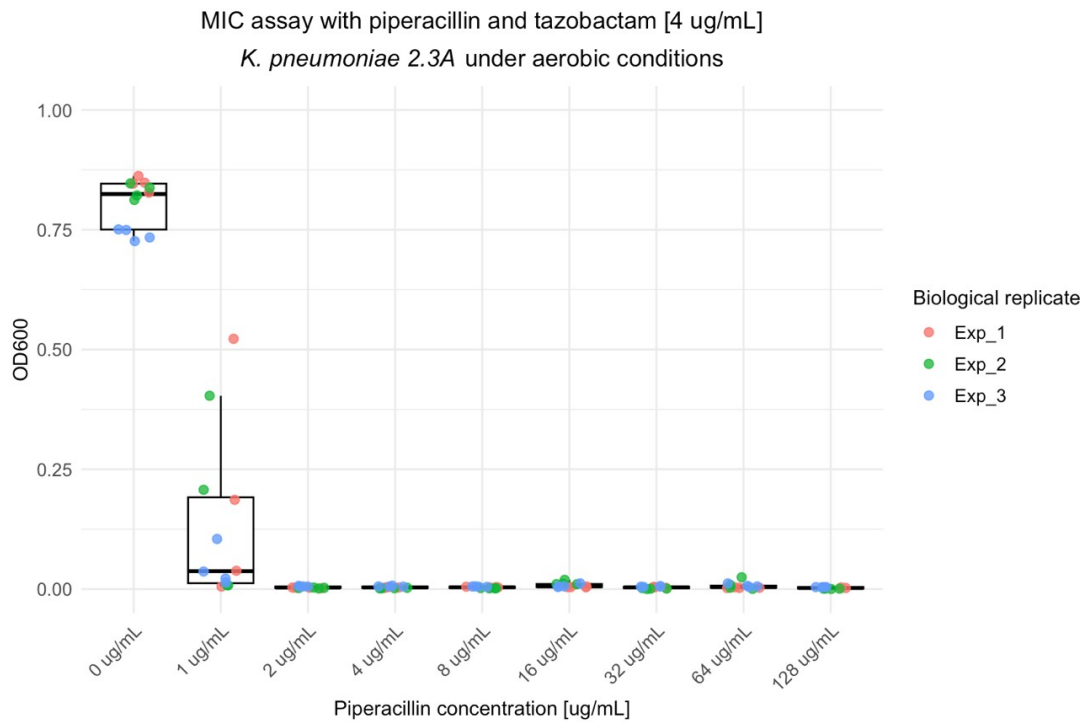

Fig. 19. MIC assay of K. pneumoniae 2.3A with piperacillin under aerobic conditions in the presence of tazobactam at a constant concentration of 4 μg/mL. Each color represents one biological replicate, including four technical replicates. The MIC was determined at 2 μg/mL.

Klebsiella michiganensis 8.3A:

This strain showed complete resistance to all tested β-lactams, including piperacillin/tazobactam, with no observable growth inhibition (Figs. 20-22). While no EUCAST breakpoints exist for this species, *K. michiganensis* is closely related to *K. oxytoca*, for which susceptibility to piperacillin/tazobactam is defined at a breakpoint of 8 µg/mL (Li, Y., et al., 2023). According to *in silico* prediction, this strain carries the *blaOXY-1-3* gene encoding an extended-spectrum β-lactamase not effectively inhibited by tazobactam (Yang, F., et al., 2022) and possesses the *oqxAB* efflux pump system, which may contribute to multidrug resistance.

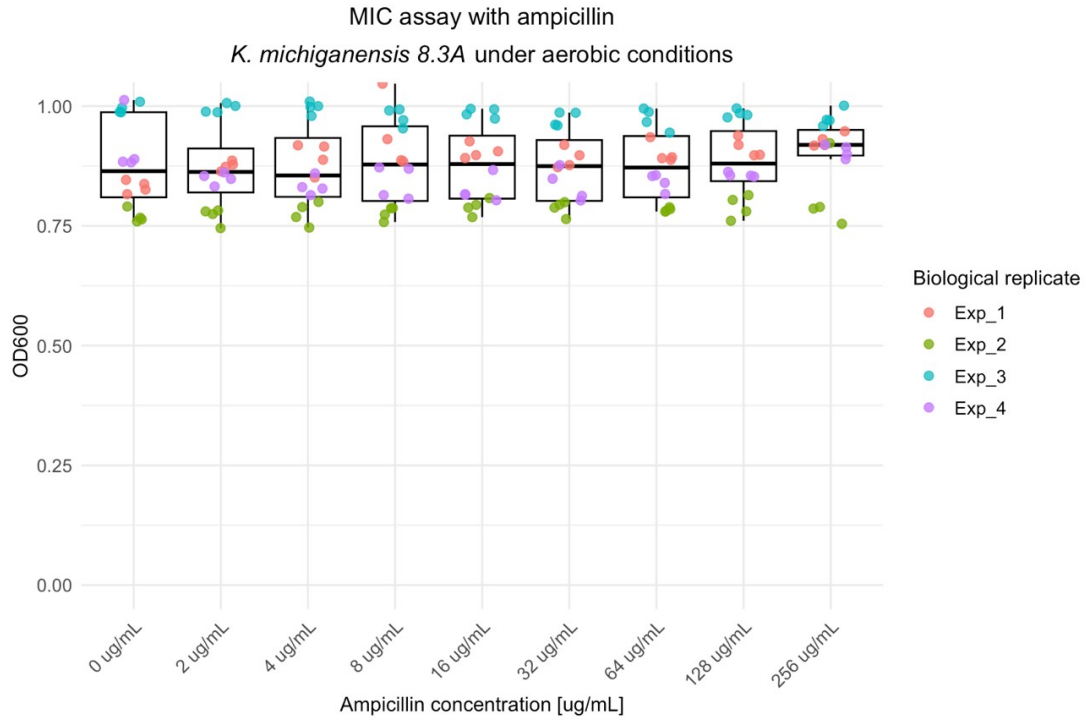

Fig. 20. MIC assay of K. michiganensis 8.3A with ampicillin under aerobic conditions. Each color represents one biological replicate, including four technical replicates. The strain was completely resistant to ampicillin.

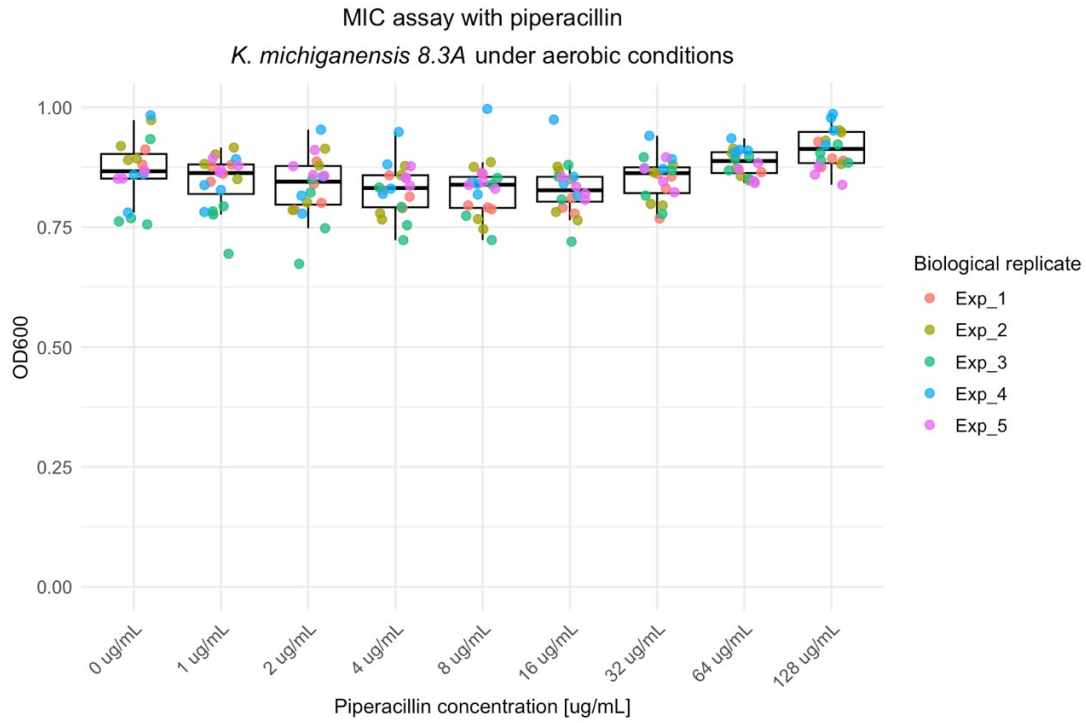

Fig. 21. MIC assay of K. michiganensis 8.3A with piperacillin under aerobic conditions. Each color represents one biological replicate, including four technical replicates. The strain was completely resistant to piperacillin.

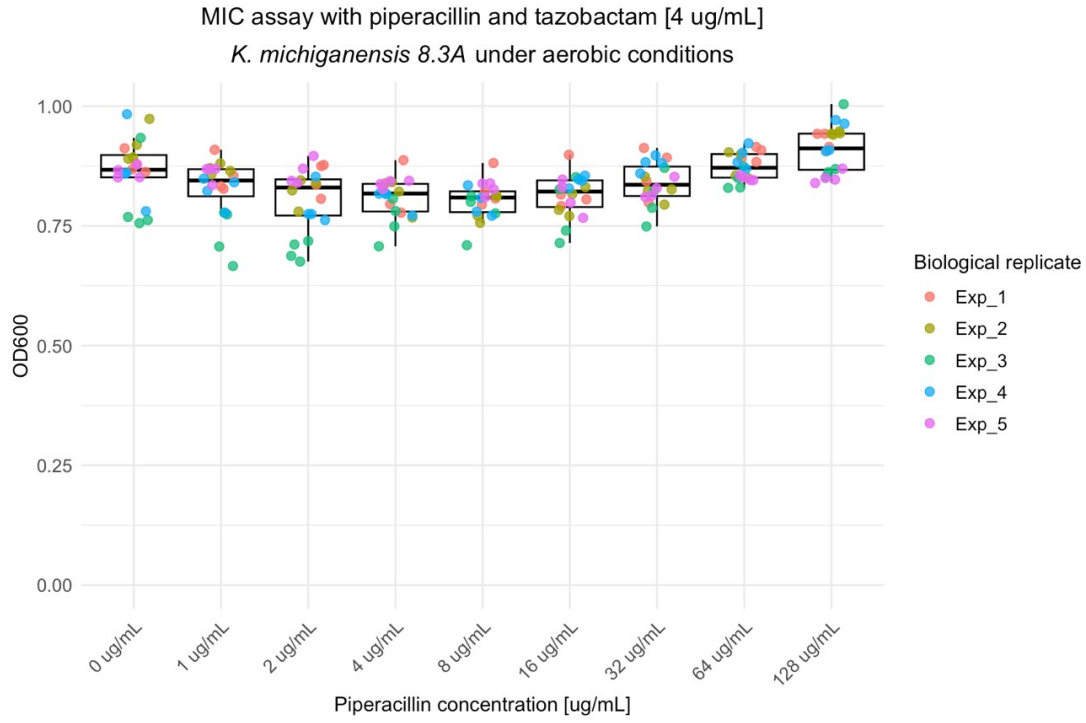

Fig. 22 MIC assay of K. michiganensis 8.3A with piperacillin under aerobic conditions in the presence of tazobactam at a constant concentration of 4 µg/mL. Each color represents one biological replicate, including four technical replicates. The strain was completely resistant to piperacillin in combination with tazobactam.

Enterococcus faecalis 5.5A:

According to EUCAST, *E. faecalis* is classified as susceptible if MIC values are ≤4 µg/mL for ampicillin, ≤8 µg/mL for piperacillin, and ≤16 µg/mL for piperacillin/tazobactam. *In silico* analysis did not show any ARGs to lactam antibiotics (Figs. 1-3). The MIC results confirmed susceptibility to ampicillin (no growth) (Fig. 23), piperacillin (MIC = 2–4 µg/mL) (Fig. 24), and piperacillin/tazobactam (MIC = 2–4 µg/mL) (Fig. 25). Notably, *E. faecalis* demonstrated limited growth capacity in MHB, with OD_{600} values rarely exceeding 0.3 after 22 hours.

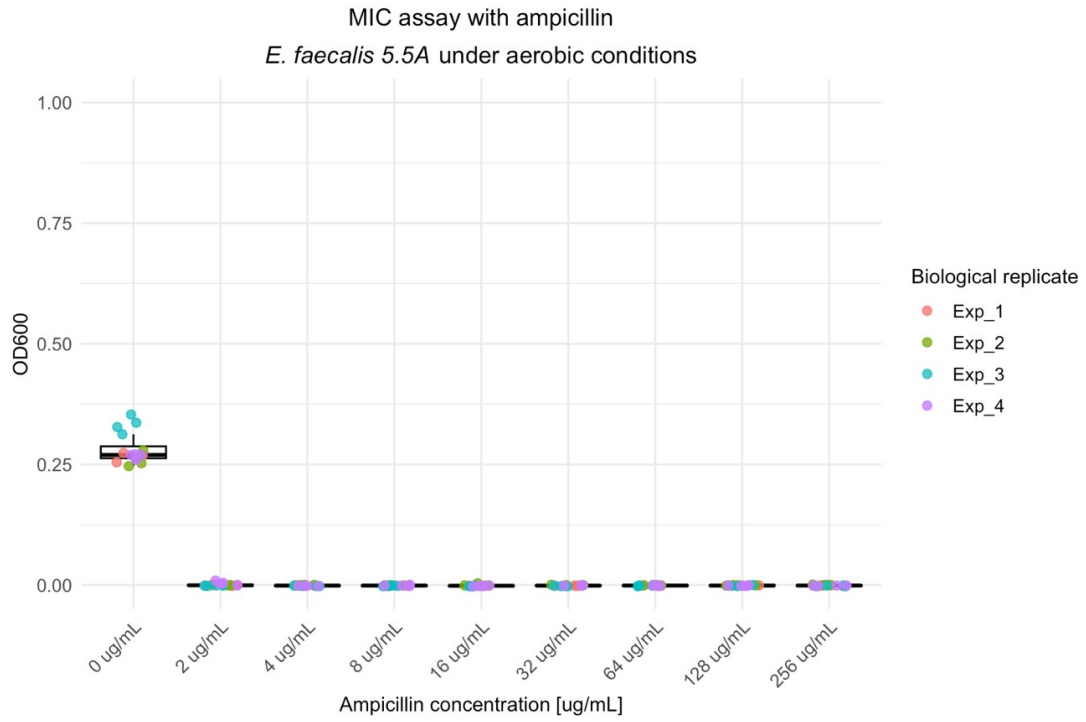

Fig. 23. MIC assay of E. faecalis 5.5A with ampicillin under aerobic conditions. Each color represents one biological replicate, including four technical replicates. The MIC was determined to be 2 µg/mL.

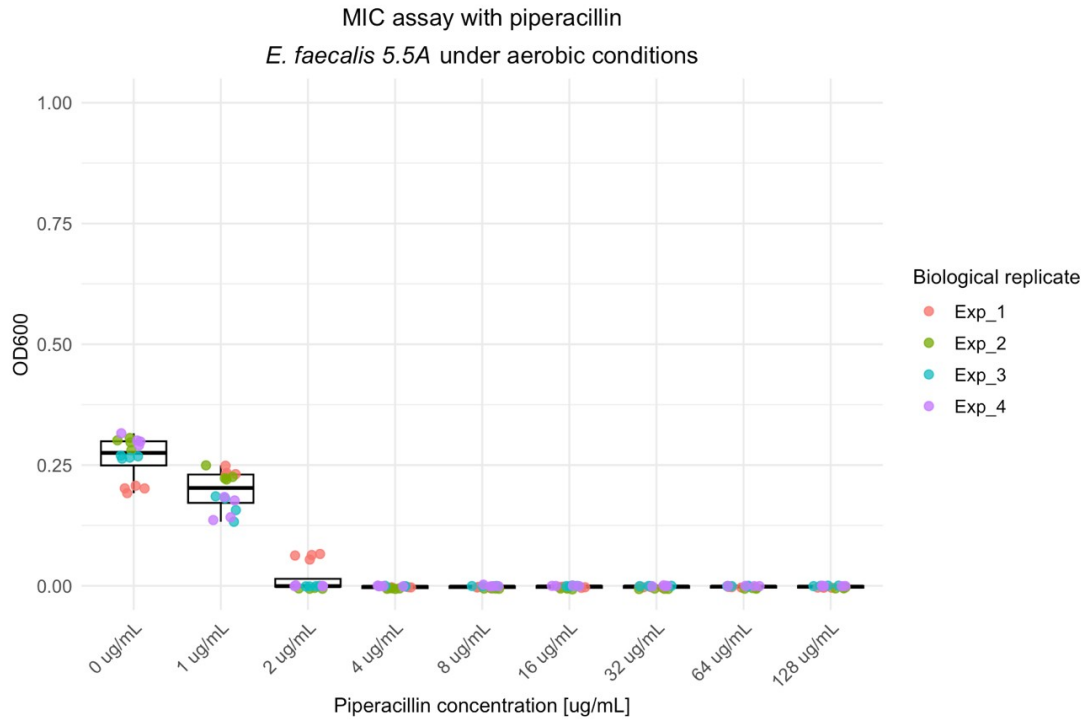

Fig. 24. MIC assay of E. faecalis 5.5A with piperacillin under aerobic conditions. Each color represents one biological replicate, including four technical replicates. The MIC was determined to be 4 μg/mL.

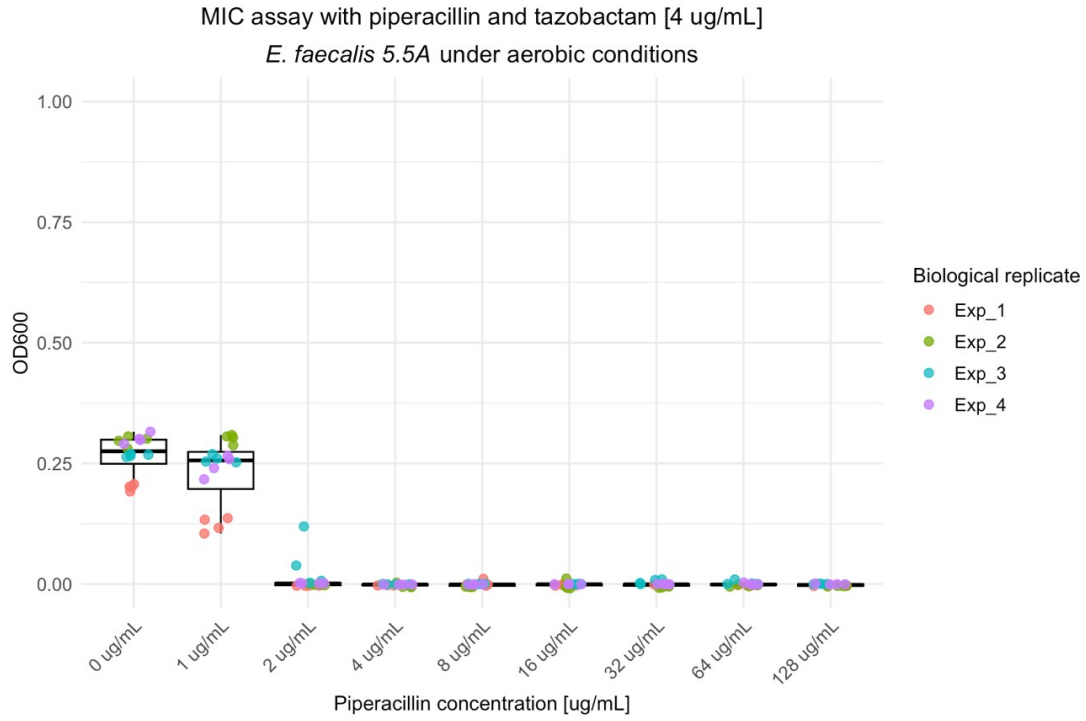

Fig. 25. MIC assay of E. faecalis 5.5A with piperacillin under aerobic conditions in the presence of tazobactam at a constant concentration of 4 μg/mL. Each color represents one biological replicate, including four technical replicates. The MIC was determined to be 4 μg/mL.

Staphylococcus epidermidis LH_NM_637:

Genomic analysis identified a complete β-lactamase operon consisting of *blaZ*, *blaR1*, and *blaI*, a cluster reported in multiple Staphylococcus species (Schwendener, S., et al., 2022), suggesting resistance to β-lactam antibiotics. However, MIC testing (Figs. 26-28) revealed a different phenotype: the strain was moderately susceptible to ampicillin (MIC = 2–8 µg/mL) and piperacillin (MIC = 4–16 µg/mL), and fully susceptible to piperacillin/tazobactam (no growth). This discrepancy may reflect differential gene expression or incomplete functionality of the *blaZ-blaR1-blaI* operon under the test conditions, as previously reported (Rocha, G., et al., 2022). EUCAST provides no ECOFF values for *S. epidermidis* for these antibiotics. Nevertheless, the MIC results indicate partial susceptibility despite the predicted genetic profile.

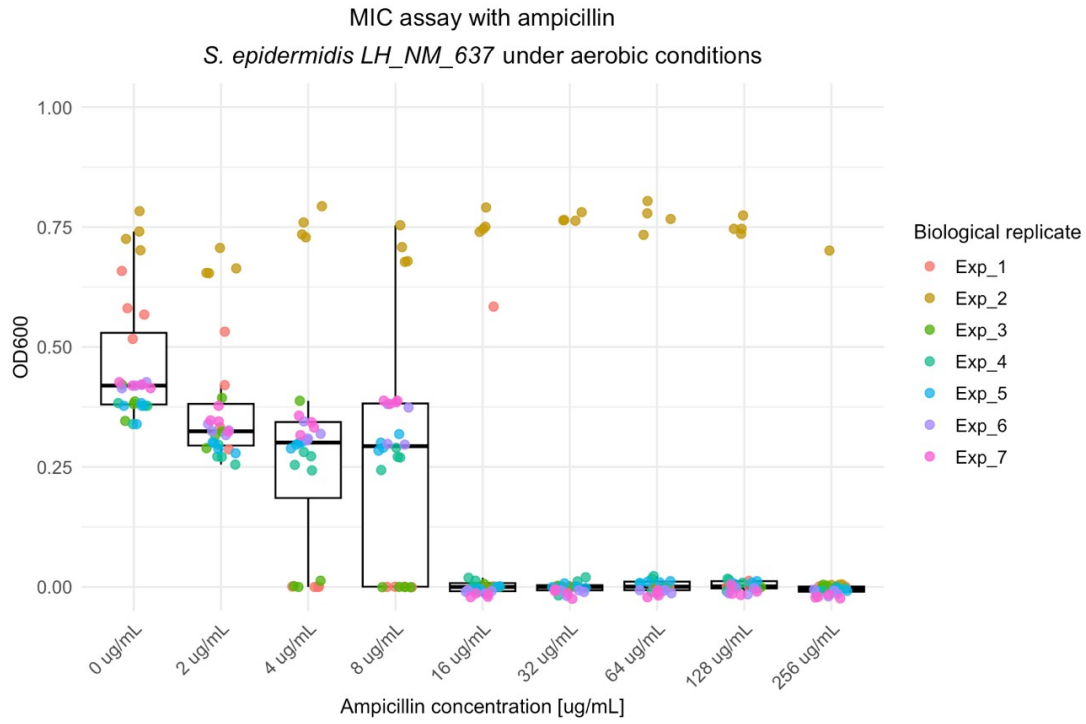

Fig. 26. MIC assay of S. epidermidis LH_NM_637 with ampicillin under aerobic conditions. Each color represents one biological replicate, including four technical replicates. The MIC was determined at 16 µg/mL ampicillin. Some outliers can be observed at all concentrations, likely indicating a heterogeneous growth pattern between biological replicates.

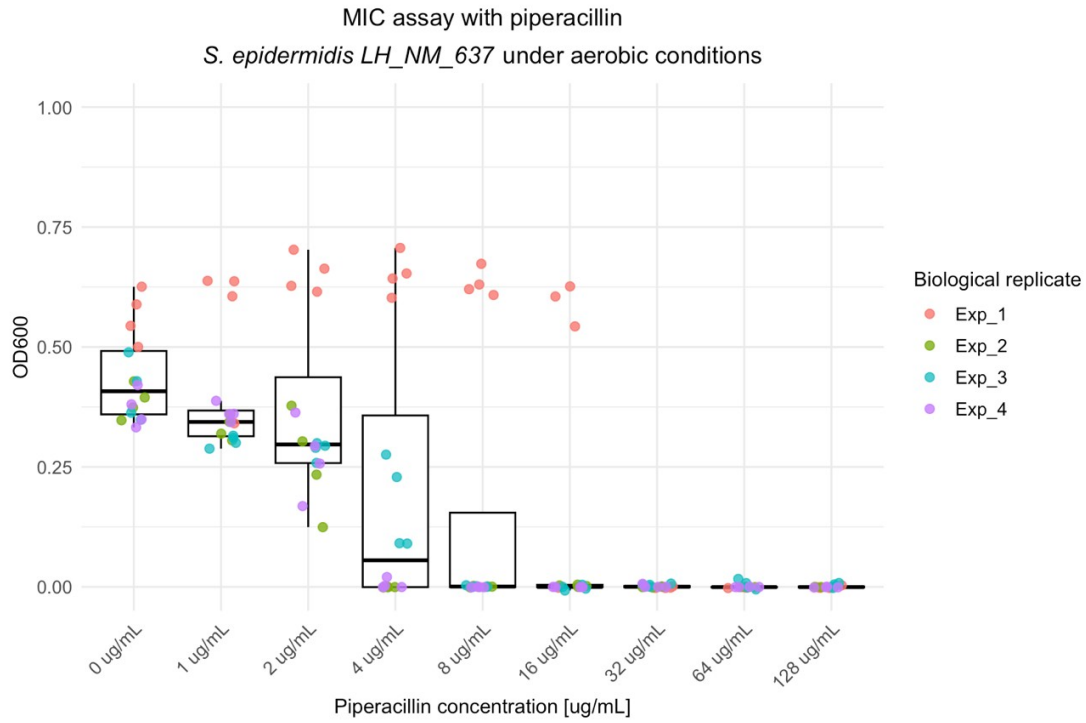

Fig. 27. MIC assay of S. epidermidis LH_NM_637 with piperacillin under aerobic conditions. Each color represents one biological replicate, including four technical replicates. The MIC was determined to be 8 μg/mL. Some outliers can be observed at concentrations of 8 and 16 μg/mL, likely indicating a heterogeneous growth pattern between biological replicates.

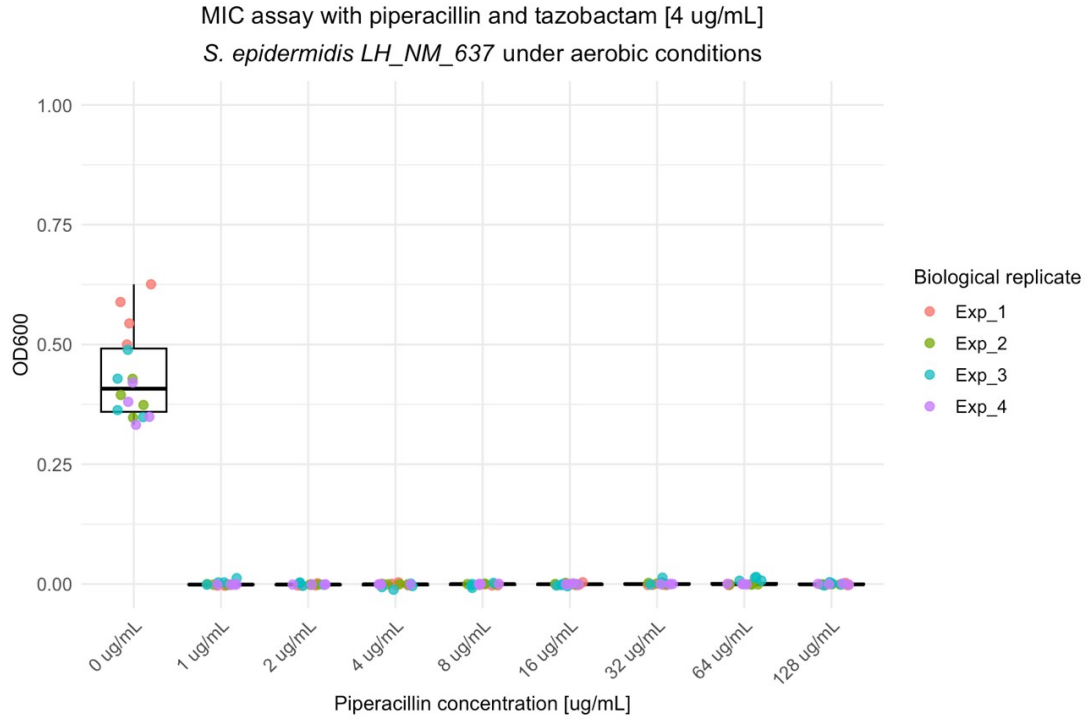

Fig. 28. MIC assay of S. epidermidis LH_NM_637 with piperacillin under aerobic conditions in the presence of tazobactam at a constant concentration of 4 μg/mL. Each color represents one biological replicate, including four technical replicates. The MIC was determined to be 1 μg/mL.

Staphylococcus epidermidis 8.2A:

As *S. epidermidis 8.2A* was included at a later stage of the study, MIC testing was performed only with ampicillin. As mentioned previously, EUCAST provides no ECOFFs for these antibiotics. It is well established that *Staphylococci* frequently carry β-lactam resistance genes (Samarra, A. et al., 2025). Consistent with this, genome analysis revealed the presence of a complete *blaZ* operon (Figs. 1-3), and *in vitro* analysis confirmed resistance to ampicillin, with a MIC value of 128 µg/mL (Fig. 29).

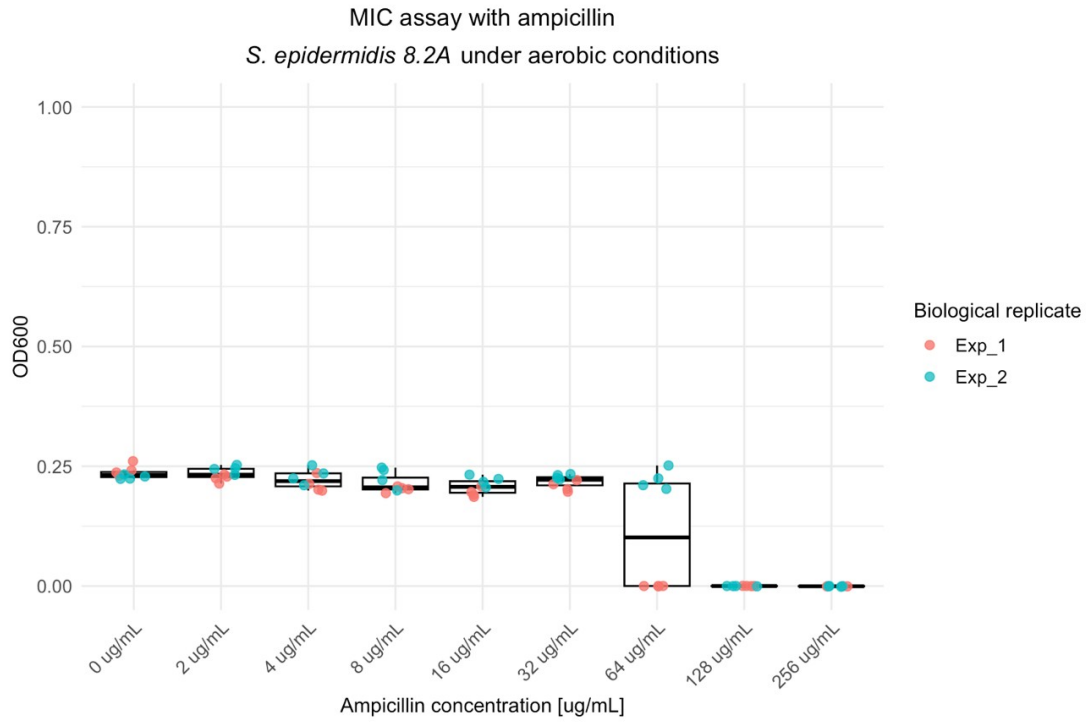

Fig. 29. MIC assay of S. epidermidis 8.2A with ampicillin under aerobic conditions. Each color represents one biological replicate, including four technical replicates. The MIC was determined to be 128 µg/mL.

Lactobacillus spp.:

Lactobacillus plantarum 37.6A:

In silico analysis did not identify any ARGs encoded in *Lactobacillus plantarum 37.6A* and *Lactobacillus fermentum 10.2E* suggesting that they are completely susceptible to β-lactam antibiotics. EUCAST does not provide ECOFF values for this species for ampicillin, piperacillin, and piperacillin/tazobactam. MIC assays were consistent with the genomic predictions, as bacterial growth was inhibited in the presence of ampicillin even at the lowest concentration measured, demonstrating susceptibility (Figs. 30-31).

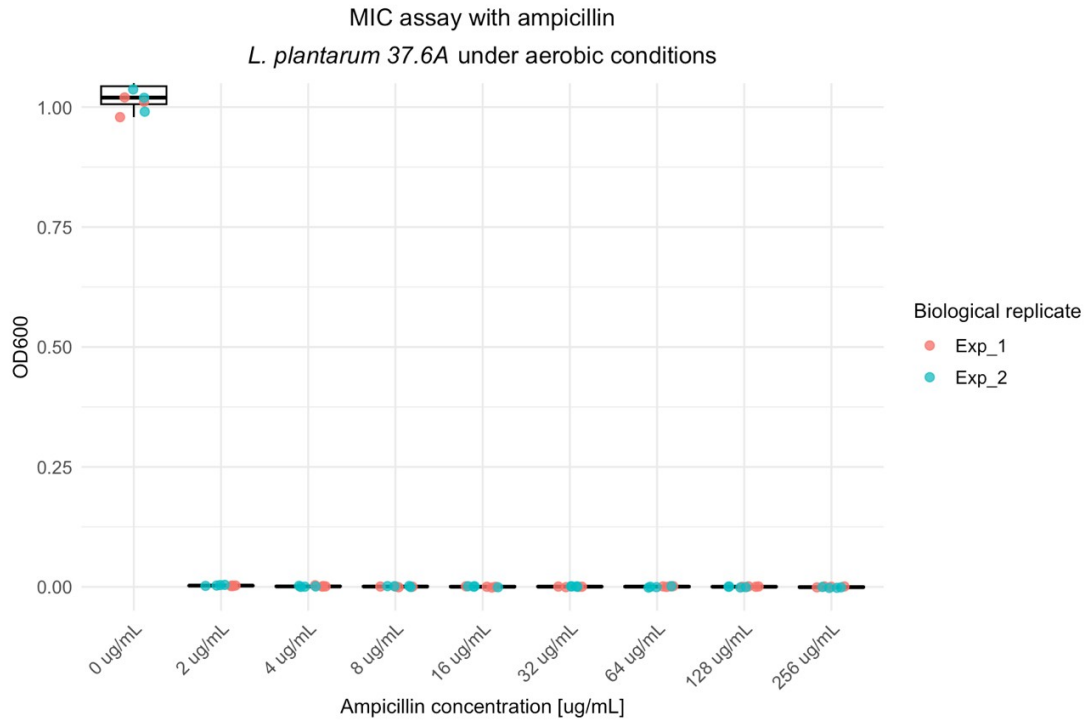

Fig. 30. MIC assay of L. plantarum 37.6A with ampicillin under aerobic conditions. Each color represents one biological replicate, including four technical replicates. The MIC was determined to be 2 μg/mL.

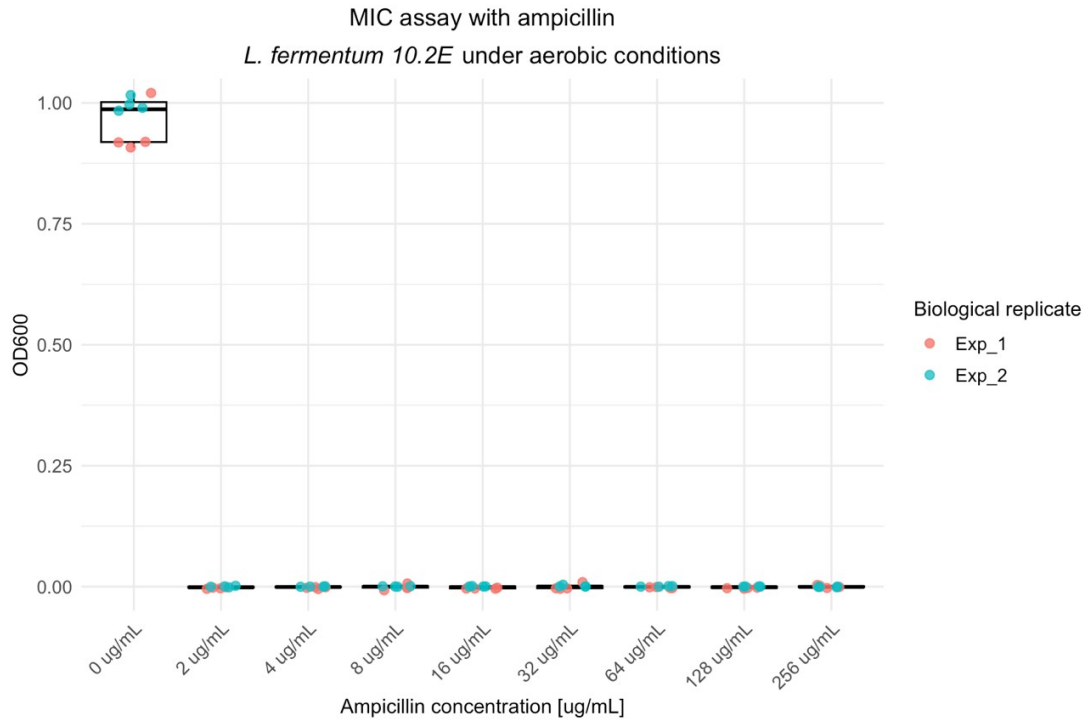

Fig. 31. MIC assay of L. fermentum 10.2E with ampicillin under aerobic conditions. Each color represents one biological replicate, including four technical replicates. The MIC was determined to be 2 μg/mL.

Bifidobacterium spp.:

Bifidobacterium bifidum WS111, Bifidobacterium breve WS23, Bifidobacterium infantis WS13, and *Bifidobacterium pseudocatenulatum WS19* were all analysed for the presence of ARGs. No β-lactam resistance genes were detected *in silico* in any of these strains, suggesting susceptibility to ampicillin, piperacillin, and piperacillin/tazobactam. EUCAST does not provide ECOFF values for *Bifidobacterium* species, likely because those bacteria are considered non-pathogenic commensals and are not typically targets of antibiotic therapy. All strains demonstrated consistent susceptibility to ampicillin, with MIC values of 2 µg/mL.

A

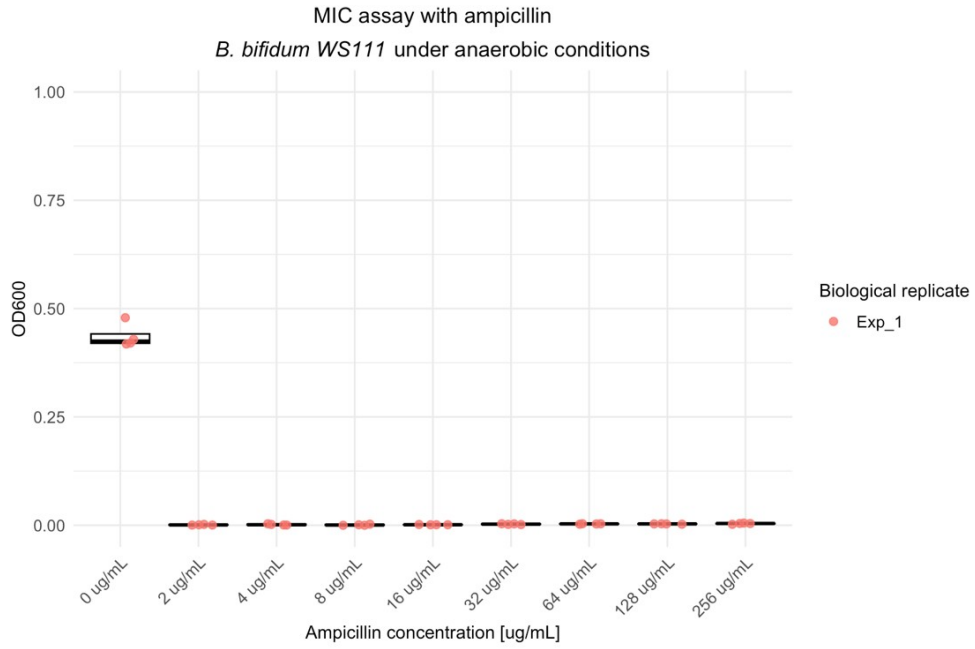

B

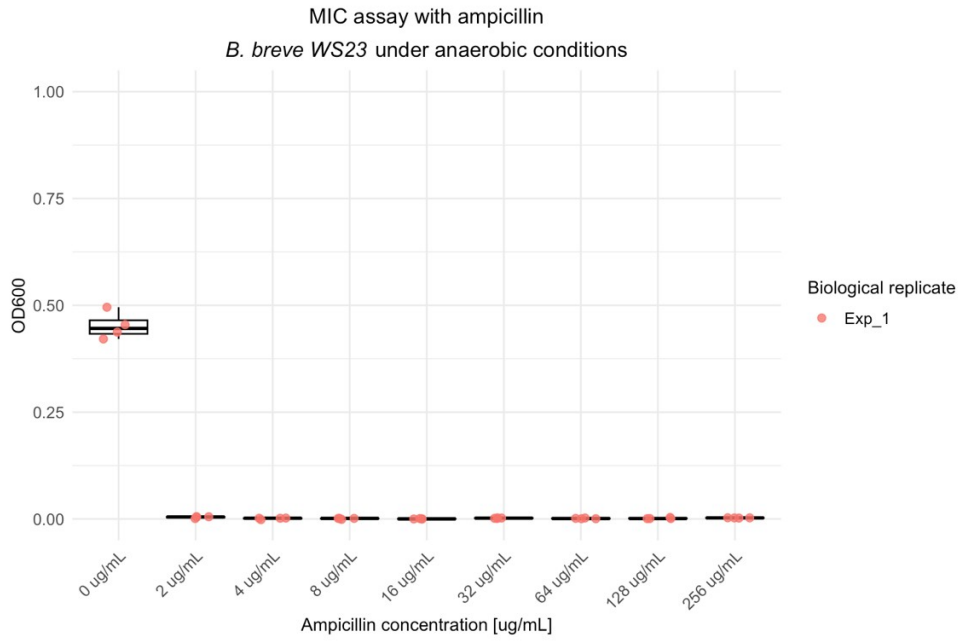

C

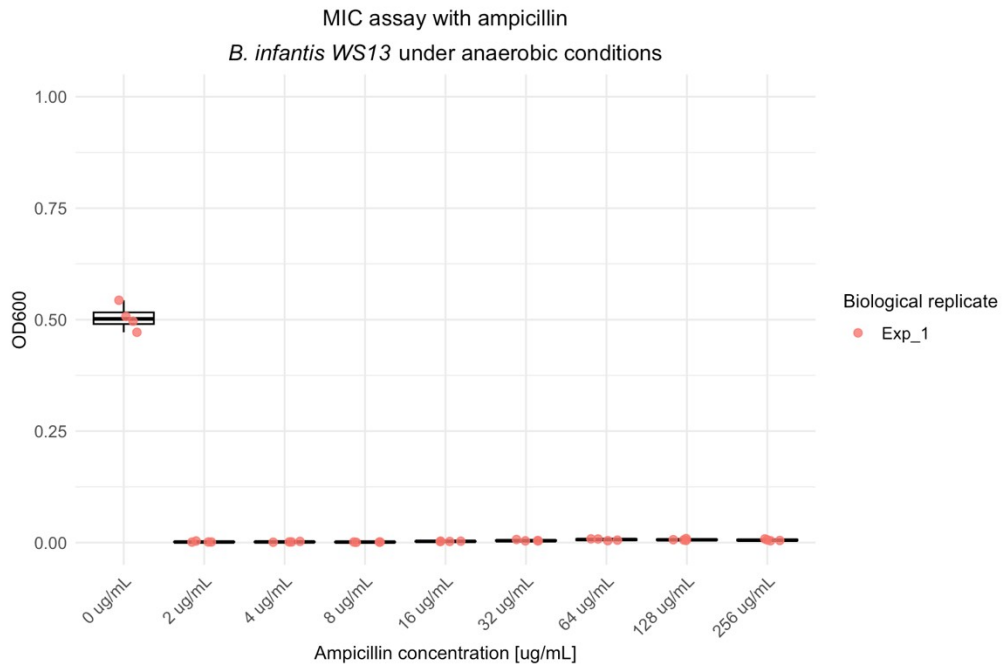

D

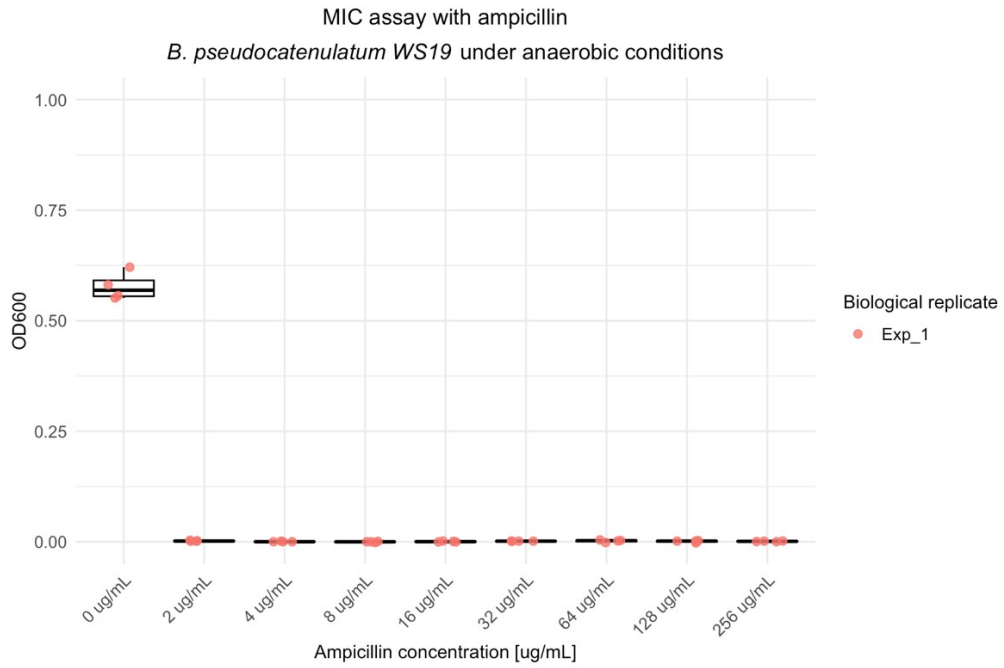

Fig. 32. MIC assay of Bifidobacterium strains with ampicillin. Individual data points represent one technical replicate within the experiment. ***A****) B. bifidum WS111;* ***B****) B. breve WS23;* ***C****) B. infantis WS13;* ***D****) B. pseudocatenulatum WS19. MIC values were determined to be 2 μg/mL for all strains.*

β-lactam susceptibility generally matched genomic predictions, with resistant strains carrying β-lactamase genes and susceptible strains lacking them. Tazobactam effectively reduced resistance in all but one strain. In some cases, exceptions and differences between genotype and phenotype were observed. Overall, the results highlight both predictable resistance patterns and strain-specific variability (Table 8).

Strain	**ARGs**	**Growth conditions**	**MIC [µg/mL] Ampicillin**	**MIC [µg/mL] Piperacillin**	**MIC [µg/mL] Piperacillin + Tazobactam**
E. coli 13.3C	*ampC, ampH, (CRP, acrABEFS, evgAS, gadWX, marA, mdtEF, H-NS)*	Aerobic	8	2	2
		Anaerobic	2*	-	-
E. coli 14.3B	*TEM-1, ampC1, (CRP, acrABEF, evgAS, gadWX, marA, mdtEF, H-NS)*	Aerobic	>256	>128	2
		Anaerobic	>256	-	-
K. pneumoniae 40.9B	*OXA-10, SHV-187, (OmpK37, acrA)*	Aerobic	256	64	4*
		Anaerobic	>256	-	-
K. pneumoniae 2.3A	*SHV-172, (OmpK37, acrA)*	Aerobic	128	16	2
		Anaerobic	256	-	-
K. michiganensis 8.3A	*OXY-1-3*	Aerobic	>256	>128	>128
S. epidermidis LH_NM_637	*blaZ*	Aerobic	16*	8*	1
S. epidermidis 8.2A	*blaZ, mecA*	Aerobic	128	-	-
E. faecalis 5.5A	-	Aerobic	2	4	4
L. fermentum 10.2E	-	Aerobic	2	-	-
L. plantarum 37.6A	-	Aerobic	2	-	-
B. bifidum WS111	-	Anaerobic	2	-	-
B. breve WS23	-	Anaerobic	2	-	-
B. infantis WS13	-	Anaerobic	2	-	-
B. pseudocatenulatum WS19	-	Anaerobic	2	-	-

Table 8. Summary of MIC assay results for β-lactam antibiotics (ampicillin, piperacillin, piperacillin/tazobactam). "" indicates that outliers were detected in some replicates at higher antibiotic concentrations, likely indicating heterogeneous growth pattern among biological replicates. "-" indicates that no measurements were performed. In the ARGs column, "-" indicates that no ARGs were detected in silico. ARGs shown in parentheses represent genes associated with multidrug resistance mechanisms (e.g. multidrug efflux pump systems).*

MIC of aminoglycoside: gentamicin

Escherichia coli 13.3C:

Focusing on aminoglycosides, specifically gentamicin in this study, *in silico* predictions did not identify any ARGs associated with this class of antibiotics (Figs. 1-3). It is important to note that gentamicin has an oxygen-dependent mechanism of action, suggesting reduced activity under anaerobic conditions. MIC assays results confirmed these predictions (Fig. 33). Despite lacking ARGs specific to aminoglycosides, *E. coli 13.3C* was resistant to gentamicin under aerobic conditions, as the observed MIC value was 4 µg/mL, exceeding the EUCAST threshold of 2 µg/mL. Moreover, resistance increased under anoxic conditions (MIC = 16 µg/mL), supporting the reduced effectiveness of gentamicin in the absence of oxygen (Fig. 34). According to *in silico* predictions, this strain carries several ARGs associated with multidrug efflux pumps, which may be induced in the presence of the antibiotic.

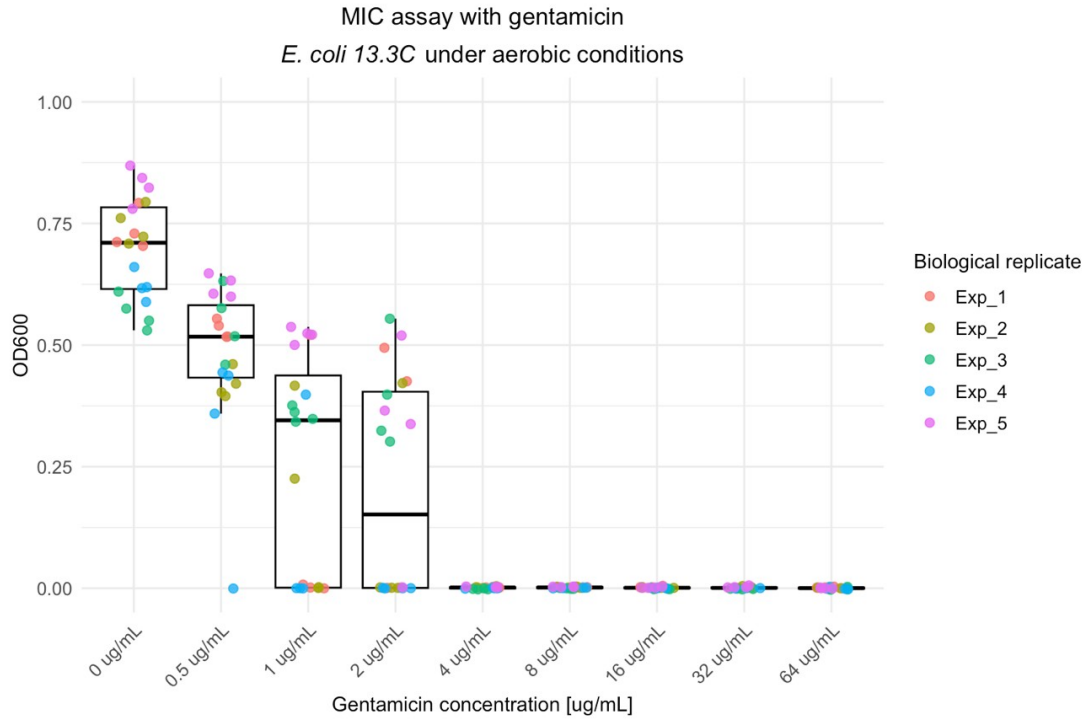

Fig. 33. MIC assay of E. coli 13.3C with gentamicin under aerobic conditions. Each color represents one biological replicate with four technical replicates. The MIC was determined to be 4 µg/mL.

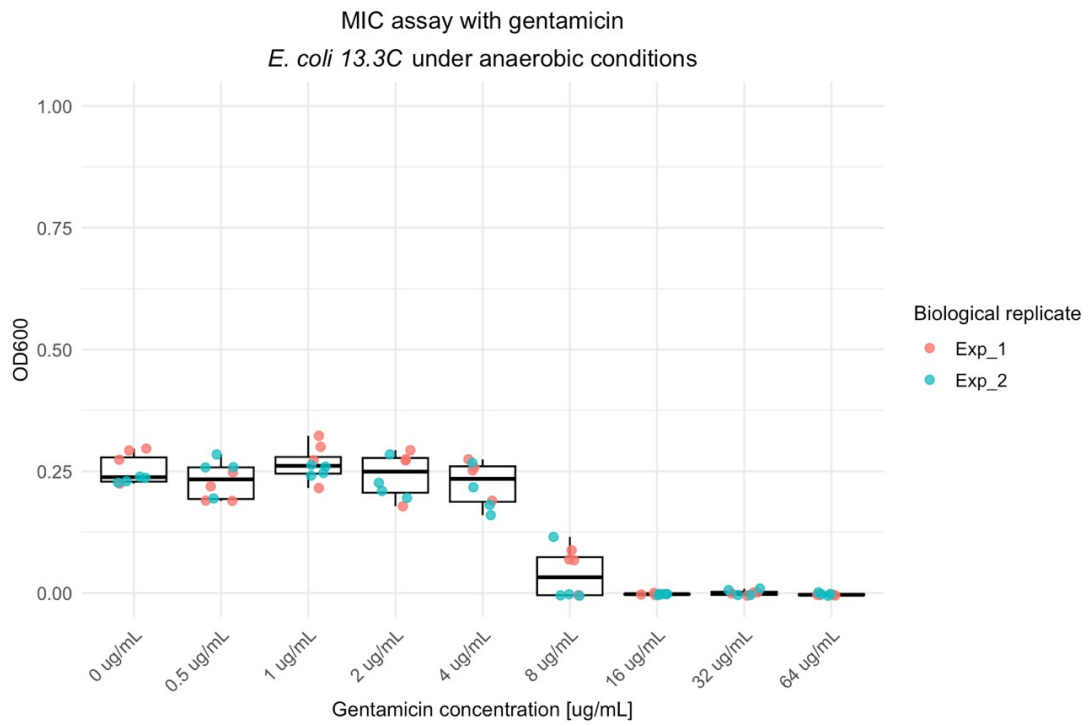

Fig. 34. MIC assay of E. coli 13.3C with gentamicin under anaerobic conditions. Each color represents one biological replicate with four technical replicates. The MIC is determined to be 16 µg/mL.

Escherichia coli 14.3B:

Analysis of MIC assays of this strain led to a similar conclusion. *E. coli 14.3B* was resistant to gentamicin under both aerobic and anaerobic conditions (Figs. 35-36), with increased resistance (higher MIC values) in an anoxic environment. *In silico* analysis identified aminoglycoside-related genes such as *aph(3")-Ib and aph(6)-Id*, encoding aminoglycoside phosphotransferase. However, these enzymes are primarily specific to streptomycin and are not expected to inactivate gentamicin based on the chemical structure (Zárate, S., et al., 2018). In addition, this strain encodes multiple ARGs associated with multidrug efflux systems, which may contribute to the observed phenotype under antibiotic exposure.

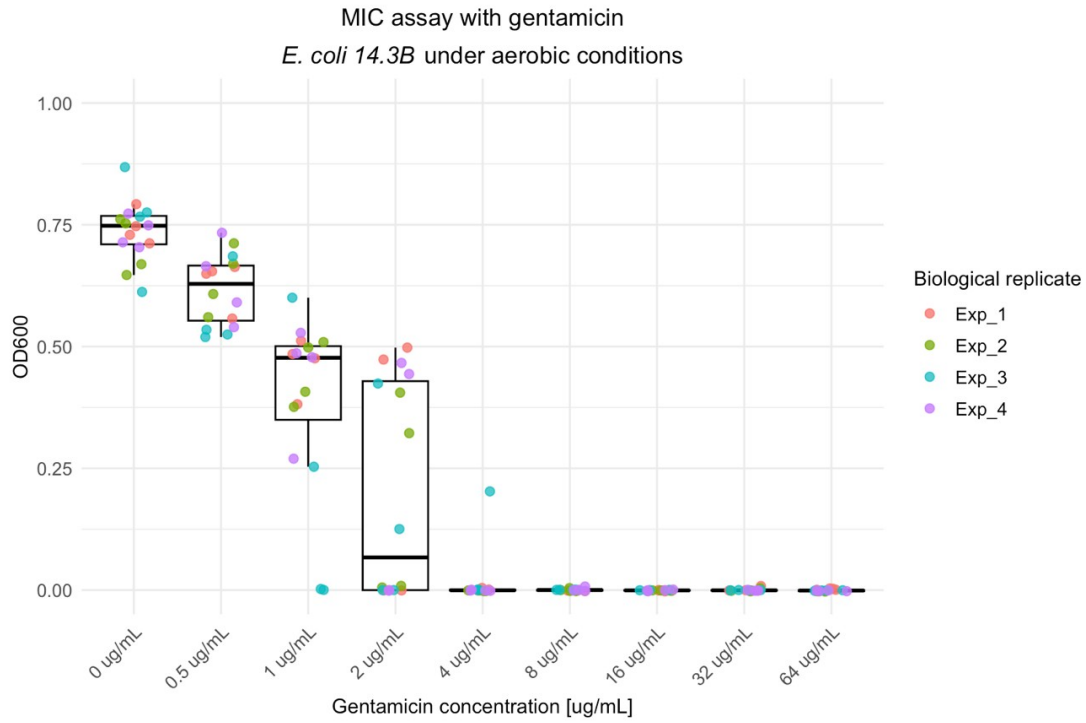

Fig. 35. MIC assay of E. coli 14.3B with gentamicin under aerobic conditions. Each color represents one biological replicate with four technical replicates. The MIC was determined to be 4 μg/mL.

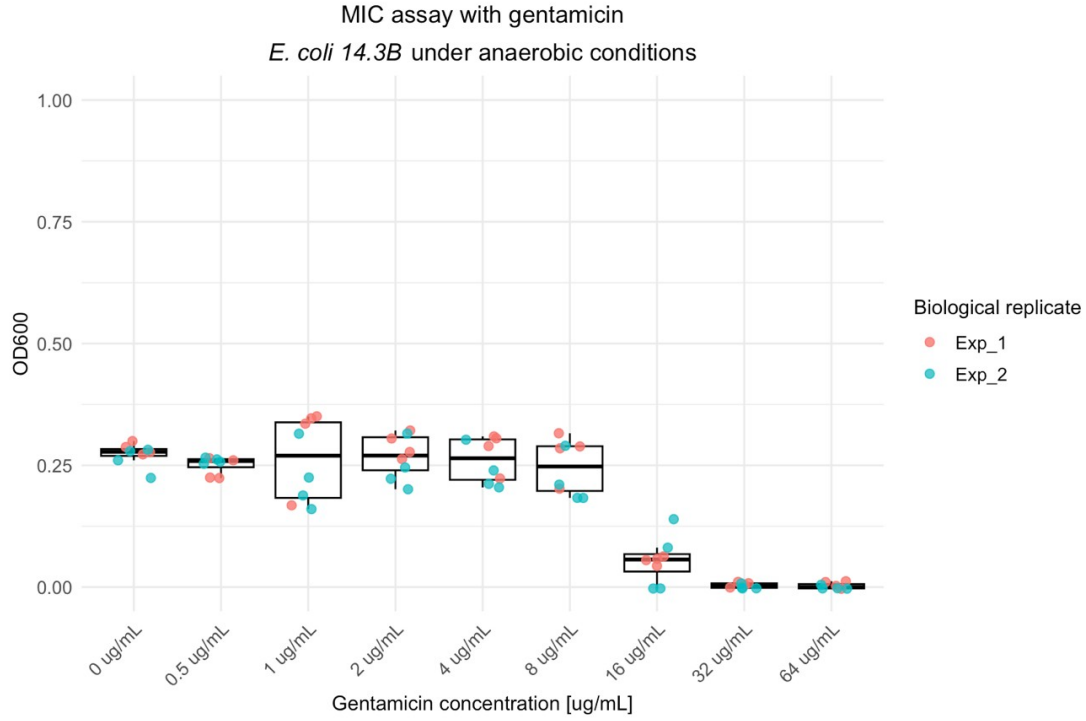

Fig. 36. MIC assay of E. coli 14.3B with gentamicin under anaerobic conditions. Each color represents one biological replicate with four technical replicates. The MIC is determined to be 32 μg/mL.

Klebsiella pneumoniae 40.9B:

According to EUCAST, wild-type *K. pneumoniae* strains have an ECOFF for gentamicin of 2 µg/mL. No gentamicin resistance genes were detected *in silico*, and consistent with this, no growth was observed in MIC assays under aerobic conditions (Figs. 37-38). However, MIC values increased in the absence of oxygen (MIC = 8 µg/mL), further supporting the oxygen-dependent activity of gentamicin.

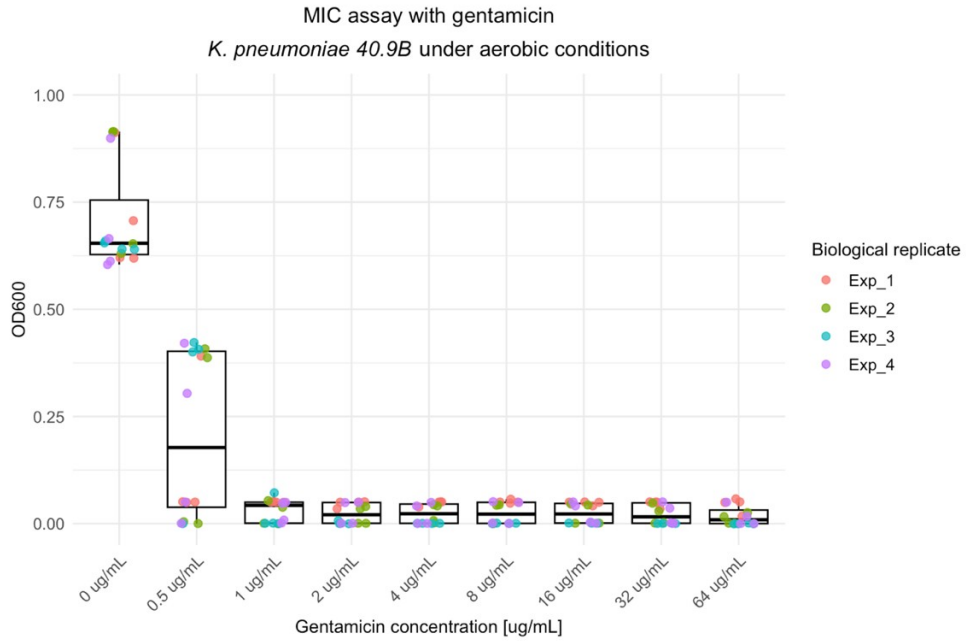

Fig. 37. MIC assay of K. pneumoniae 40.9B with gentamicin under aerobic conditions. Each color represents one biological replicate with four technical replicates. The MIC was determined to be 1 µg/mL.

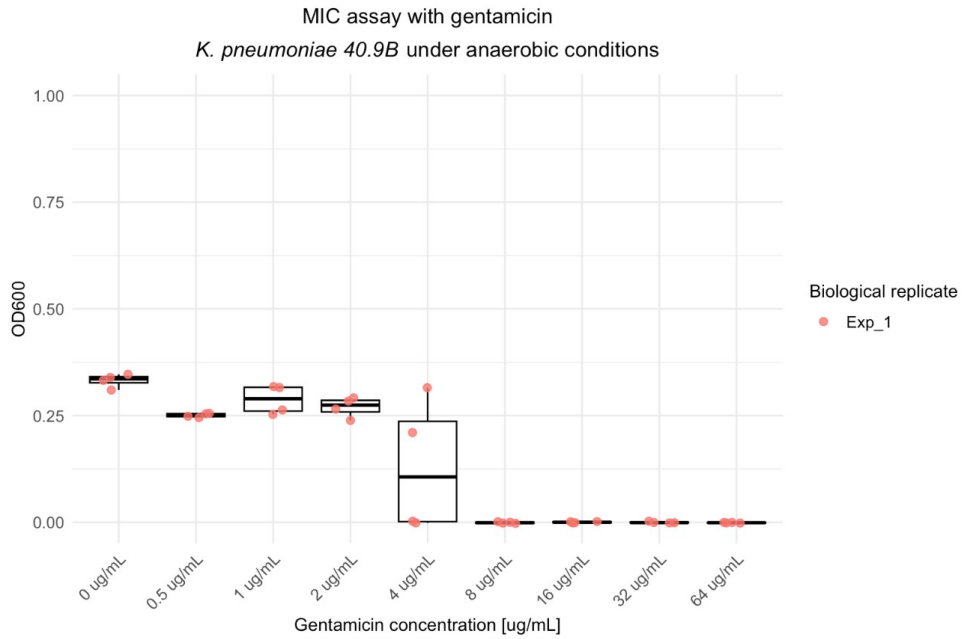

Fig. 38. MIC assay of K. pneumoniae 40.9B with gentamicin under anaerobic conditions. Each color represents one biological replicate with four technical replicates. The MIC was determined to be 8 µg/mL.

Klebsiella pneumoniae 2.3A:

The strain was susceptible to gentamicin (MIC = 1–2 µg/mL), consistent with the absence of gentamicin-specific resistance genes (Fig. 39), despite carrying the aminoglycoside resistance genes *aph(6)-Id* and *aph(3")-Ib,* which encode aminoglycoside O-phosphotransferases typically conferring resistance to streptomycin (Collins, A., et al., 2007). Notably, while most MIC values across technical replicates were 1 µg/mL, some variation was observed in two of the biological replicates, where MIC values reached 4 µg/mL. Under anaerobic conditions, similar to the other *Klebsiella pneumoniae* strain, resistance increased, with MIC values at 8 µg/mL (Fig. 40).

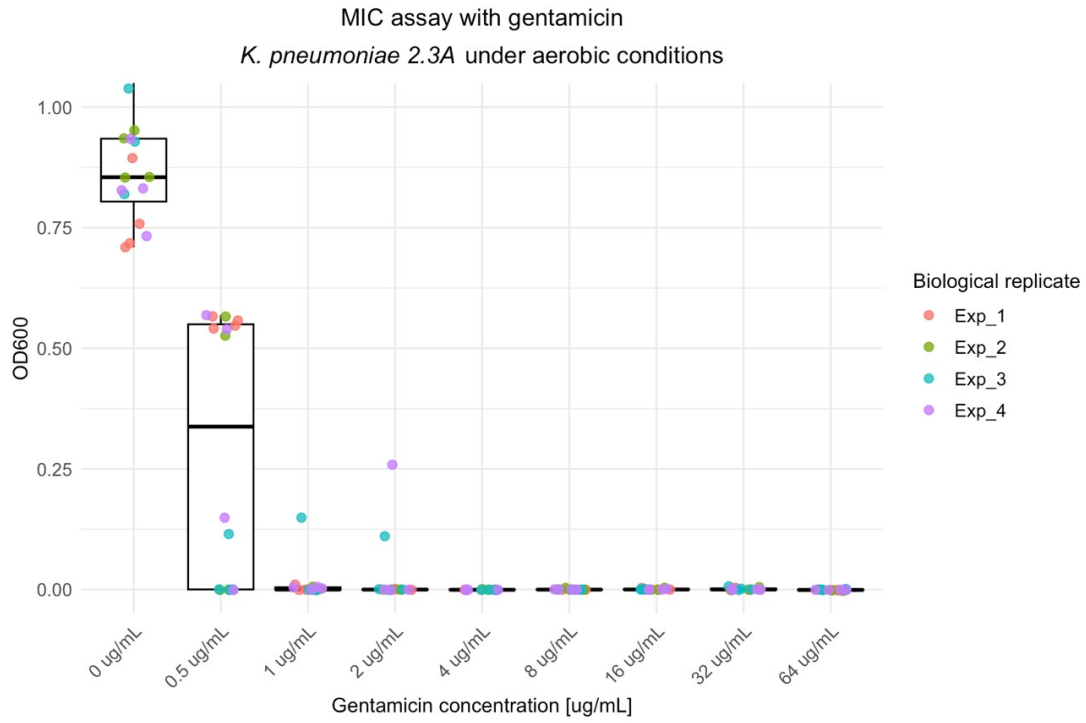

Fig. 39. MIC assay of K. pneumoniae 2.3A with gentamicin under aerobic conditions. Each color represents one biological replicate with four technical replicates. The MIC was determined to be 1 µg/mL. Some outliers can be observed at concentrations of 1 and 2 µg/mL, likely indicating a heterogeneous pattern within biological replicates.

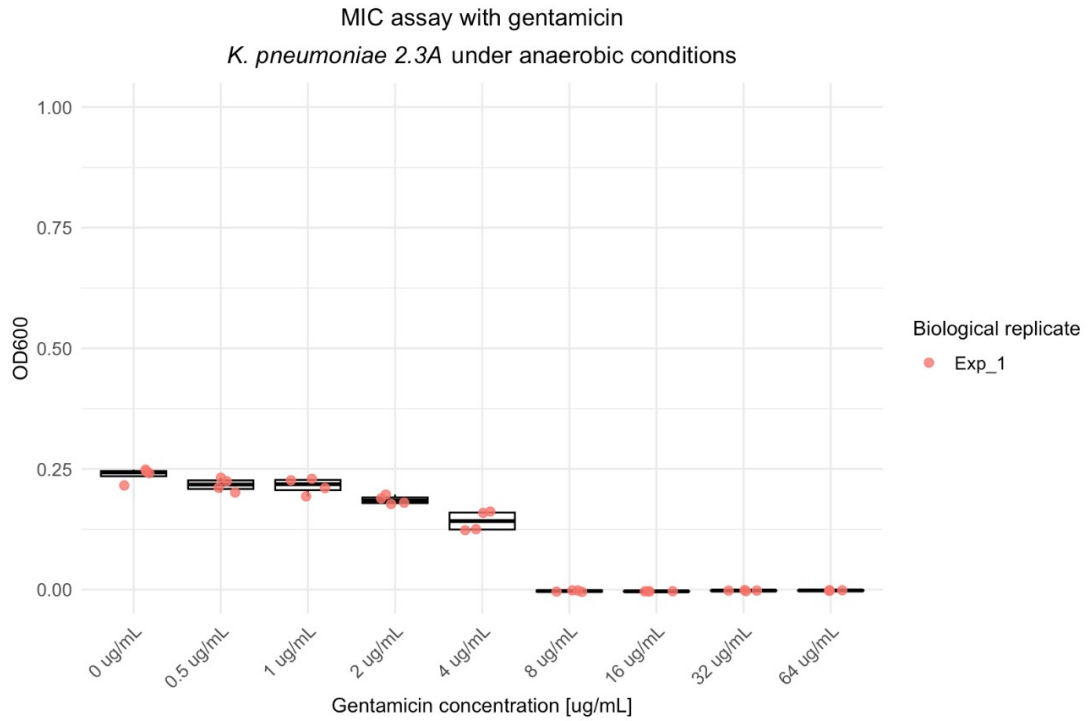

Fig. 40. MIC assay of K. pneumoniae 2.3A with gentamicin under anaerobic conditions. Individual data points represent one technical replicate. The MIC was determined to be 8 μg/mL.

Klebsiella michiganensis 8.3A:

The strain remained susceptible to gentamicin (MIC = 1 µg/mL), in accordance with the *in silico* analysis (Fig. 41). According to EUCAST, the breakpoint for *K. oxytoca* (the closest related species) is 2 µg/mL.

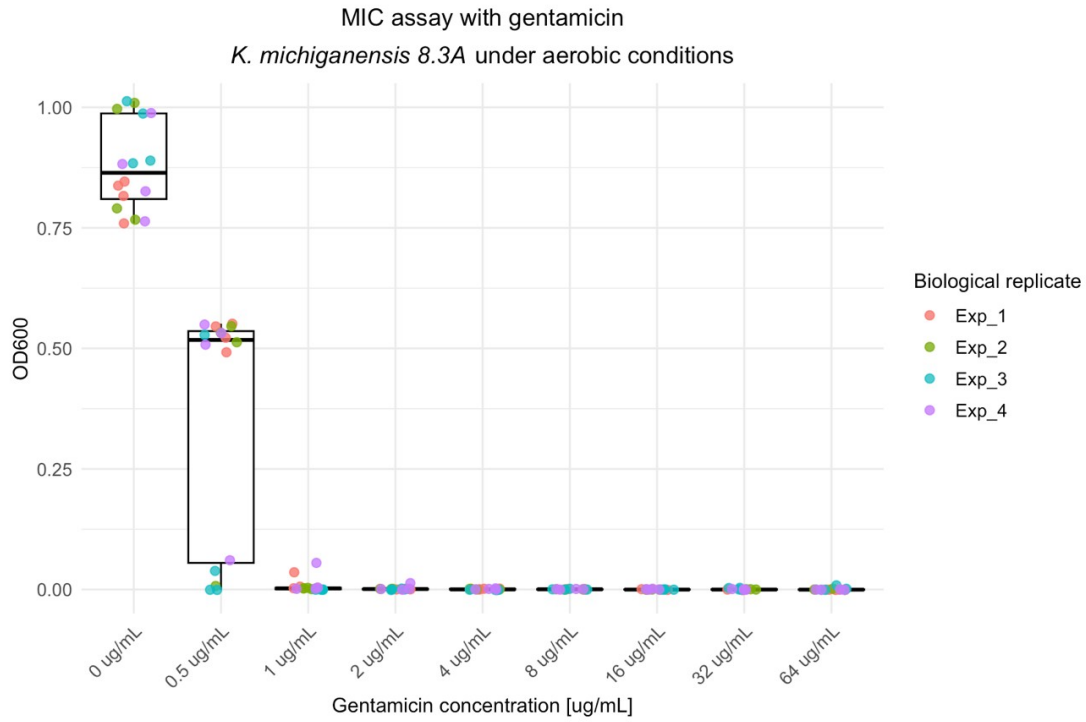

Fig. 41. MIC assay of K. michiganensis 8.3A with gentamicin under aerobic conditions. Each color represents one biological replicate with four technical replicates. The MIC was determined to be 1 µg/mL.

Enterococcus faecalis 5.5A:

According to EUCAST, *E. faecalis* is classified as susceptible to gentamicin if no growth is observed at concentrations of ≤64 µg/mL. *In vitro*, the MIC was determined to be 32 µg/mL, indicating susceptibility (Fig. 42). Genome analysis revealed the presence of the *spw* and *aad6* genes encoding aminoglycoside nucleotidyltransferases, as well as *aph(3')-III* encoding an aminoglycoside phosphotransferase; however, none of them are specifically effective against gentamicin (Fabre, A., et al., 2018; Zárate, S., et al., 2018).

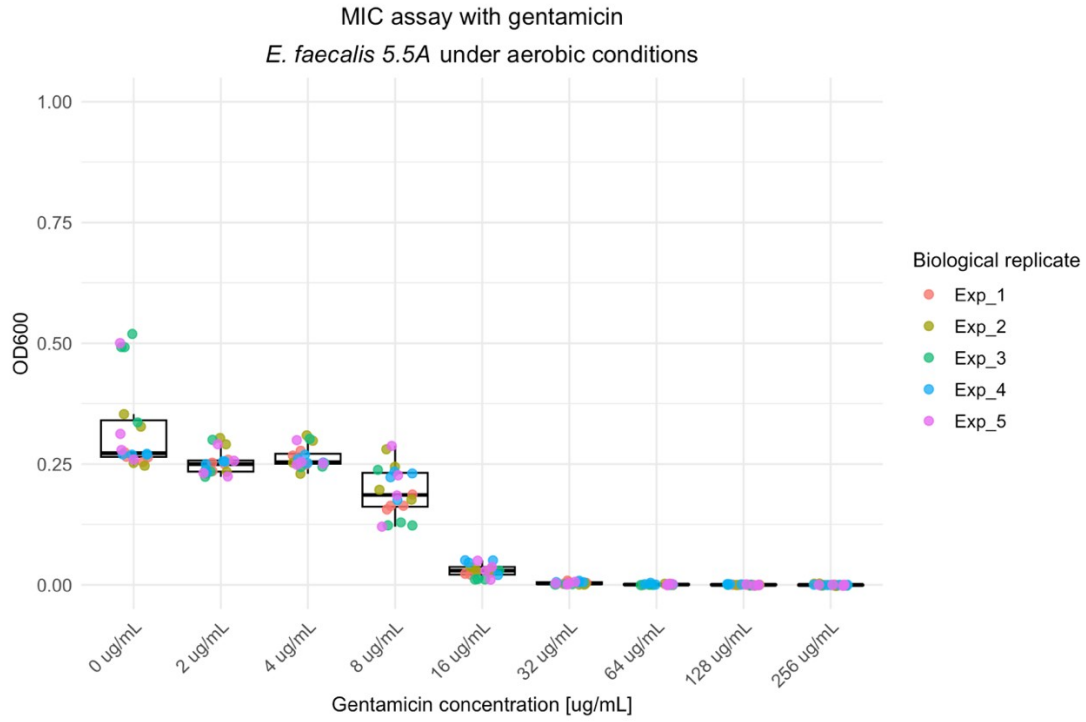

Fig. 42. MIC assay of E. faecalis 5.5A with gentamicin under aerobic conditions. Each color represents one biological replicate with four technical replicates. The MIC was determined to be 32 µg/mL.

Staphylococcus epidermidis LH_NM_637:

For *S. epidermidis*, EUCAST defines an ECOFF for gentamicin of 0.25 µg/mL. No gentamicin resistance determinants were identified in the genome, and phenotypic analysis confirmed susceptibility in all replicates (Fig. 43).

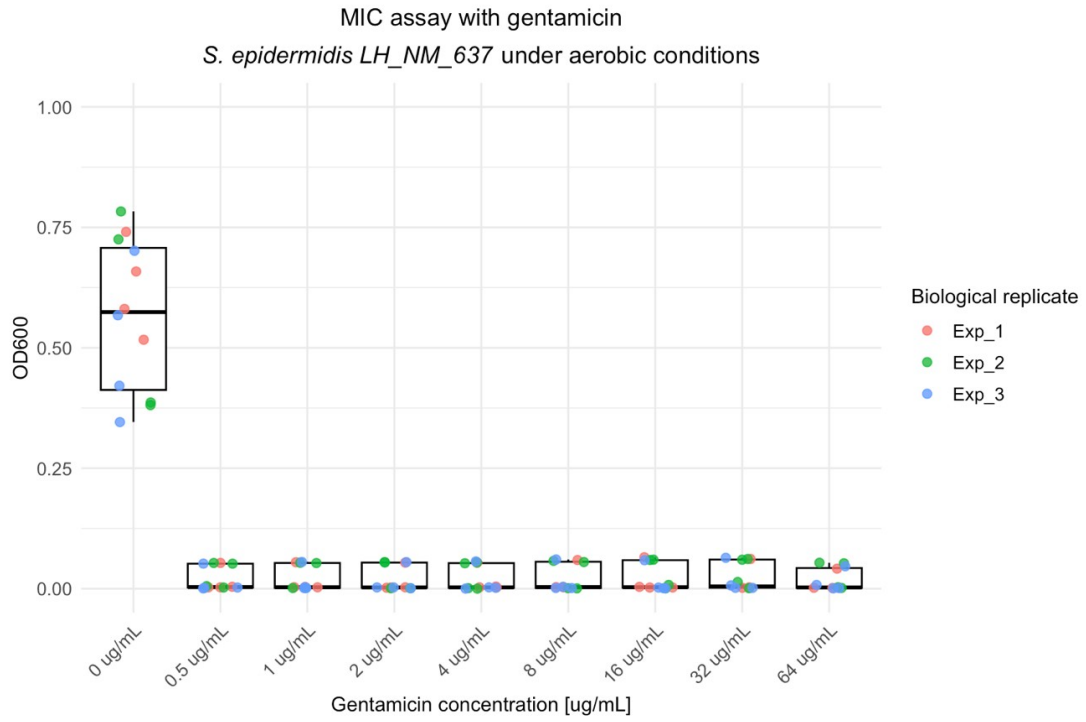

Fig. 43. MIC assay of S.epidermidis LH_NM_637 with gentamicin under aerobic conditions. Each color represents one biological replicate with four technical replicates. The MIC was determined to be 0.5 µg/mL.

Staphylococcus epidermidis 8.2A:

Genome analysis revealed the presence of the *aac(6')-Ie-aph(2'')-Ia* gene, encoding an aminoglycoside acetyltransferase associated with resistance to multiple aminoglycosides, including gentamicin. According to EUCAST, the ECOFF for gentamicin for *S. epidermidis* is 0.25 µg/mL. Consistently, MIC assays demonstrated strong resistance, with a MIC value of 256 µg/mL (Fig. 44).

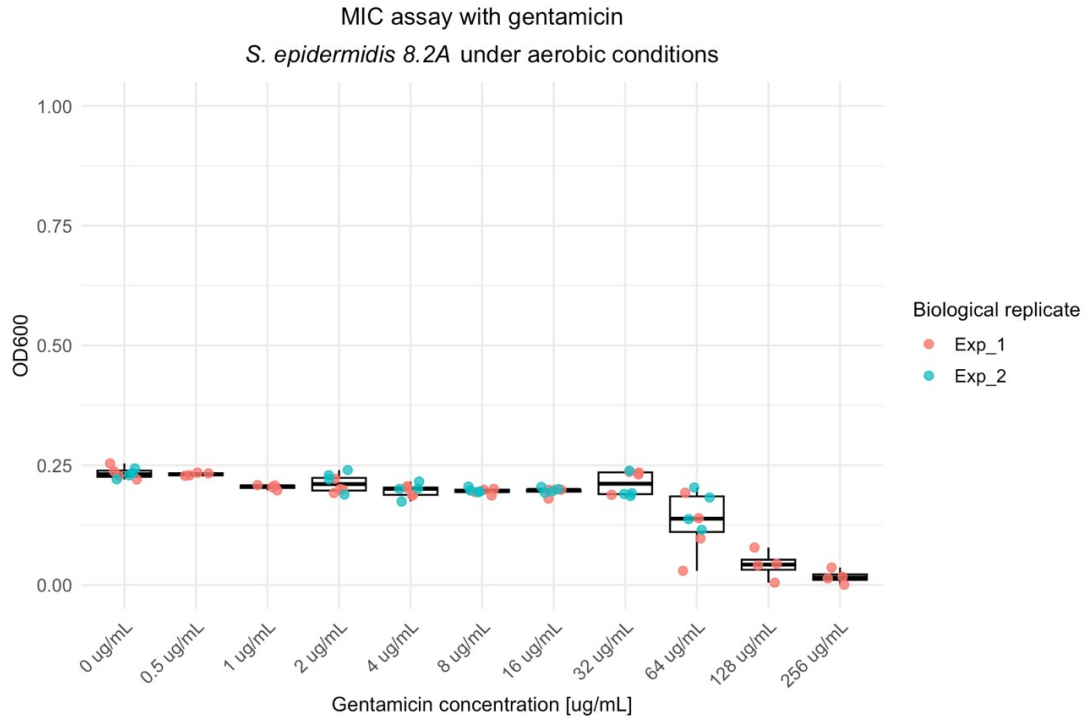

Fig. 44. MIC assay of S. epidermidis 8.2A with gentamicin under aerobic conditions. Each color represents one biological replicate with four technical replicates. The MIC was determined to be 256 µg/mL.

Lactobacillus spp.:

Lactobacillus plantarum 37.6A and Lactobacillus fermentum 10.2E did not encode any ARGs related to aminoglycosides according to genome analysis, and EUCAST does not provide breakpoint values for these species. However, phenotypic analysis showed that both strains were resistant to gentamicin under aerobic conditions, with MIC values of 128 µg/mL (Figs. 45-46). According to the literature, most lactobacilli are intrinsically resistant to aminoglycosides, including gentamicin, without requiring specific ARGs. This resistance is at

least partially attributed to the lack of cytochrome-mediated, energy-dependent transport of aminoglycosides across the membrane (Dec, M., et al., 2017; Abriouel, H., et al., 2015).

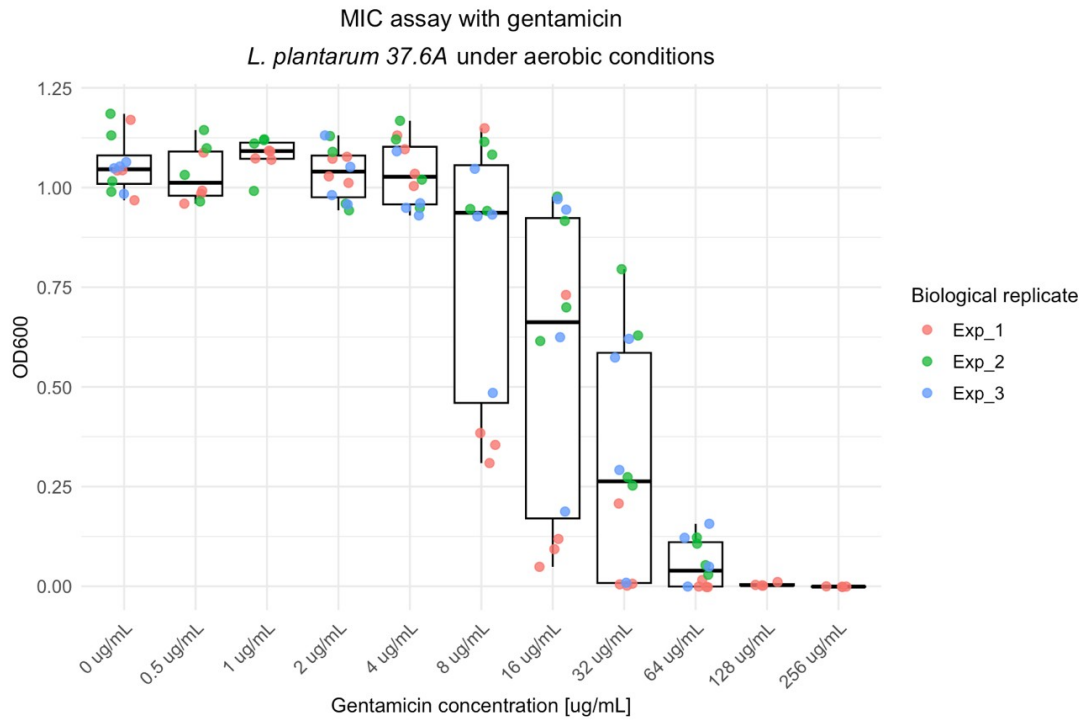

Fig. 45. MIC assay of L.plantarum 37.6A with gentamicin under aerobic conditions. Each color represents one biological replicate with four technical replicates. The MIC was determined to be 128 µg/mL.

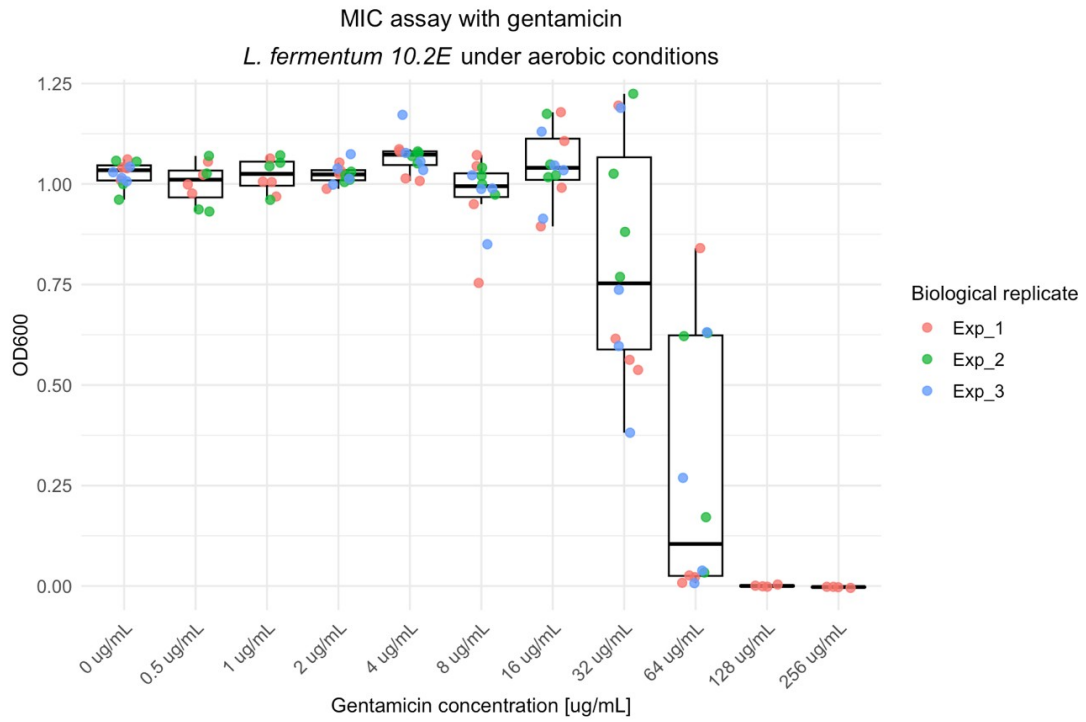

Fig. 46 MIC assay of L.fermentum 10.2E with gentamicin under aerobic conditions. Each color represents one biological replicate with four technical replicates. The MIC was determined to be 128 µg/mL.

Bifidobactrium spp.:

Bifidobacterium bifidum WS111, Bifidobacterium breve WS23, Bifidobacterium infantis WS13, and *Bifidobacterium pseudocatenulatum WS19* are strictly anaerobic; therefore, MIC assays were performed under anoxic conditions. Although no ARGs related to aminoglycosides were detected, resistance to gentamicin was expected due to its oxygen-dependent mechanism of action. EUCAST does not provide ECOFF values for these species. MIC assays confirmed these expectations: all strains were able to grow in the presence of gentamicin under anaerobic conditions, although MIC values varied between species (Fig. 47).

A

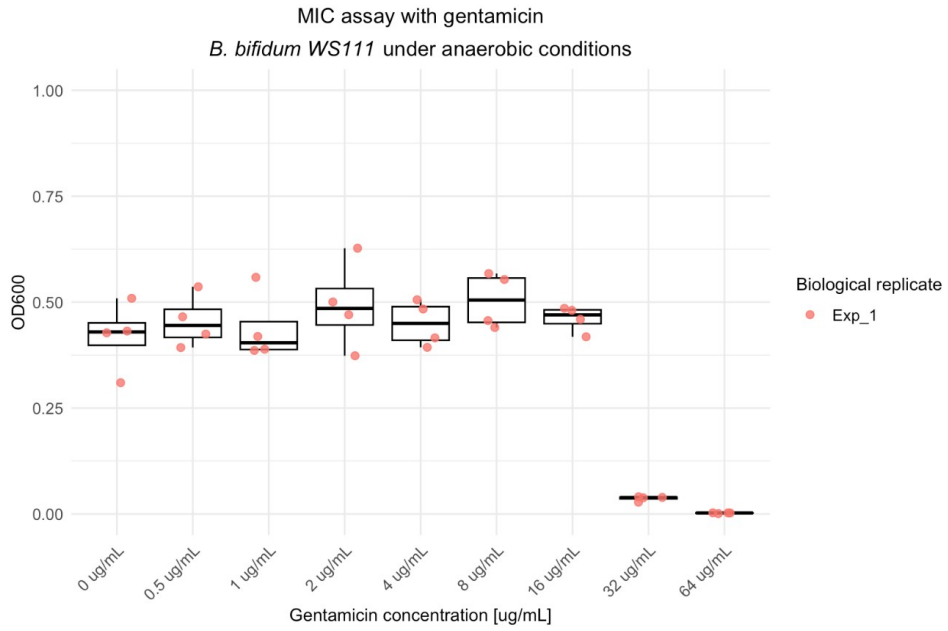

B

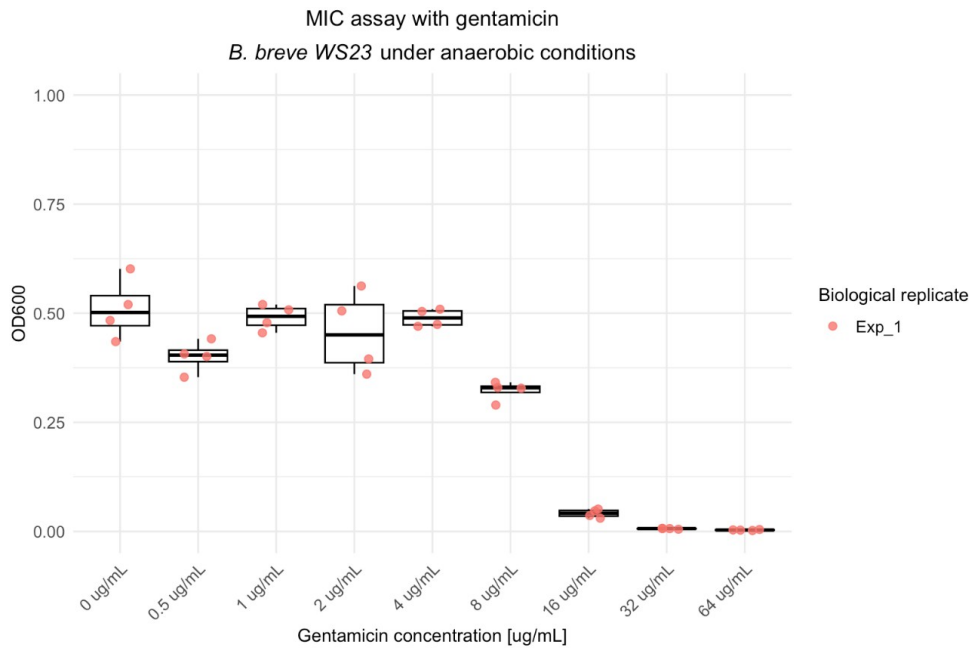
MIC assay with gentamicin
B. breve WS23 under anaerobic conditions
OD600
1.00
0.75
0.50
0.25
0.00
0 ug/mL
0.5 ug/mL
1 ug/mL
2 ug/mL
4 ug/mL
8 ug/mL
16 ug/mL
32 ug/mL
64 ug/mL
Gentamicin concentration [ug/mL]
Biological replicate
Exp_1

C

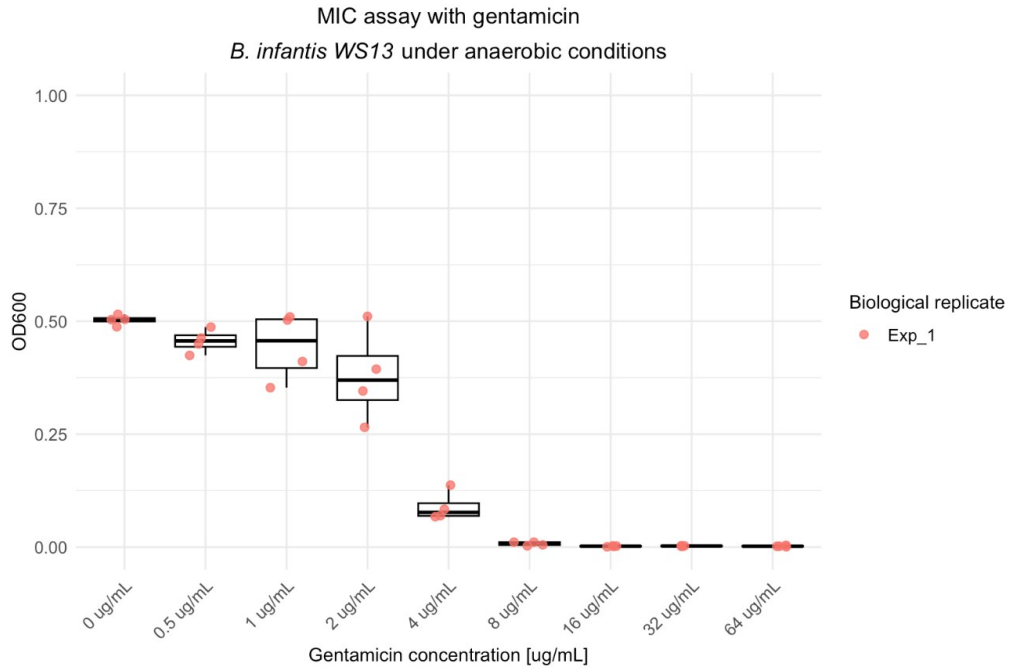
MIC assay with gentamicin
B. infantis WS13 under anaerobic conditions
OD600
1.00
0.75
0.50
0.25
0.00
0 ug/mL
0.5 ug/mL
1 ug/mL
2 ug/mL
4 ug/mL
8 ug/mL
16 ug/mL
32 ug/mL
64 ug/mL
Gentamicin concentration [ug/mL]
Biological replicate
Exp_1

D

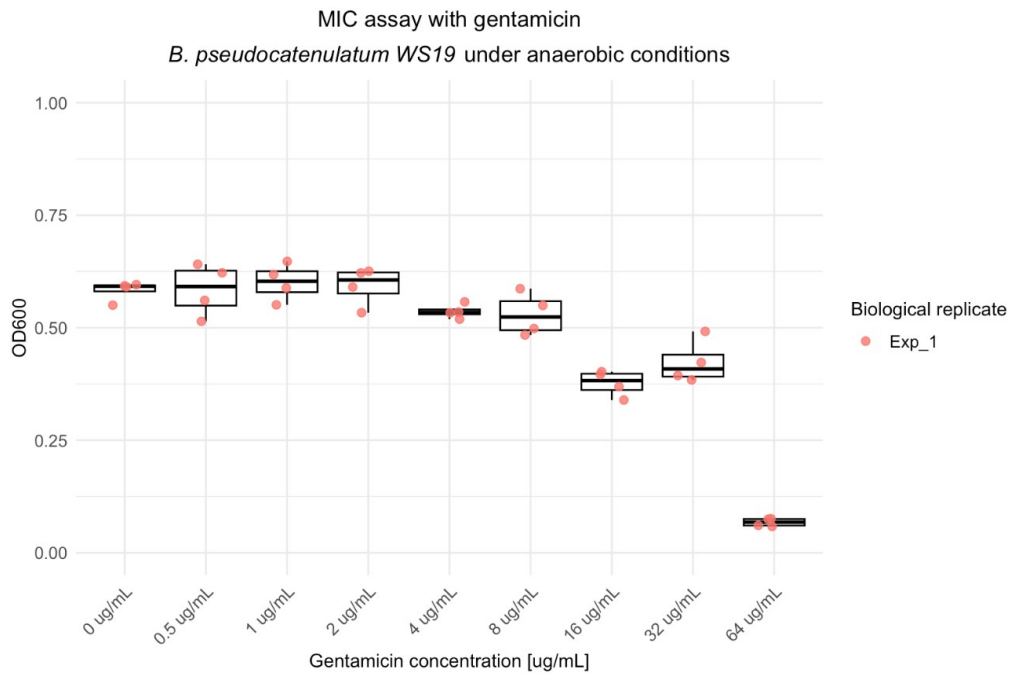

Fig. 47. MIC assay of Bifidobacteria strains with gentamicin under anaerobic conditions. Individual data points represent one technical replicate within the experiment. ***A****) B. bifidum WS111 (MIC = 32-64 μg/mL);* ***B****) B. breve WS23 (MIC = 32 μg/mL);* ***C****) B. infantis WS13 (MIC = 8 μg/mL);* ***D****) B. pseudocatenulatum WS19 (MIC = 64 μg/mL).*

Aminoglycoside susceptibility testing revealed that gentamicin activity strongly depends on oxygen availability, with increased resistance observed under anaerobic conditions. While some strains (e.g., *E. coli 13.3C* and *14.3B*) exhibited resistance despite lacking specific gentamicin-targeting ARGs, others showed susceptibility consistent with genomic predictions. Overall, the results highlight the complex relationship between genotype, phenotype, and environmental conditions (Table 9). Genomic predictions appeared to be more reliable for β-lactam resistance rather than for gentamicin, that was strongly influenced by oxygen availability and intrinsic resistance mechanisms.

Strain	**ARGs**	**Growth conditions**	**MIC [μg/mL] Gentamicin**
E. coli 13.3C	*(acrD, baeRS, cpxA, kdpE, tolC)*	Aerobic	4
		Anaerobic	16
E. coli 14.3B	*aph(3'')-Ib, aph(6)-Id, (acrD, baeRS, cpxA, kdpE, tolC)*	Aerobic	4
		Anaerobic	32
K. pneumoniae 40.9B	*aph(3'')-Ib, aph(6)-Id, ant(3")-IIa, LAP-2, (KpnEF, KpnG)*	Aerobic	1
		Anaerobic	8
K. pneumoniae 2.3A	*aph(3'')-Ib, aph(6)-Id,*	Aerobic	1*

	(KpnEF, KpnG)	Anaerobic	8
K. michiganensis 8.3A	-	Aerobic	1
S. epidermidis LH_NM_637	-	Aerobic	0.5
S. epidermidis 8.2A	*aac(6')-Ie-aph(2'')-Ia, ant(4')-Ib*	Aerobic	256
E. faecalis 5.5A	*aph(3')-IIIa, aad(6)*	Aerobic	32
L. fermentum 10.2E	-	Aerobic	128
L. plantarum 37.6A	-	Aerobic	128
B. bifidum WS111	-	Anaerobic	32-64
B. breve WS23	-	Anaerobic	32
B. infantis WS13	-	Anaerobic	8
B. pseudocatenulatum WS19	-	Anaerobic	64

Table 9. Summary of MIC assay results for gentamicin. "" indicates that outliers were detected in some replicates at higher antibiotic concentrations, likely indicating heterogeneous growth pattern among biological replicates. In the ARGs column, "-" indicates that no ARGs were detected in silico. ARGs shown in parentheses represent genes associated with multidrug resistance mechanisms (e.g. multidrug efflux pump systems).*

Growth analysis

To further characterize the strains, growth curve experiments were performed. Notably, *Bifidobacterium* and *Lactobacillus* species did not grow in our main experimental medium, MHB, even after the addition of L-cysteine (1%), an essential supplement for *Bifidobacteria.* Therefore, alternative media were tested for all strains. Media selection was based on literature data. Brain Heart Infusion (BHI), supplemented with L-cysteine, was included as a standard medium commonly used in gut microbiome studies (Kovács R, et al., 2022). In addition, two media based on De Man, Rogosa, Sharpe Broth (MRS), a medium specifically designed for *Lactobacillus* spp., were tested. These were prepared as mixtures of MRS and MHB at ratios of 1:1 and 9:1 (MHB:MRS), referred to as 50/50 and 90/10, respectively (Klare, I., et al., 2005). Strains belonging to the *Enterobacteriaceae* family (*E. coli 13.3C, E. coli 14.3B, K. pneumoniae 40.9B, K. pneumoniae 2.3A,* and *K. michiganensis 8.3A*) consistently exhibited

robust and reproducible growth across all four tested media, following typical growth dynamics (Figs. 48-52).

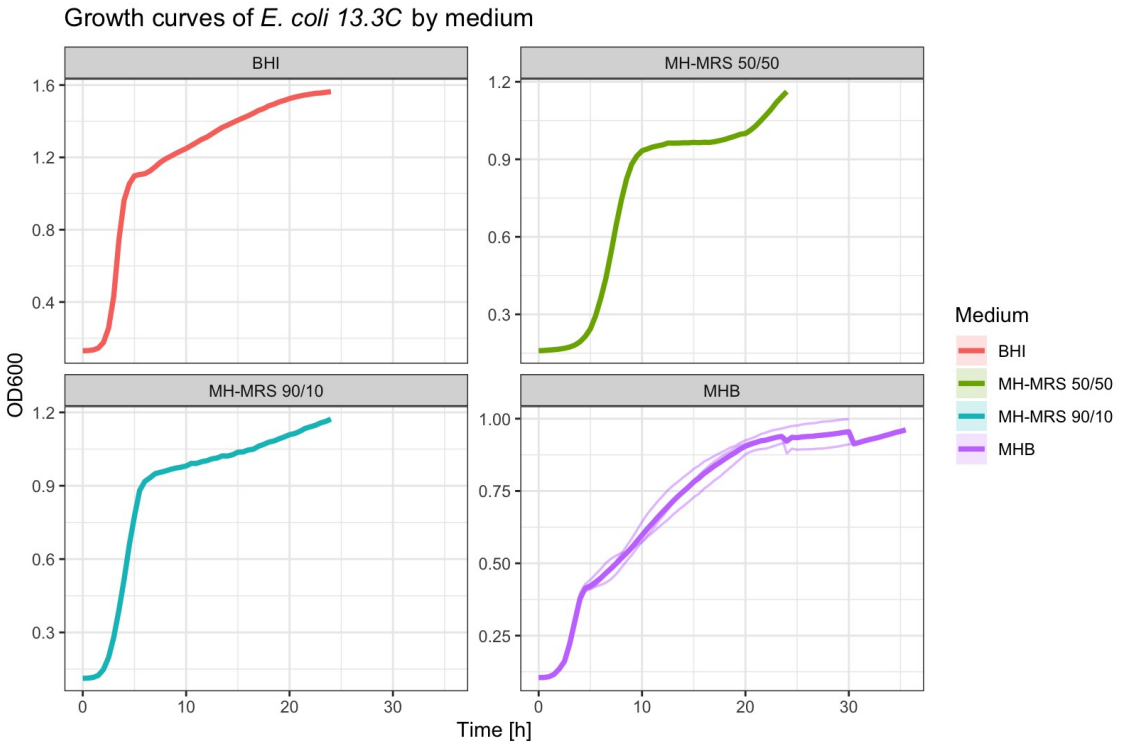

Fig. 48. Growth curves of E. coli 13.3C in four different media: BHI, MH-MRS 50/50, MH-MRS 90/10, and MHB. The x-axis shows time in hours, and the y-axis shows the optical density of the culture measured at 600 nm using a plate reader. Thick line represents the mean value of the technical replicates, thin lines represent individual technical replicates distinguished from mean value.

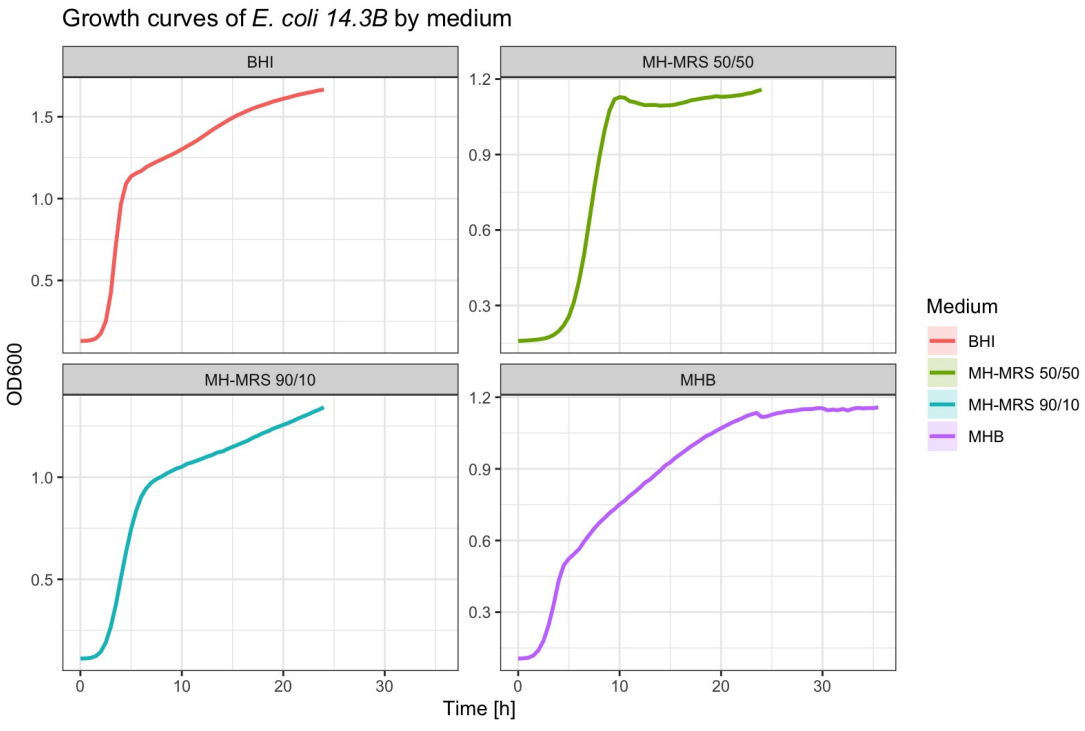

Fig. 49. Growth curves of E. coli 14.3B in four different media: BHI, MH-MRS 50/50, MH-MRS 90/10, and MHB. The x-

axis shows time in hours, and the y-axis shows the optical density of the culture measured at 600 nm using a plate reader. Thick line represents the mean value of the technical replicates, thin lines represent individual technical replicates distinguished from the mean value.

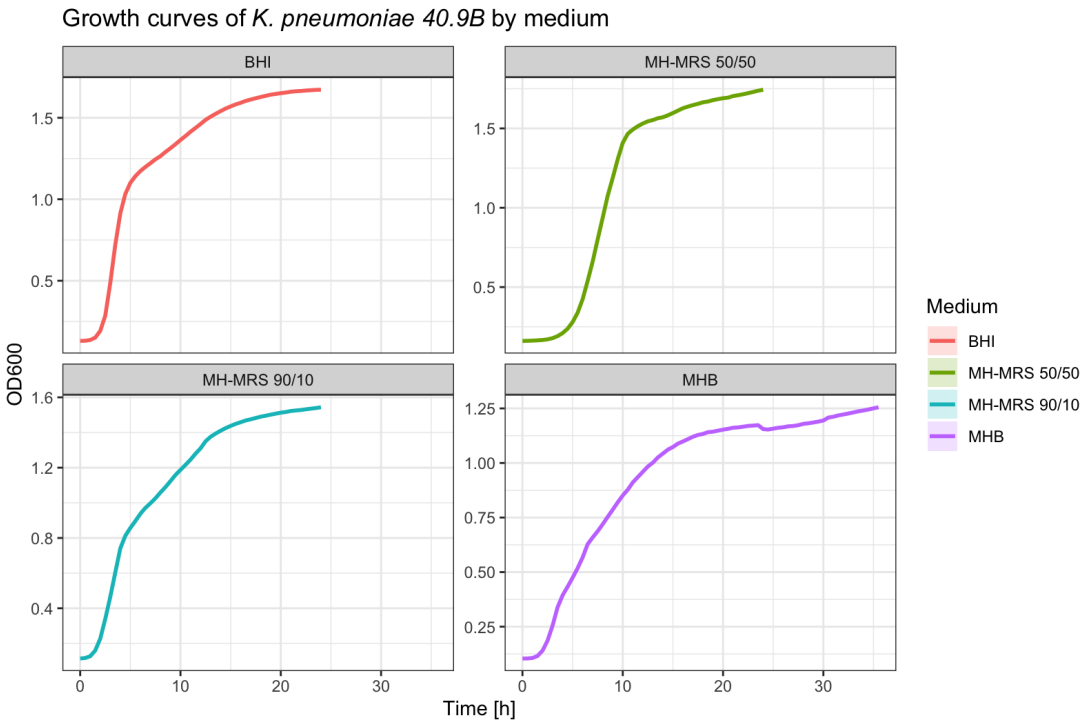

Fig. 50. Growth curves of K. pneumoniae 40.9B in four different media: BHI, MH-MRS 50/50, MH-MRS 90/10, and MHB. The x-axis shows time in hours, and the y-axis shows the optical density of the culture measured at 600 nm using a plate reader. Thick line represents the mean value of the technical replicates, thin lines represent individual technical replicates distinguished from the mean value.

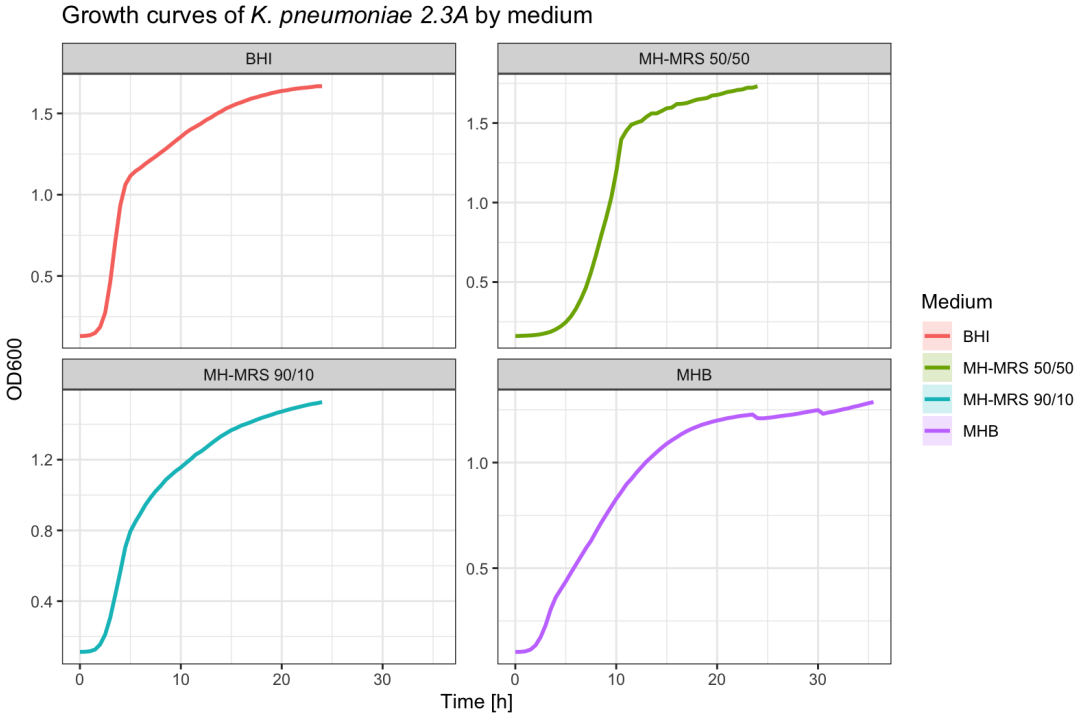

Fig. 51. Growth curves of K. pneumoniae 2.3A in four different media: BHI, MH-MRS 50/50, MH-MRS 90/10, and MHB. The x-axis shows time in hours, and the y-axis shows the optical density of the culture measured at 600 nm using a plate reader. Thick line represents the mean value of the technical replicates, thin lines represent individual technical replicates distinguished from the mean value.

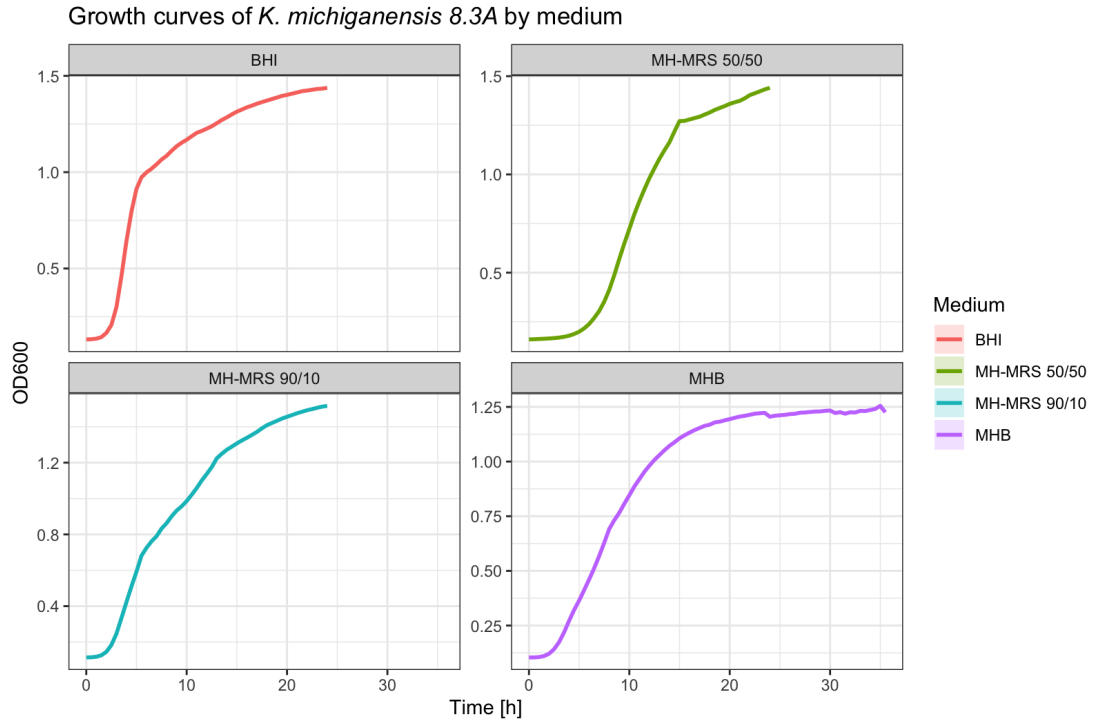

Fig. 52. Growth curves of K. michiganensis 8.3A in four different media: BHI, MH-MRS 50/50, MH-MRS 90/10, and MHB. The x-axis shows time in hours, and the y-axis shows the optical density of the culture measured at 600 nm using a plate reader. Thick line represents the mean value of the technical replicates, thin lines represent individual technical replicates distinguished from the mean value.

Staphylococcus epidermidis LH_NM_637 (Fig. 53) and *Enterococcus faecalis 5.5A* (Fig. 54) demonstrated variable, replicate-specific growth patterns in MHB medium across both technical and biological replicates. In contrast, in alternative media their growth curves followed the expected growth dynamics.

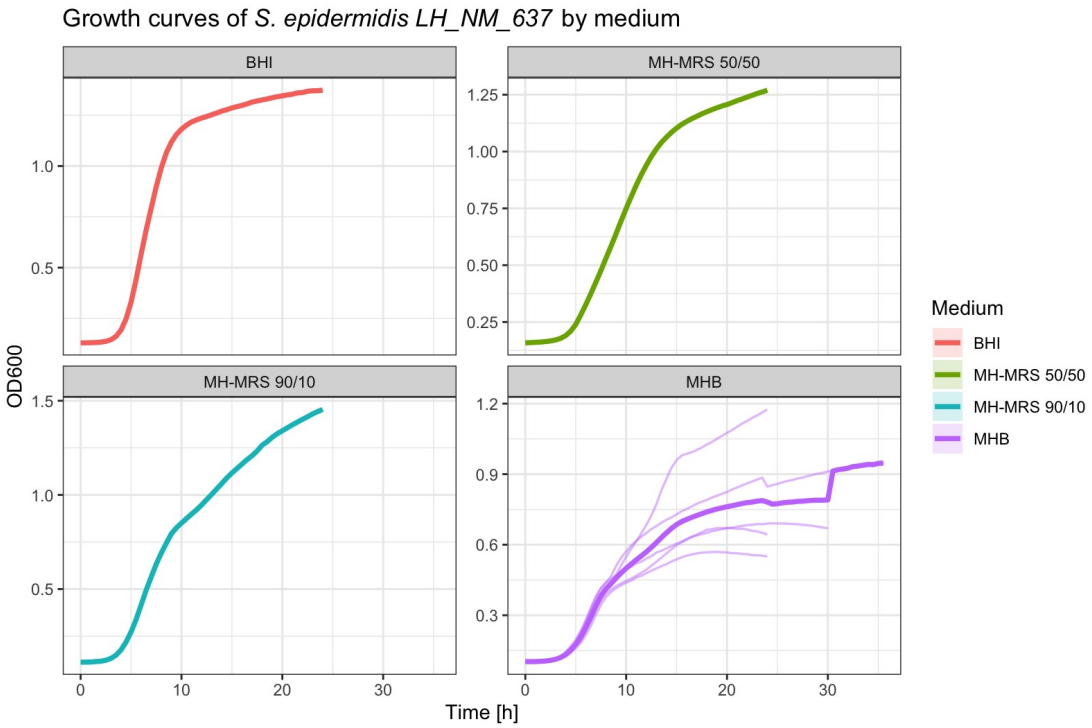

Fig. 53. Growth curves of S. epidermidis LH_NM_637 in four different media: BHI, MH-MRS 50/50, MH-MRS 90/10, and MHB. The x-axis shows time in hours, and the y-axis shows the optical density of the culture measured at 600 nm using a plate reader. Thick line represents the mean value of the technical replicates, thin lines represent individual technical replicates distinguished from the mean value.

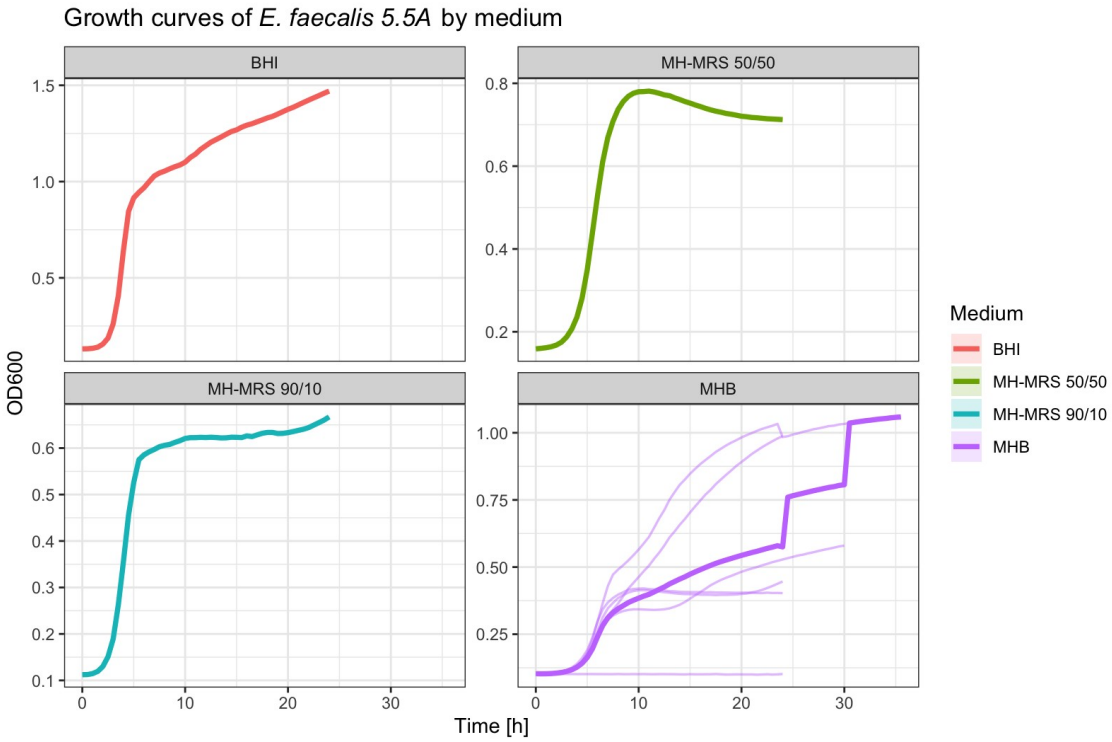

Fig. 54. Growth curves of E. faecalis 5.5A in four different media: BHI, MH-MRS 50/50, MH-MRS 90/10, and MHB. The x-axis shows time in hours, and the y-axis shows the optical density of the culture measured at 600 nm using a plate reader. Thick line represents the mean value of the technical replicates, thin lines represent individual technical replicates

distinguished from the mean value.

Growth analyses for *Lactobacillus* and for *Bifidobacterium* species were conducted in three media (BHI, 50/50 MH-MRS, and 90/10 MH-MRS). *Lactobacilli* showed optimal growth in 50/50 MH-MRS, where growth was reproducible and consistent with standard bacterial growth behaviour (Fig. 55). *L. plantarum 37.6A* was cultivated under both aerobic and anaerobic conditions. The main difference observed was a lower maximum optical density under anoxic conditions. Aerobic cultivation of *L. fermentum 10.2E* was not successful; therefore, growth analysis was performed only under anaerobic conditions.

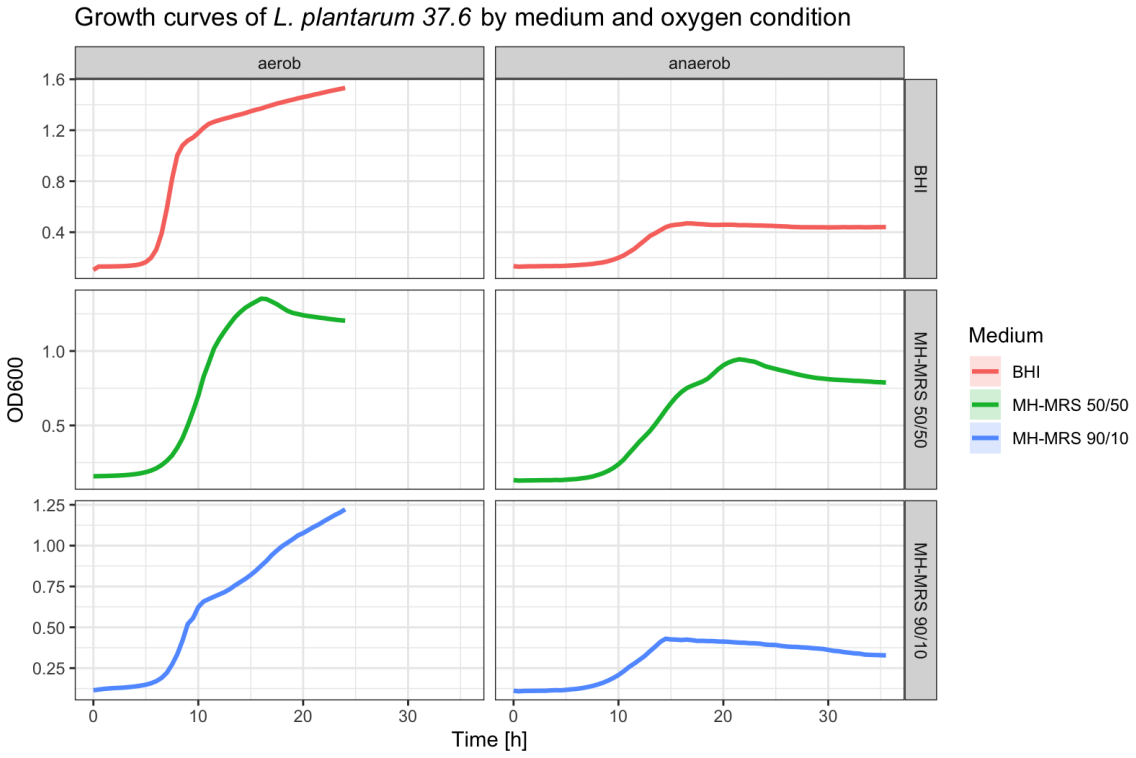

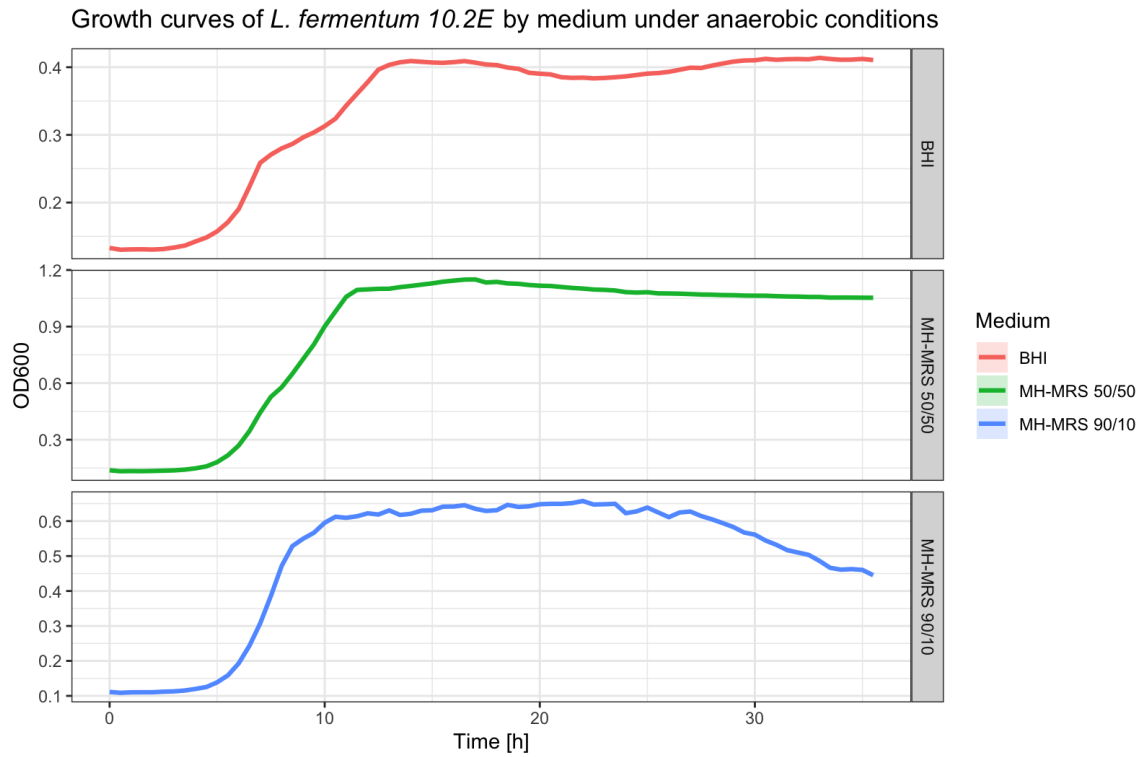

Fig. 55. Growth curves of Lactobacilli in three different media: BHI, MH-MRS 50/50, and MH-MRS 90/10. The x-axis shows time in hours, and the y-axis shows the optical density of the culture measured at 600 nm using a plate reader. Thick line represents the mean value of the technical replicates, thin lines represent individual technical replicates distinguished from the mean value. The upper plot shows growth curves of L. plantarum 37.6A, the lower – L. fermentum 10.2E.

In contrast, *Bifidobacterium* spp. exhibited a typical bacterial growth pattern in BHI medium.

A

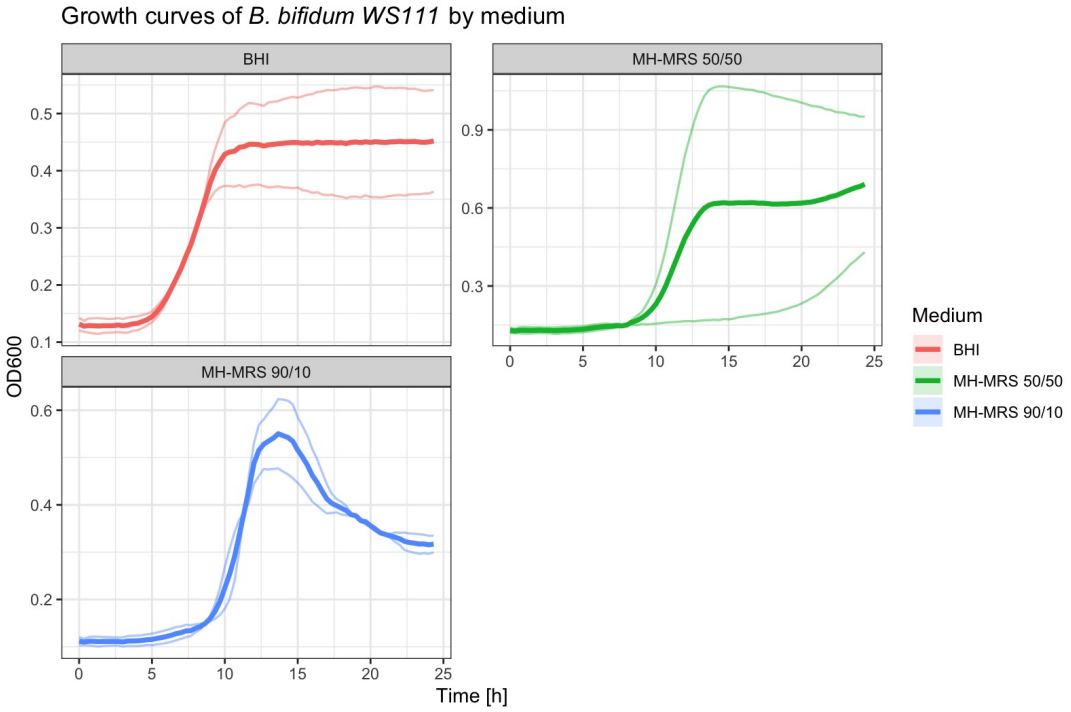
Growth curves of B. bifidum WS111 by medium
BHI
MH-MRS 50/50
MH-MRS 90/10
OD600
Time [h]
Medium
BHI
MH-MRS 50/50
MH-MRS 90/10

B

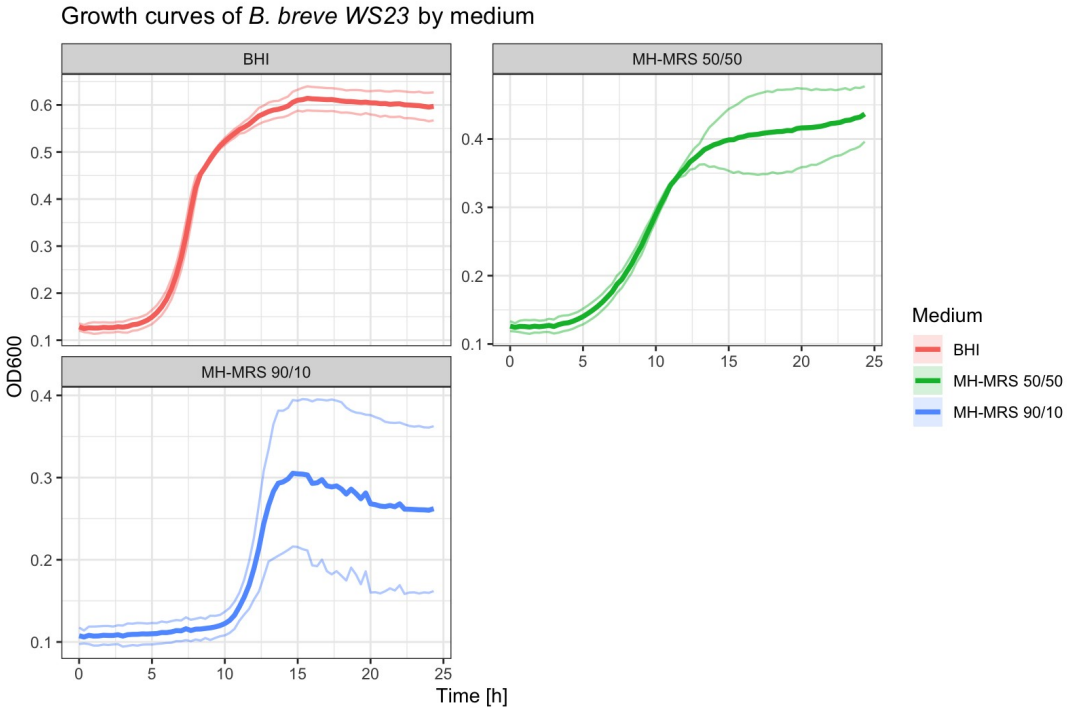
Growth curves of B. breve WS23 by medium
BHI
MH-MRS 50/50
MH-MRS 90/10
OD600
Time [h]
Medium
BHI
MH-MRS 50/50
MH-MRS 90/10

C

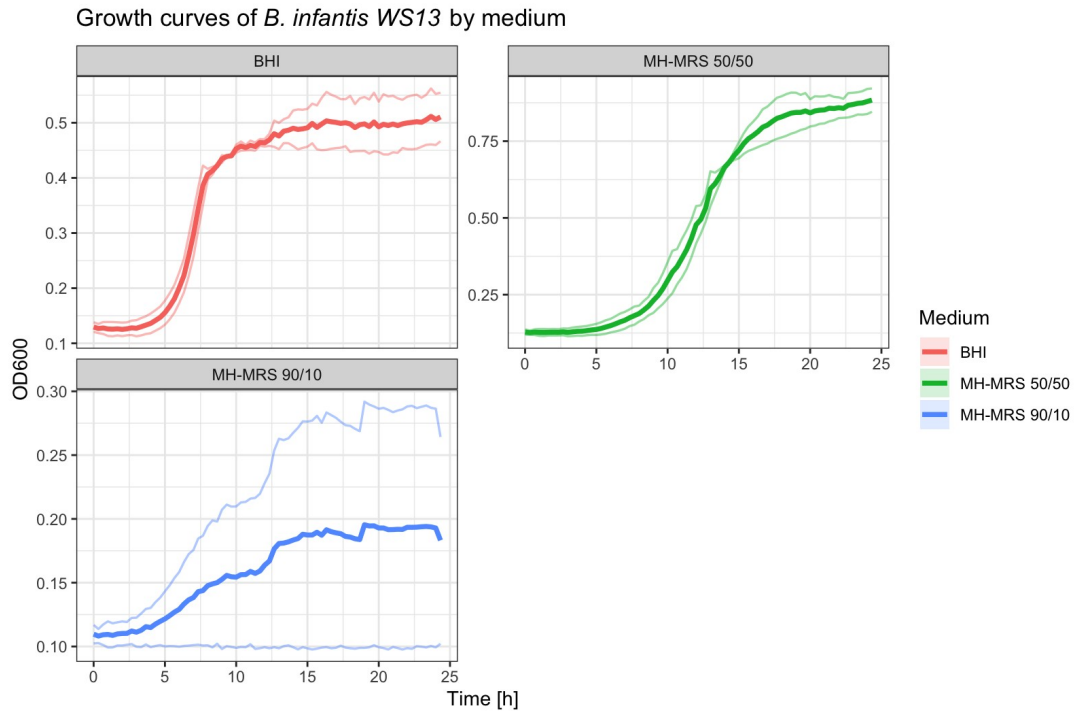

D

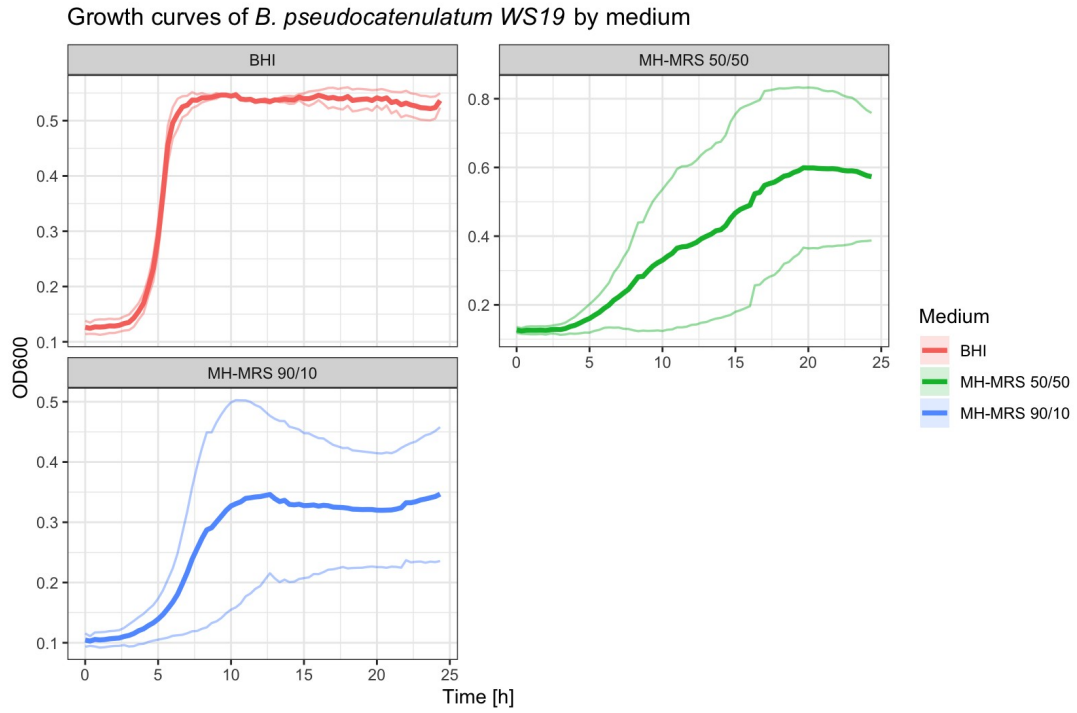

*Fig. 56. Growth curves of Bifidobacteria in three different media: BHI, MH-MRS 50/50, and MH-MRS 90/10. **A**) B. bifidum WS111; **B**) B. breve WS23; **C**) B. infantis WS13; **D**) B. pseudocatenulatum WS19. The x-axis shows time in hours, the y-axis shows the optical density of the culture measured at 600 nm using a plate reader. Thick line represents the mean value of the technical replicates, thin lines represent individual technical replicates distinguished from mean value.*

Overall, growth analysis provided important information on suitable media for the strains included in this study. The observed variability in growth patterns across media highlights the

need to select appropriate cultivation conditions for different bacterial groups, especially for more sensitive and strictly anaerobic microorganisms such as *Bifidobacterium* spp. and certain *Lactobacillus* spp. In contrast, members of the *Enterobacteriaceae* family showed robust growth under all tested conditions (Table 10). These findings will be important for selecting suitable and consistent cultivation conditions in future studies investigating potential cross-protection using these strains.

		Maximum optical density (OD_{600})			
Strain	**Growth conditions**	**BHI**	**MH-MRS 90/10**	**MH-MRS 50/50**	**MHB**
E. coli 13.3C	Aerobic	1.56 ± 0.019	1.19 ± 0.025	1.16 ± 0.362	1.17 ± 0.052
E. coli 14.3B	Aerobic	1.66 ± 0.011	1.34 ± 0.008	1.157 ± 0.051	1.15 ± 0.017
K. pneumoniae 40.9B	Aerobic	1.67 ± 0.011	1.54 ± 0.017	1.74 ± 0.013	1.20 ± 0.048
K. pneumoniae 2.3A	Aerobic	1.67 ± 0.009	1.52 ± 0.038	1.73 ± 0.014	1.26 ± 0.035
K. michiganensis 8.3A	Aerobic	1.44 ± 0.014	1.51 ± 0.013	1.44 ± 0.037	1.23 ± 0.017
S. epidermidis LH_NM_637	Aerobic	1.37 ± 0.011	1.45 ± 0.048	1.27 ± 0.009	0.79 ± 0.263
E. faecalis 5.5A	Aerobic	1.47 ± 0.054	0.67 ± 0.039	0.71 ± 0.079	0.81 ± 0.42
L. plantarum 37.6A	Aerobic	1.53 ± 0.017	1.22 ± 0.072	1.20 ± 0.035	-
L. plantarum 37.6A	Anaerobic	0.45 ± 0.033	0.32 ± 0.024	0.93 ± 0.047	-
L. fermentum 10.2E	Anaerobic	0.41 ± 0.017	0.63 ± 0.064	1.06 ± 0.17	-
B. bifidum WS111	Anaerobic	0.45 ± 0.048	0.55 ± 0.179	0.69 ± 0.253	-
B. breve WS23	Anaerobic	0.60 ± 0.033	0.30 ± 0.203	0.44 ± 0.082	-
B. infantis WS13	Anaerobic	0.51 ± 0.056	0.18 ± 0.033	0.88 ± 0.284	-
B. pseudocatenulatum WS19	Anaerobic	0.54 ± 0.016	0.35 ± 0.066	0.57 ± 0.124	-

Table 10. Growth curves assay summary. Mean OD_{600} values with standard deviation of each strain in different media.

Co-cultivation for determination of potential cross-protection

To investigate the potential cross-protection against antibiotics, combinations of two bacterial strains were initially selected, consisting of one resistant and one susceptible strain. To maintain consistency across experiments, conditions were aligned with those used for MIC

assays, including cultivation in liquid MHB, a starting inoculum optical density at 0.001 and incubation at 37°C for 20-22 hours. As an initial experimental setup for co-cultivation, it was decided to begin with combinations of facultative anaerobes under aerobic conditions. Different antibiotic concentrations were tested, corresponding to the MIC values of the susceptible strain, four times MIC (4xMIC), and the highest concentration used in MIC assays, at which the resistant strain clearly survived. Growth and survival of strains in co-cultures were evaluated by strain-specific dPCR. Additionally, optical density measurements (OD_{600}) were performed and used to support interpretation of the results. It is important to note that, although dPCR is considered a highly sensitive quantitative method, these co-cultivation assays were not optimized for precise quantitative comparison. The variability in sample processing may influence the absolute number of detected gene copies. DNA extraction efficiency can differ between bacterial strains. In addition, low level of positive signals may arise from stochastic amplification events, differences in amplification efficiency or minimal cross-contamination during sample processing, all of which have been previously described as limitations of dPCR assays (Quan, P., et al., 2018). Therefore, dPCR results were interpreted in qualitative way, rather than focusing on absolute quantitative differences between samples.

Combinations with ampicillin

Cross-protection against ampicillin was first examined using *E. coli 13.3C* as the susceptible strain in combination with four resistant strains: *E. coli 14.3B, K. pneumoniae 40.9B, K. pneumoniae 2.3A* and *K. michiganensis 8.3A*. No evidence of cross-protection was observed for the combinations *E. coli 13.3C* + *E. coli 14.3B* (Fig. 57), as dPCR results did not show survival of the susceptible strain in co-culture in the presence of ampicillin. Similarly, no clear cross-protection was observed in co-cultures of *E. coli 13.3C* with *K. michiganensis 8.3A* (Fig. 58) and *K. pneumoniae 40.9B* (Fig. 59). Although weak positive dPCR signals for susceptible strains were identified in some antibiotic-containing co-cultures, comparable signals were also detected in control monocultures where the second strain should not have been present (Fig. 59). As the specificity of the primers has been checked (Fig. S1) and contamination was excluded by conventional PCR, these low-abundance signals were interpreted as background or technical noise during dPCR. Nevertheless, the results suggest that additional optimization of experimental conditions may be necessary for more sensitive detection of community effects. The corresponding dPCR-derived copy numbers for monocultures and co-cultures are summarized in Tables 11-14. As discussed above, these values should be interpreted qualitatively rather than quantitatively due to the variability observed between biological

replicates and the need for further optimization of the experimental setup. The tables provide an overview of trends across different strain combinations and antibiotic concentrations.

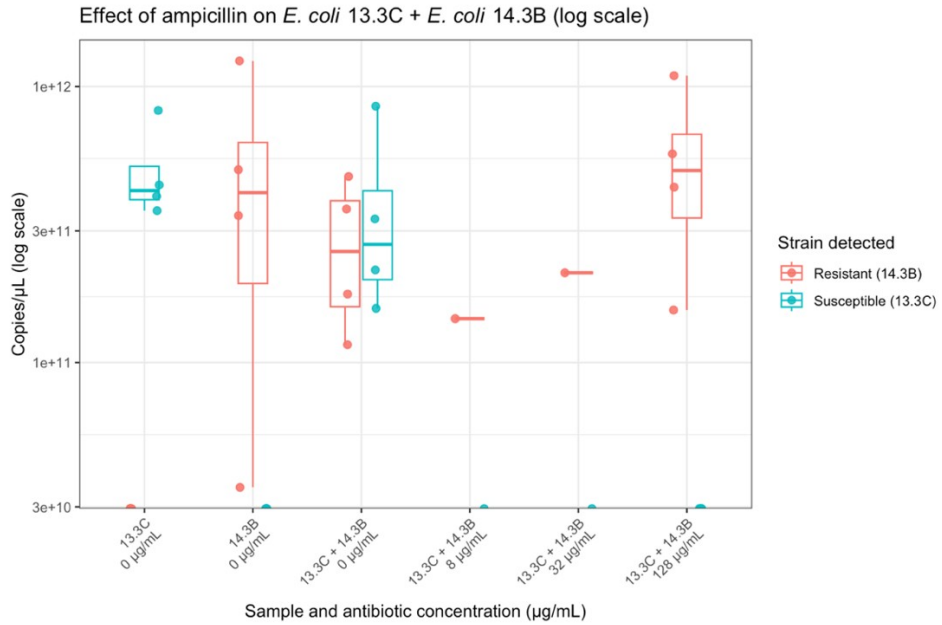

Fig. 57 Co-culture of E. coli 13.3C and E. coli 14.3B with and without ampicillin plotted on logarithmic scale. The x-axis shows different samples of mono- and co-cultures with different ampicillin concentrations. On the logarithmic y-axis number of gene copies per µL of sample detected by dPCR are marked. Individual data points represent one biological replicate. No growth of the susceptible strain (blue) was detected in combination with the resistant (red) strain in the presence of ampicillin.

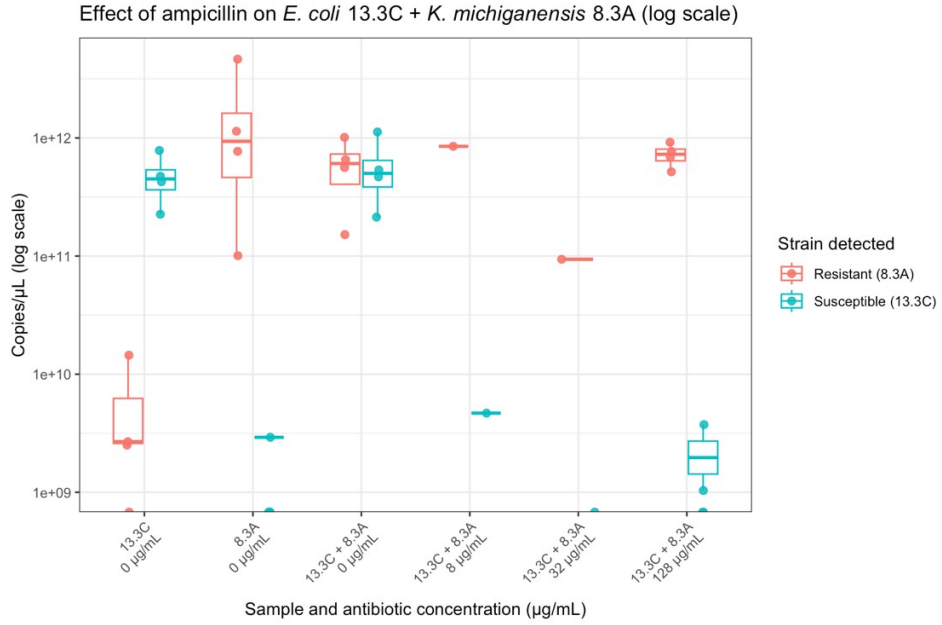

Fig. 58. Co-culture of E. coli 13.3C and K. michiganensis 8.3A with and without ampicillin plotted on logarithmic scale. The x-axis shows different samples of mono- and co-cultures with different ampicillin concentrations. On the logarithmic y-axis number of gene copies per µL of sample detected by dPCR are marked. Individual data points represent one biological replicate. Weak positive signals of a susceptible strain (blue) are detected in co-cultures with antibiotic

concentrations at 4 and 128 µg/mL, however they remain comparable to the background signal observed in monocultures controls, therefore are not considered significant.

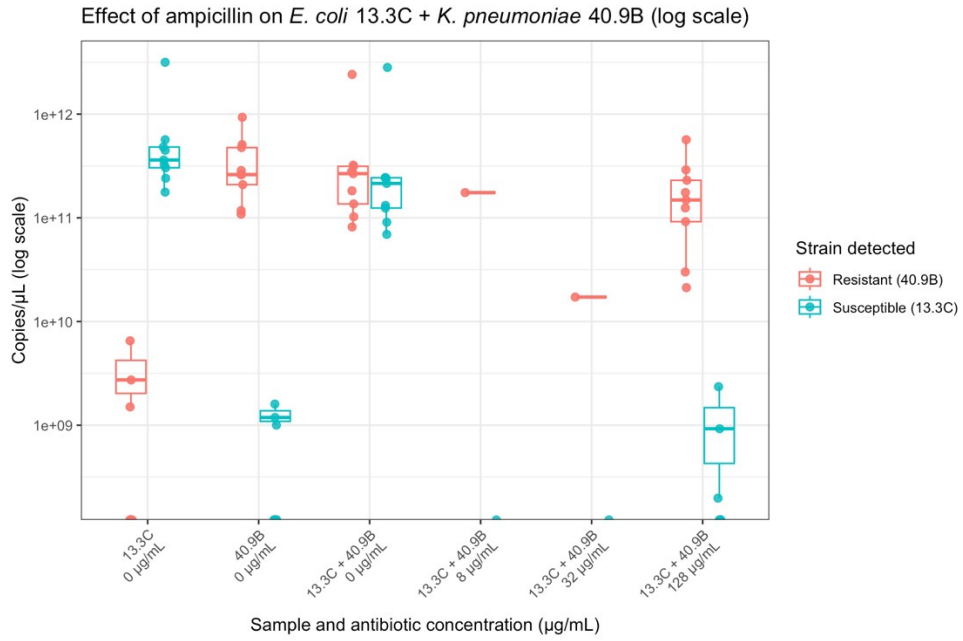

Fig. 59. Co-culture of E. coli 13.3C and K. pneumoniae 40.9B with and without ampicillin plotted on logarithmic scale. The x-axis shows different samples of mono- and co-cultures with different ampicillin concentrations. On the logarithmic y-axis number of gene copies per µL of sample detected by dPCR are marked. Individual data points represent one biological replicate. A weak positive signal of a susceptible strain (blue) was detected in co-culture at antibiotic concentration of 128 µg/mL, however it remained comparable to the background signal observed in monoculture controls, and was therefore not considered significant.

In contrast, a potential cross-protection effect was observed for the combination of *E. coli 13.3C* with *K. pneumoniae 2.3A*. In one biological replicate, the susceptible strain survived in co-culture at 32 µg/mL of ampicillin (Fig. 60), despite the absence of growth at lower concentrations. Additional optical density measurement of the plate confirmed that *E. coli 13.3C* did not grow in monoculture at 32 and 64 µg/mL of ampicillin, supporting the possibility of cross-protection (Fig. 61).

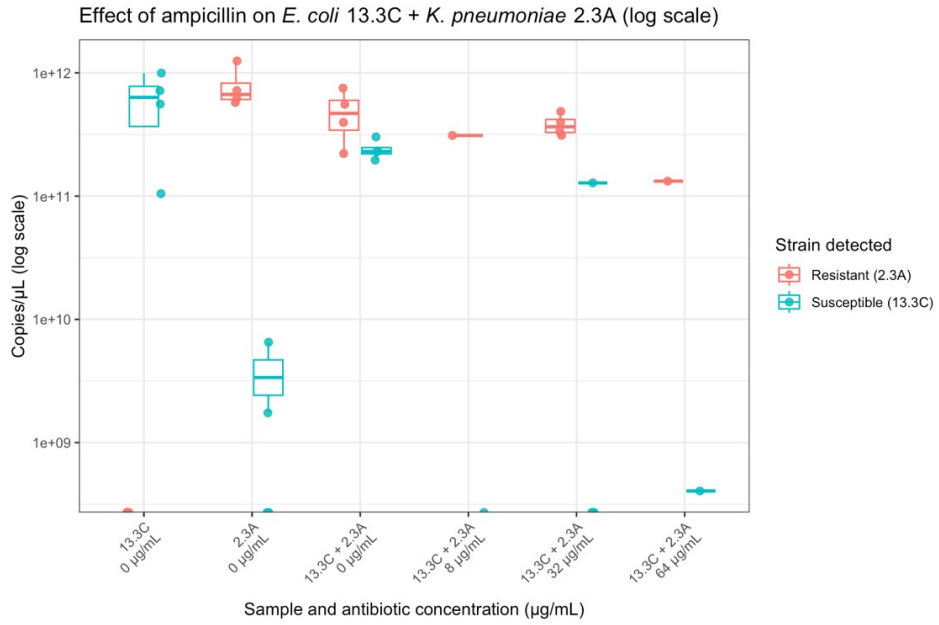

Fig. 60 Co-culture of E. coli 13.3C and K. pneumoniae 2.3A with and without ampicillin plotted on logarithmic scale. The x-axis shows different samples of mono- and co-cultures with different ampicillin concentrations. On the logarithmic y-axis number of gene copies per µL of sample detected by dPCR are marked. Individual data points represent one biological replicate. A positive signal of the susceptible strain (blue) was detected in co-culture at antibiotic concentration of 32 µg/mL.

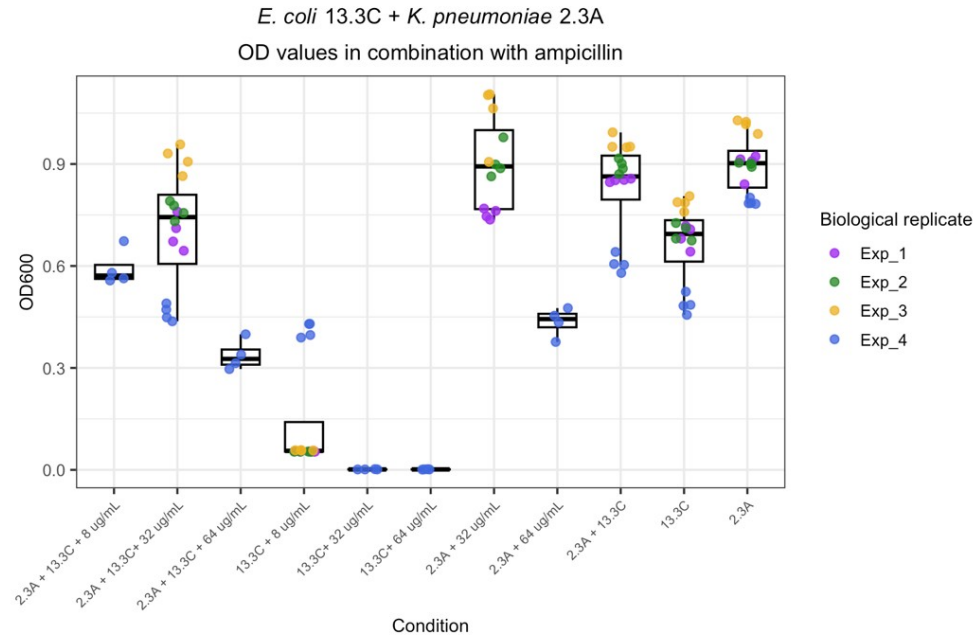

Fig. 61. Optical density measured from co-cultivation experiments of the combination E. coli 13.3C and K. pneumoniae 2.3A with ampicillin. The x-axis shows different samples of mono- and co-cultures with different piperacillin concentrations. The y-axis shows OD_{600} values of the samples. It demonstrates the growth inhibition of susceptible E. coli 13.3C in monoculture controls with ampicillin concentration at 32 and 64 µg/mL.

Ampicillin concentration [µg/mL]	Strain	Growth in monoculture (Copies per µL)	Growth in co-culture (Copies per µL)	Change in growth between mono- and co-culture	Relative abundance in co-culture
0	*E. coli 14.3B* Resistant	$5.29 * 10^{11}$ $\pm 5.11 * 10^{11}$	$2.81 * 10^{11}$ $\pm 1.64 * 10^{11}$	-46.78%	42%
	E. coli 13.3C Susceptible	$5.04 * 10^{11}$ $\pm 2.13 * 10^{11}$	$3.88 * 10^{11}$ $\pm 3.15 * 10^{11}$	-22.88%	58%
8	*E. coli 14.3B* Resistant		$1.44 * 10^{11}$	-72.71%	100%
	E. coli 13.3C Susceptible		0	-100%	0%
32	*E. coli 14.3B* Resistant		$2.11 * 10^{11}$	-59.99%	100%
	E. coli 13.3C Susceptible		0	-100%	0%
128	*E. coli 14.3B* Resistant		$5.63 * 10^{11}$ $\pm 3.94 * 10^{11}$	6.52%	100%
	E. coli 13.3C Susceptible		0	-100%	0%

Table 11. dPCR analysis of resistant E. coli 14.3B and susceptible E. coli 13.3C during co-cultivation under different ampicillin concentrations. Growth is expressed as DNA copy number per µL (mean ± SD, where applicable). Relative abundance indicates the contribution of each strain to the total bacterial population in co-culture. Percentage changes in growth were calculated relative to the corresponding monoculture grown without antibiotic treatment.

Ampicillin concentration [μg/mL]	Strain	Growth in monoculture (Copies per μL)	Growth in co-culture (Copies per μL)	Change in growth between mono- and co-culture	Relative abundance in co-culture
0	*K. pneumoniae 40.9B* Resistant	$3.58 * 10^{11}$ $\pm 2.44 * 10^{11}$	$4.36 * 10^{11}$ $\pm 7 * 10^{11}$	21.81%	49.59%
	E. coli 13.3C Susceptible	$6.23 * 10^{11}$ $\pm 8.99 * 10^{11}$	$4.43 * 10^{11}$ $\pm 8.38 * 10^{11}$	-29.17%	50.41%
8	*K. pneumoniae 40.9B* Resistant		$1.75 * 10^{11}$	-51.07%	100%
	E. coli 13.3C Susceptible		0	-100%	0%
32	*K. pneumoniae 40.9B* Resistant		$1.72 * 10^{10}$	-95.19%	100%
	E. coli 13.3C Susceptible		0	-100%	0%
128	*K. pneumoniae 40.9B* Resistant		$1.71 * 10^{11}$ $\pm 1.65 * 10^{11}$	-52.13%	99.8%
	E. coli 13.3C Susceptible		$3.48 * 10^{8}$ $\pm 7.62 * 10^{8}$	-99.94%	0.2%

Table 12. dPCR analysis of resistant K. pneumoniae 40.9B and susceptible E. coli 13.3C during co-cultivation under different ampicillin concentrations. Growth is expressed as DNA copy number per μL (mean ± SD, where applicable). Relative abundance indicates the contribution of each strain to the total bacterial population in co-culture. Percentage changes in growth were calculated relative to the corresponding monoculture grown without antibiotic treatment.

Ampicillin concentration [μg/mL]	Strain	Growth in monoculture (Copies per μL)	Growth in co-culture (Copies per μL)	Change in growth between mono- and co-culture	Relative abundance in co-culture
0	*K. pneumoniae 2.3A* Resistant	$7.91 * 10^{11} \pm 3.12 * 10^{11}$	$4.81 * 10^{11} \pm 2.26 * 10^{11}$	-39.16%	66.75%
	E. coli 13.3C Susceptible	$5.94 * 10^{11} \pm 3.74 * 10^{11}$	$2.40 * 10^{11} \pm 4.49 * 10^{10}$	-59.68%	33.25%
8	*K. pneumoniae 2.3A* Resistant		$3.11 * 10^{11}$	-60.73%	100%
	E. coli 13.3C Susceptible		0	-100%	0%
32	*K. pneumoniae 2.3A* Resistant		$3.83 * 10^{11} \pm 7.81 * 10^{10}$	-51.64%	92.28%
	E. coli 13.3C Susceptible		$3.20 * 10^{10} \pm 6.40 * 10^{10}$	-94.62%	7.72%
64	*K. pneumoniae 2.3A* Resistant		$1.32 * 10^{11}$	-83.28%	99.69%
	E. coli 13.3C Susceptible		$4.05 * 10^{8}$	-99.93%	0.31%

Table 13. dPCR analysis of resistant K. pneumoniae 2.3A and susceptible E. coli 13.3C during co-cultivation under different ampicillin concentrations. Growth is expressed as DNA copy number per μL (mean ± SD, where applicable). Relative abundance indicates the contribution of each strain to the total bacterial population in co-culture. Percentage changes in growth were calculated relative to the corresponding monoculture grown without antibiotic treatment.

Ampicillin concentration [µg/mL]	Strain	Growth in monoculture (Copies per µL)	Growth in co-culture (Copies per µL)	Change in growth between mono- and co-culture	Relative abundance in co-culture
0	*K. michiganensis 8.3A* Resistant	$1.66 * 10^{12} \pm 2.03 * 10^{12}$	$5.95 * 10^{11} \pm 3.53 * 10^{11}$	-64.23%	50.41%
	E. coli 13.3C Susceptible	$4.77 * 10^{11} \pm 2.31 * 10^{11}$	$5.85 * 10^{11} \pm 3.85 * 10^{11}$	22.63%	49.59%
8	*K. michiganensis 8.3A* Resistant		$8.49 * 10^{11}$	-48.96%	99.45%
	E. coli 13.3C Susceptible		$4.67 * 10^{9}$	-99.02%	0.55%
32	*K. michiganensis 8.3A* Resistant		$9.39 * 10^{10}$	-94.36%	100%
	E. coli 13.3C Susceptible		0	-100%	0%
128	*K. michiganensis 8.3A* Resistant		$7.23 * 10^{11} \pm 1.68 * 10^{11}$	-56.52%	99.84%
	E. coli 13.3C Susceptible		$1.19 * 10^{9} \pm 1.77 * 10^{9}$	-99.75%	0.16%

Table 14. dPCR analysis of resistant K. michiganensis 8.3A and susceptible E. coli 13.3C during co-cultivation under different ampicillin concentrations. Growth is expressed as DNA copy number per µL (mean ± SD, where applicable). Relative abundance indicates the contribution of each strain to the total bacterial population in co-culture. Percentage changes in growth were calculated relative to the corresponding monoculture grown without antibiotic treatment.

Combinations with piperacillin and tazobactam

Cross-protection against piperacillin/tazobactam was investigated using *K. michiganensis 8.3A* as the resistant strain. It encodes OXY1-3 β-lactamases which has been reported to be resistant to β-lactams. Tazobactam was added at a constant concentration of 4 μg/mL as in the MIC assays. No cross-protection was observed for combinations of *K. michiganensis 8.3A* with *E. coli 13.3C* (Fig. 62), *K. pneumoniae 40.9B* (Fig. 63) and *K. pneumoniae 2.3A* (Fig. 64). As for combinations of *E. coli 13.3C* with *K. pneumoniae 40.9B* and *K. michiganensis 8.3A* with ampicillin described above (Figs. 58-59), weak positive signals were detected in some antibiotic-containing co-cultures, however, they were below the level of background signals present in monoculture controls and were not therefore interpreted as evidence of cross-protection.

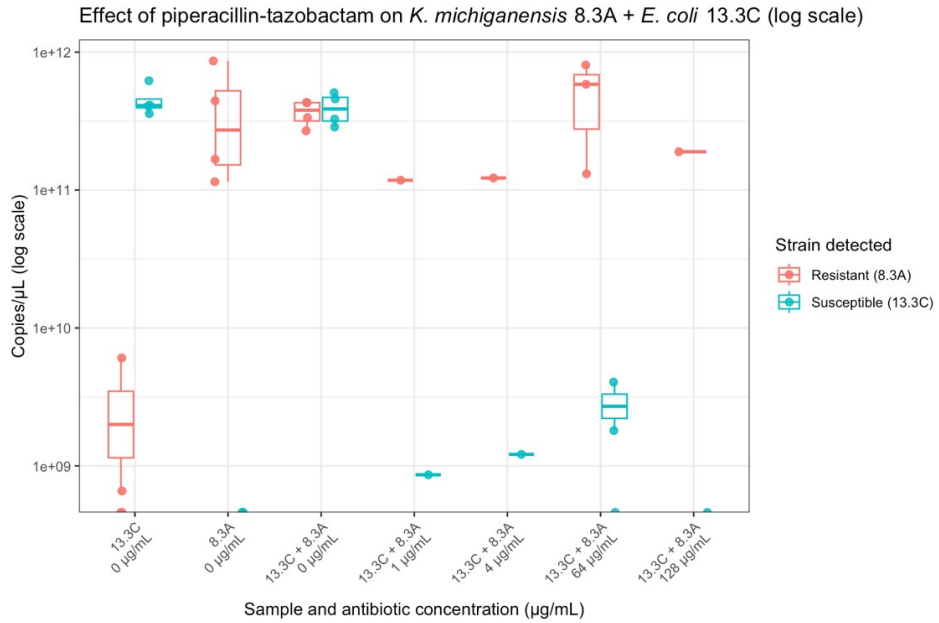

Fig. 62. Co-culture of K. michiganensis 8.3A and E. coli 13.3C with and without piperacillin/tazobactam plotted on logarithmic scale. The x-axis shows different samples of mono- and co-cultures with different piperacillin concentrations. On the logarithmic y-axis number of gene copies per μL of sample detected by dPCR are marked. Individual data points represent one biological replicate. Weak positive signals of the susceptible strain (blue) were detected in co-cultures at antibiotic concentrations of 1, 4, and 64 μg/mL, however, they remained comparable to the background signal observed in monoculture controls and therefore not considered significant.

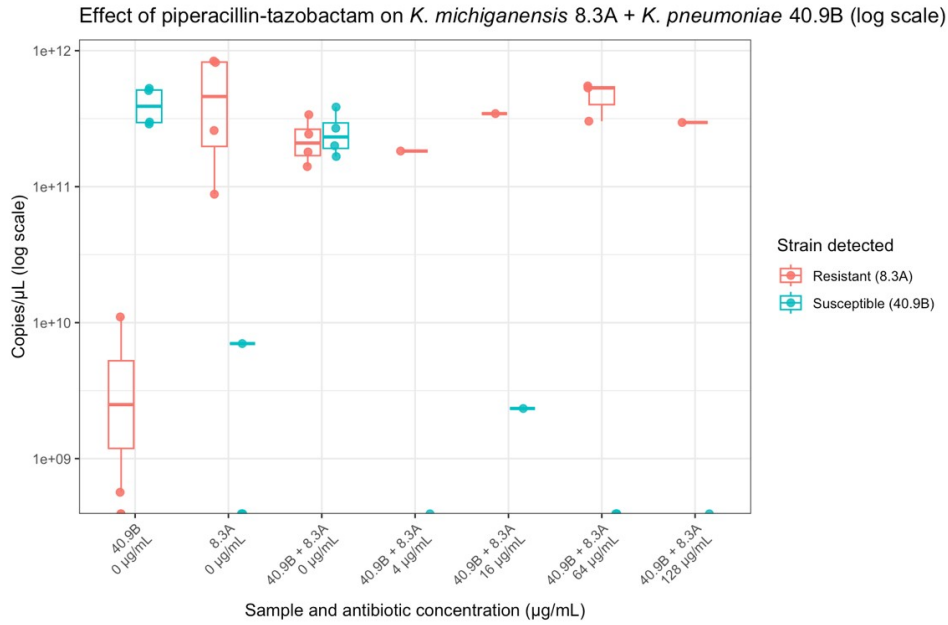

Fig. 63. Co-culture of K. michiganensis 8.3A and K. pneumoniae 40.9B with and without piperacillin/tazobactam plotted on logarithmic scale. The x-axis shows different samples of mono- and co-cultures with different piperacillin concentrations. On the logarithmic y-axis number of gene copies per µL of sample detected by dPCR are marked. Individual data points represent one biological replicate. A weak positive signal of a susceptible strain (blue) was detected in co-culture with antibiotic concentration at 16 µg/mL, however, it remained comparable to the background signal observed in monoculture controls and was therefore not considered significant.

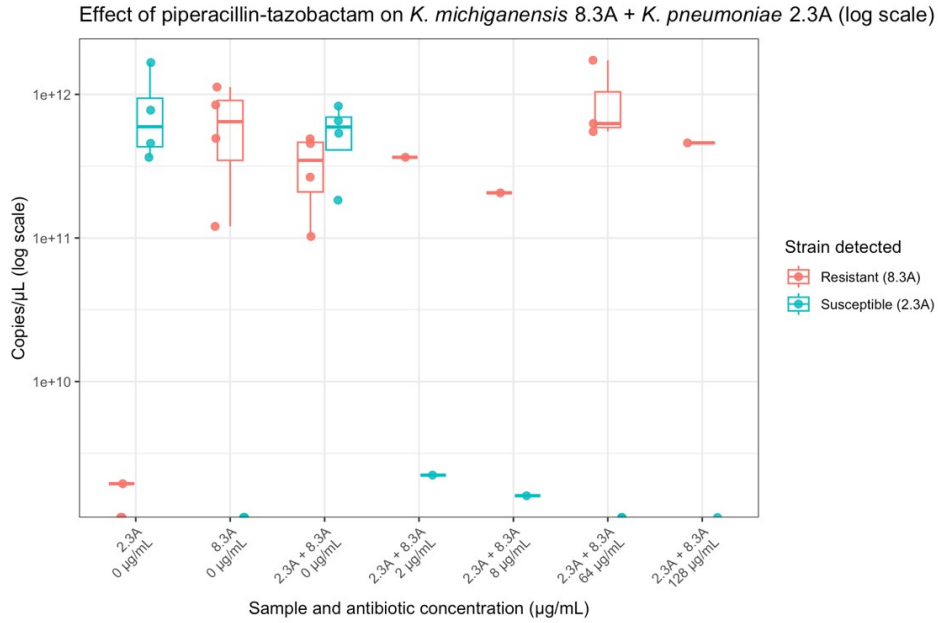

Fig. 64. Co-culture of K. michiganensis 8.3A and K. pneumoniae 2.3A with and without piperacillin/tazobactam plotted on logarithmic scale. The x-axis shows different samples of mono- and co-cultures with different piperacillin concentrations. On the logarithmic y-axis number of gene copies per µL of sample detected by dPCR are marked. Individual data points represent one biological replicate. Weak positive signals of a susceptible strain (blue) were detected in co-cultures with antibiotic concentrations at 2 and 8 µg/mL, however, they remained comparable to the background signal observed in monoculture controls and were therefore not considered significant.

In the combination of *E. coli 14.3B* with *K. michiganensis 8.3A,* a potential cross-protection effect was detected (Fig. 65). The susceptible *E. coli 14.3B* strain survived in co-culture at piperacillin concentration of 64 µg/mL, whereas it did not grow in monoculture with this concentration (Fig. 66). Interestingly, *E. coli 14.3B* also demonstrated unexpected growth in monoculture at MIC and 4x MIC concentration of piperacillin (1 and 4 µg/mL, respectively) (Fig. 66), despite its full susceptibility in previous MIC assays (Fig. 11). This observation may indicate activation of ARGs not specifically related to β-lactams, such as multidrug efflux pumps, encoded by the *marA, mdtEF, arcAB, and evgAS* genes which were predicted *in silico* for this strain (Fig. 3).

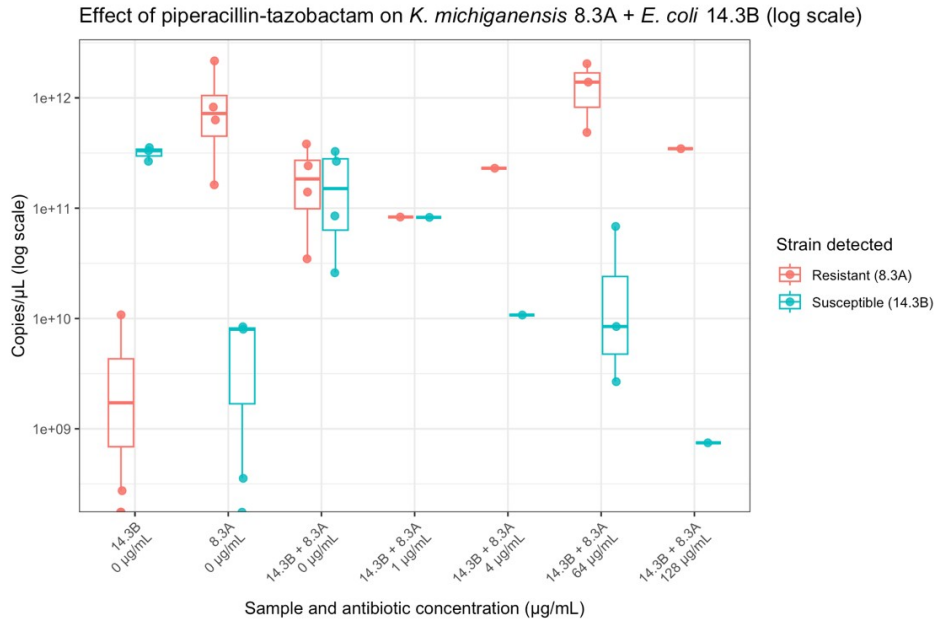

Fig. 65. Co-culture of K. michiganensis 8.3A and E. coli 14.3B with and without piperacillin/tazobactam plotted on logarithmic scale. The x-axis shows different samples of mono- and co-cultures with different piperacillin concentrations. On the logarithmic y-axis number of gene copies per µL of sample detected by dPCR are marked. Individual data points represent one biological replicate. Positive signals of the susceptible strain (blue) were detected in co-cultures with all antibiotic concentrations. Except for 1 and 64 µg/mL, signals remained comparable to the background signals observed in monoculture controls and were therefore not considered significant. The positive signal of susceptible strain in one biological replicate in the combination with ampicillin at 64 µg/mL suggests potential cross-protection.

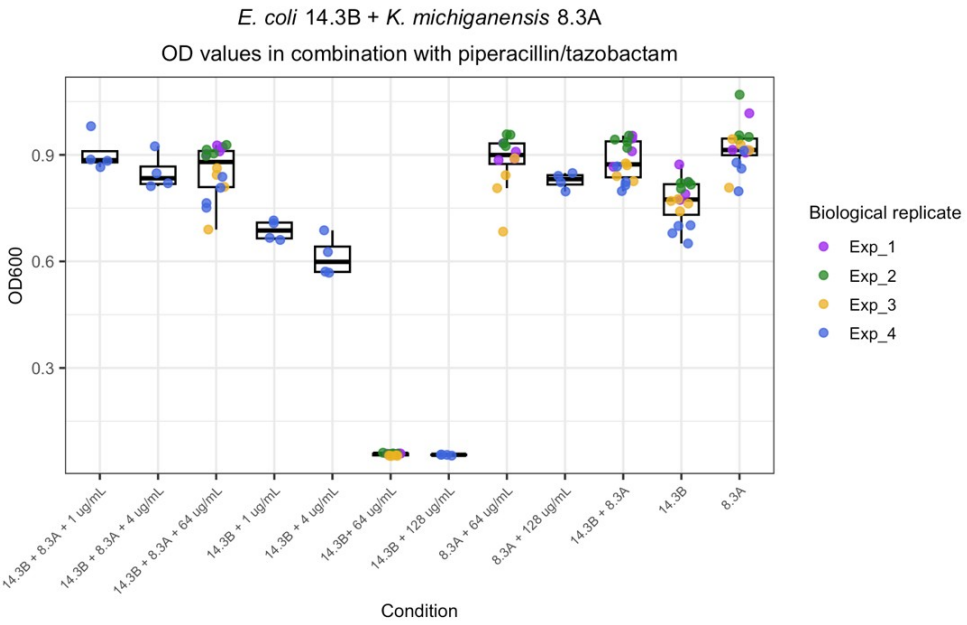

Fig. 66. Optical density measured from co-cultivation experiments of the combination K. michiganensis 8.3A and E. coli 14.3B with piperacillin/tazobactam. The x-axis shows different samples of mono- and co-cultures with different piperacillin concentrations. The y-axis shows OD_{600} values of the samples. It demonstrates the growth of susceptible E. coli 14.3B strain in monoculture with piperacillin at 1 μg/mL (MIC values) and 4 μg/mL (4xMIC).

A summary of the dPCR-derived copy numbers is presented in Tables 15-18. As discussed previously, quantitative interpretation of these values is limited by experimental variability and the need for further optimization of the assay. Therefore, the data were used primarily to identify qualitative trends in bacterial growth and survival under different co-cultivation conditions.

Piperacillin concentration [µg/mL]	**Strain**	**Growth in monoculture (Copies per µL)**	**Growth in co-culture (Copies per µL)**	**Change in growth between mono- and co-culture**	**Relative abundance in co-culture**
0	*K. michiganensis 8.3A* Resistant	$3.97 * 10^{11} \pm 3.42 * 10^{11}$	$3.66 * 10^{11} \pm 7.91 * 10^{10}$	-7.76%	48.12%
	E. coli 13.3C Susceptible	$4.49 * 10^{11} \pm 1.16 * 10^{11}$	$3.95 * 10^{11} \pm 1.05 * 10^{11}$	-12.14%	51.88%
1	*K. michiganensis 8.3A* Resistant		$1.78 * 10^{11}$	-70.35%	99.27%
	E. coli 13.3C Susceptible		$8.62 * 10^{8}$	-99.81%	0.73%
4	*K. michiganensis 8.3A* Resistant		$1.22 * 10^{11}$	-69.22%	99.02%
	E. coli 13.3C Susceptible		$1.21 * 10^{9}$	-99.73%	0.98%
64	*K. michiganensis 8.3A* Resistant		$3.80 * 10^{11} \pm 3.44 * 10^{11}$	-4.27%	99.62%
	E. coli 13.3C Susceptible		$1.47 * 10^{9} \pm 1.93 * 10^{9}$	-99.67%	0.38%
128	*K. michiganensis 8.3A* Resistant		$1.89 * 10^{11}$	-55.29%	100%
	E. coli 13.3C Susceptible		0	-100%	0%

Table 15. dPCR analysis of resistant K. michiganensis 8.3A and susceptible E. coli 13.3C during co-cultivation under different piperacillin concentrations with constant tazobactam concentration at 4 µg/mL. Growth is expressed as DNA copy number per µL (mean ± SD, where applicable). Relative abundance indicates the contribution of each strain to the total bacterial population in co-culture. Percentage changes in growth were calculated relative to the corresponding monoculture grown without antibiotic treatment.

Piperacillin concentration [µg/mL]	Strain	Growth in monoculture (Copies per µL)	Growth in co-culture (Copies per µL)	Change in growth between mono- and co-culture	Relative abundance in co-culture
0	*K. michiganensis 8.3A* Resistant	$9.46 * 10^{11} \pm 8.59 * 10^{11}$	$1.99 * 10^{11} \pm 1.48 * 10^{11}$	-78.89%	53.16%
	E. coli 14.3B Susceptible	$3.17 * 10^{11} \pm 4.57 * 10^{10}$	$1.76 * 10^{11} \pm 1.43 * 10^{11}$	-44.55%	46.84%
1	*K. michiganensis 8.3A* Resistant		$8.31 * 10^{10}$	-91.22%	50.16%
	E. coli 14.3B Susceptible		$8.26 * 10^{10}$	-73.99%	49.84%
4	*K. michiganensis 8.3A* Resistant		$2.3 * 10^{11}$	-75.66%	95.54%
	E. coli 14.3B Susceptible		$1.08 * 10^{10}$	-96.61%	4.46%
64	*K. michiganensis 8.3A* Resistant		$9.8 * 10^{11} \pm 7.81 * 10^{11}$	3.49%	98.01%
	E. coli 14.3B Susceptible		$1.99 * 10^{10} \pm 3.25 * 10^{10}$	-93.74%	1.99%
128	*K. michiganensis 8.3A* Resistant		$3.46 * 10^{11}$	-63.4%	99.78%
	E. coli 14.3B Susceptible		$7.46 * 10^{8}$	-99.76%	0.22%

Table 16. dPCR analysis of resistant K. michiganensis 8.3A and susceptible E. coli 14.3B during co-cultivation under different piperacillin concentrations with constant tazobactam concentration at 4 µg/mL. Growth is expressed as DNA copy number per µL (mean ± SD, where applicable). Relative abundance indicates the contribution of each strain to the total bacterial population in co-culture. Percentage changes in growth were calculated relative to the corresponding monoculture grown without antibiotic treatment.

Piperacillin concentration [µg/mL]	Strain	Growth in monoculture (Copies per	Growth in co-culture (Copies per	Change in growth between	Relative abundance in co-culture

		µL)	µL)	mono- and co-culture	
0	*K. michiganensis 8.3A* Resistant	$5.01 * 10^{11} \pm 3.85 * 10^{11}$	$2.26 * 10^{11} \pm 8.63 * 10^{10}$	-54.99%	46.92%
	K. pneumoniae 40.9B Susceptible	$4.06 * 10^{11} \pm 1.33 * 10^{11}$	$2.55 * 10^{11} \pm 9.65 * 10^{10}$	-37.19%	53.08%
4	*K. michiganensis 8.3A* Resistant		$1.83 * 10^{11}$	-63.53%	100%
	K. pneumoniae 40.9B Susceptible		0	-100%	0%
16	*K. michiganensis 8.3A* Resistant		$3.44 * 10^{11}$	-31.28%	99.33%
	K. pneumoniae 40.9B Susceptible		$2.34 * 10^{9}$	-99.42%	0.67%
64	*K. michiganensis 8.3A* Resistant		$3.46 * 10^{11} \pm 1.38 * 10^{11}$	-30.9%	100%
	K. pneumoniae 40.9B Susceptible		0	-100%	0%
128	*K. michiganensis 8.3A* Resistant		$2.97 * 10^{11}$	-40.83%	100%
	K. pneumoniae 40.9B Susceptible		0	-100%	0%

Table 17. dPCR analysis of resistant K. michiganensis 8.3A and susceptible K. pneumoniae 40.9B during co-cultivation under different piperacillin concentrations with constant tazobactam concentration at 4 µg/mL. Growth is expressed as DNA copy number per µL (mean ± SD, where applicable). Relative abundance indicates the contribution of each strain to the total bacterial population in co-culture. Percentage changes in growth were calculated relative to the corresponding monoculture grown without antibiotic treatment.

Piperacillin concentration [µg/mL]	**Strain**	**Growth in monoculture (Copies per µL)**	**Growth in co-culture (Copies per µL)**	**Change in growth between mono- and co-culture**	**Relative abundance in co-culture**
0	*K. michiganensis 8.3A*	$6.46 * 10^{11}$	$3.29 * 10^{11}$	-49.16%	37.34%

	Resistant	± 4.35 * 10^{11}	± 2.23 * 10^{11}		
	K. pneumoniae 2.3A Susceptible	8.16 * 10^{11} ± 5.94 * 10^{11}	5.51 * 10^{11} ± 2.73 * 10^{11}	-32.46%	62.66%
2	*K. michiganensis 8.3A* Resistant		3.65 * 10^{11}	-43.55%	99.4%
	K. pneumoniae 2.3A Susceptible		2.23 * 10^{9}	-99.73%	0.6%
8	*K. michiganensis 8.3A* Resistant		2.06 * 10^{11}	-68.09%	99.23%
	K. pneumoniae 2.3A Susceptible		1.6 * 10^{9}	-99.8%	0.77%
64	*K. michiganensis 8.3A* Resistant		7.27 * 10^{11}	12.56%	100%
	K. pneumoniae 2.3A Susceptible		0	-100%	0%
128	*K. michiganensis 8.3A* Resistant		4.6 * 10^{11}	-28.85%	100%
	K. pneumoniae 2.3A Susceptible		0	-100%	0%

Table 18. dPCR analysis of resistant K. michiganensis 8.3A and susceptible K. pneumoniae 2.3A during co-cultivation under different piperacillin concentrations with constant tazobactam concentration at 4 μg/mL. Growth is expressed as DNA copy number per μL (mean ± SD, where applicable). Relative abundance indicates the contribution of each strain to the total bacterial population in co-culture. Percentage changes in growth were calculated relative to the corresponding monoculture grown without antibiotic treatment.

Combinations with gentamicin

Staphylococcus epidermidis 8.2A was selected as a gentamicin resistant strain for combinations, because of its clear resistance pattern in MIC assays (Fig. 44) and the presence of aminoglycoside-specific ARGs including the *aac(6')-Ie-aph(2")-Ia* gene (Fig. 3). It was combined with five susceptible strains: *E. coli 13.3C, E. coli 14.3B, K. pneumoniae 40.9B, K.*

pneumoniae 2.3A, and *K. michiganensis 8.3A*. It is important to note that in co-cultures without antibiotic only the susceptible strains showed substantial growth, while *S. epidermidis 8.2A* appeared to be outcompeted. No evidence of cross-protection was detected for the combination with *E. coli 13.3C* (Fig. 67).

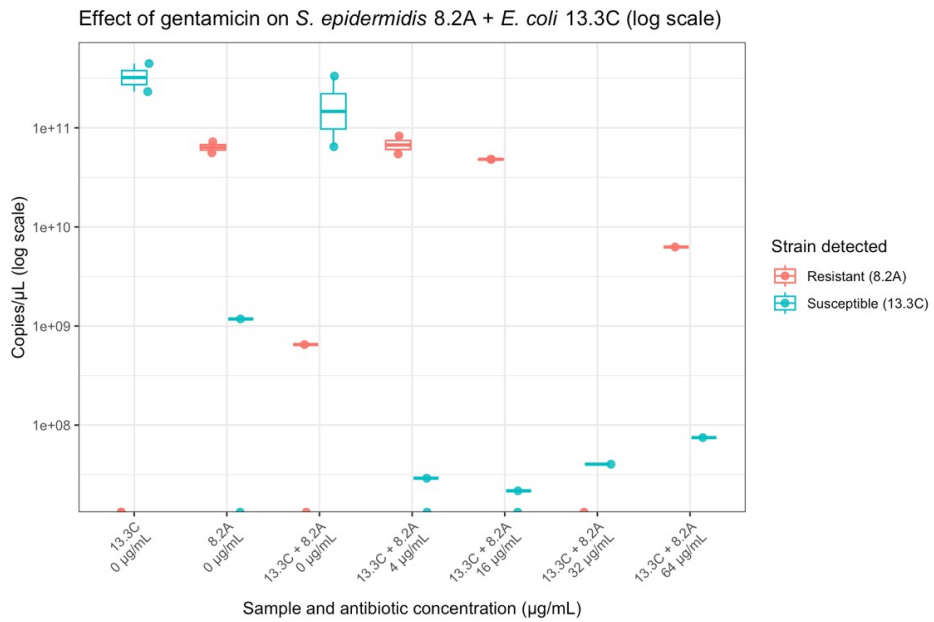

Fig. 67. Co-culture of S. epidermidis 8.2A and E. coli 13.3C with and without gentamicin plotted on logarithmic scale. The x-axis shows different samples of mono- and co-cultures with different gentamicin concentrations. On the logarithmic y-axis number of gene copies per µL of sample detected by dPCR are marked. Individual data points represent one biological replicate. Weak positive signals of the susceptible strain (blue) were detected in co-cultures with all antibiotic concentrations; however, they remained lower than the background signal observed in monoculture control and were therefore not considered significant.

However, potential cross-protection was observed in several other combinations. In co-cultures of *E. coli 14.3B* with *S. epidermidis 8.2A* (Fig. 68), weak but reproducible growth of the susceptible strain was detected at multiple gentamicin concentrations (4, 16, and 32 µg/mL), exceeding the levels observed in the monoculture control (Fig. 68: "8.2A 0 µg/mL"). At the same time, *E. coli 14.3B* demonstrated limited growth in monoculture at 4 µg/mL gentamicin (MIC concentration) in two of four technical replicates, as shown by optical density measurements (Fig. 69), indicating heterogeneous behaviour of the susceptible strain between MIC assays and co-cultivation experiments. Based on this heterogeneity, only the growth of *E. coli 14.3B* at 32 µg/mL of gentamicin could be considered potential cross-protection.

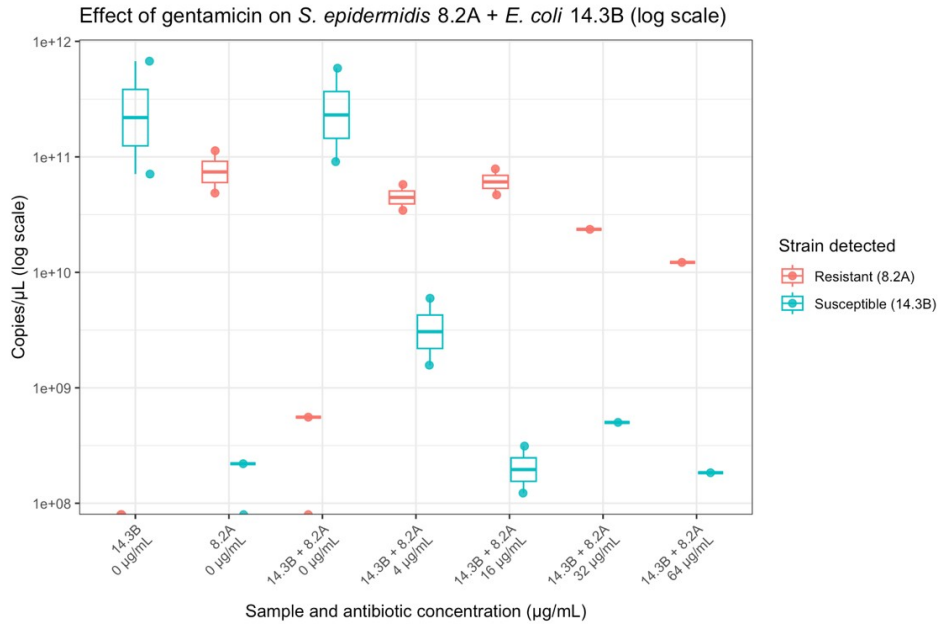

Fig. 68. Co-culture of S. epidermidis 8.2A and E. coli 14.3B with and without gentamicin plotted on logarithmic scale. The x-axis shows different samples of mono- and co-cultures with different gentamicin concentrations. On the logarithmic y-axis number of gene copies per µL of sample detected by dPCR are marked. Individual data points represent one biological replicate. Positive signals of the susceptible strain (blue) were detected in co-cultures at antibiotic concentrations of 4, 16 and 32 µg/mL. Further weak positive signal was detected in co-cultures at 64 µg/mL of gentamicin, however it remained lower than the background signal observed in monoculture control and were therefore not considered significant.

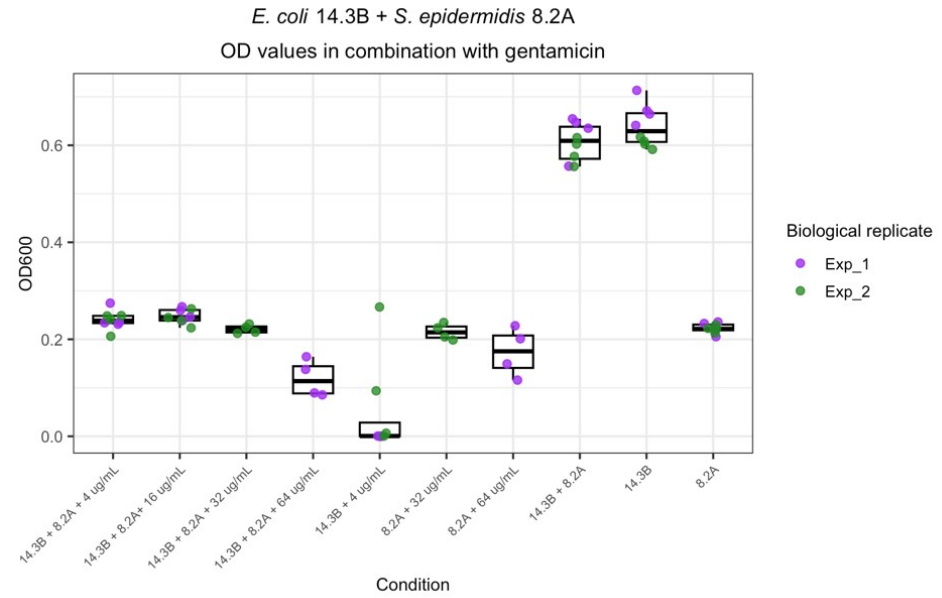

Fig. 69. Optical density of co-cultivation experiments of combination S. epidermidis 8.2A and E. coli 14.3B with gentamicin. The x-axis shows different samples of mono- and co-cultures with different gentamicin concentrations. The y-axis shows OD_{600} values of the samples. The figure demonstrates limited growth of the susceptible E. coli 14.3B strain in monoculture with gentamicin concentrations of 4 µg/mL in two out of four technical replicates.

Similar observations were made for *K. pneumoniae 40.9B* (Fig. 70) and *K. pneumoniae 2.3A* (Fig. 72). In co-cultures of *K. pneumoniae 40.9B* with *S. epidermidis 8.2A* growth of the

susceptible strain was detected at all three tested gentamicin concentrations. However, weak growth of *K. pneumoniae 40.9B* was also observed in monoculture at the MIC concentration based on optical density measurements (Fig. 71), making the results obtained at 4 and 32 µg/mL of gentamicin more relevant for interpretation as potential cross-protection. Similarly, *K. pneumoniae 2.3A* demonstrated growth in co-culture at 1, 4, and 32 µg/mL of gentamicin, although the signal at 32 µg/mL remained very weak. Since this strain was also able to grow alone at 1 µg/mL gentamicin (Fig. 73), only growth detected at 4 and 32 µg/mL was considered relevant for potential cross-protection.

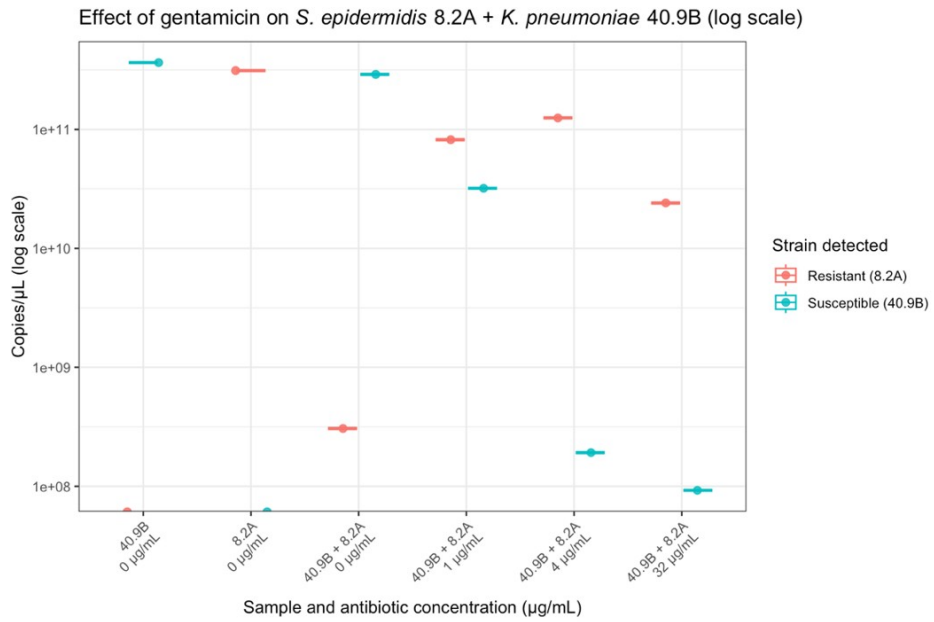

Fig. 70. Co-culture of S. epidermidis 8.2A and K. pneumoniae 40.9B with and without gentamicin plotted on logarithmic scale. The x-axis shows different samples of mono- and co-cultures with different gentamicin concentrations. On the logarithmic y-axis number of gene copies per µL of sample detected by dPCR are marked. Individual data points represent one biological replicate. Positive signals of the susceptible strain (blue) were detected in co-cultures at antibiotic concentrations of 1, 4 and 32 µg/mL

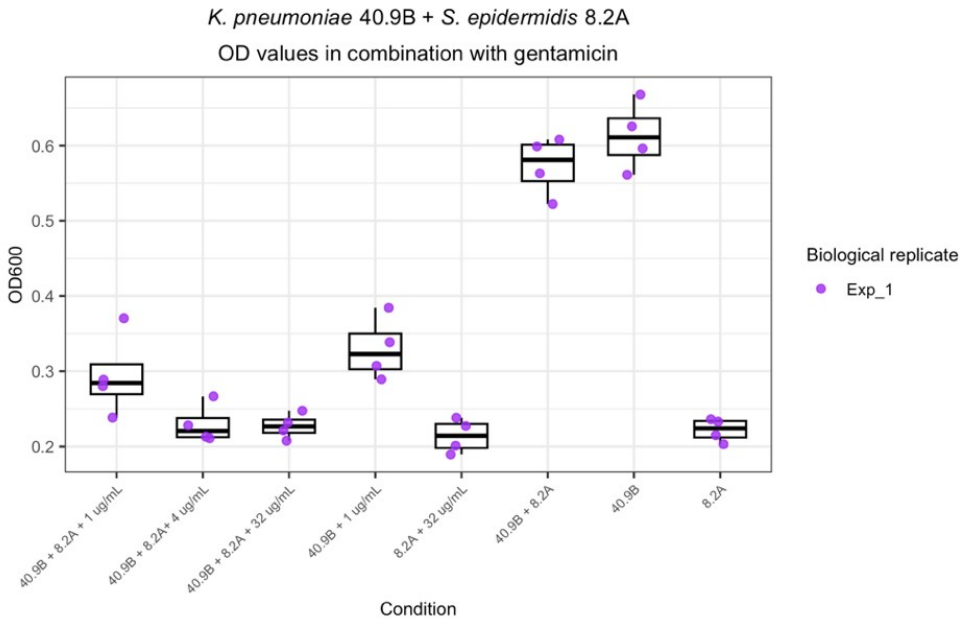

Fig. 71. Optical density of co-cultivation experiments of combination S. epidermidis 8.2A and K. pneumoniae 40.9B with gentamicin. The x-axis shows different samples of mono- and co-cultures with different gentamicin concentrations. The y-axis shows OD_{600} values of the samples. The figure demonstrates limited growth of the susceptible K. pneumoniae 40.9B strain in monoculture with gentamicin concentrations of 1 μg/mL (MIC value).

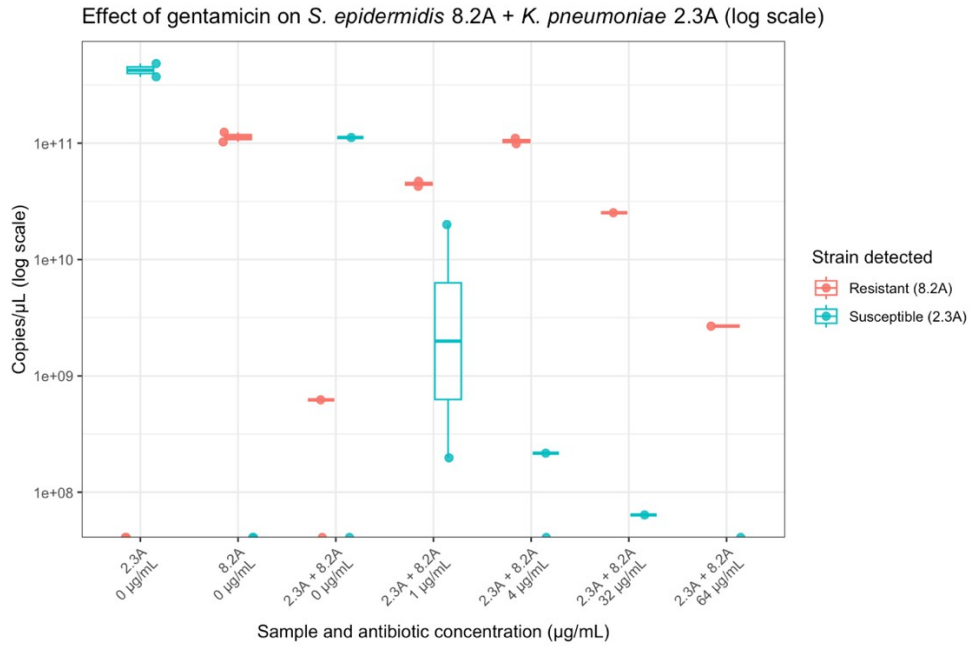

Fig. 72. Co-culture of S. epidermidis 8.2A and K. pneumoniae 2.3A with and without gentamicin plotted on logarithmic scale. The x-axis shows different samples of mono- and co-cultures with different gentamicin concentrations. On the logarithmic y-axis number of gene copies per µL of sample detected by dPCR are marked. Individual data points represent one biological replicate. Positive signals of the susceptible strain (blue) were detected in co-cultures at antibiotic concentrations of 1, 4 and 32 µg/mL.

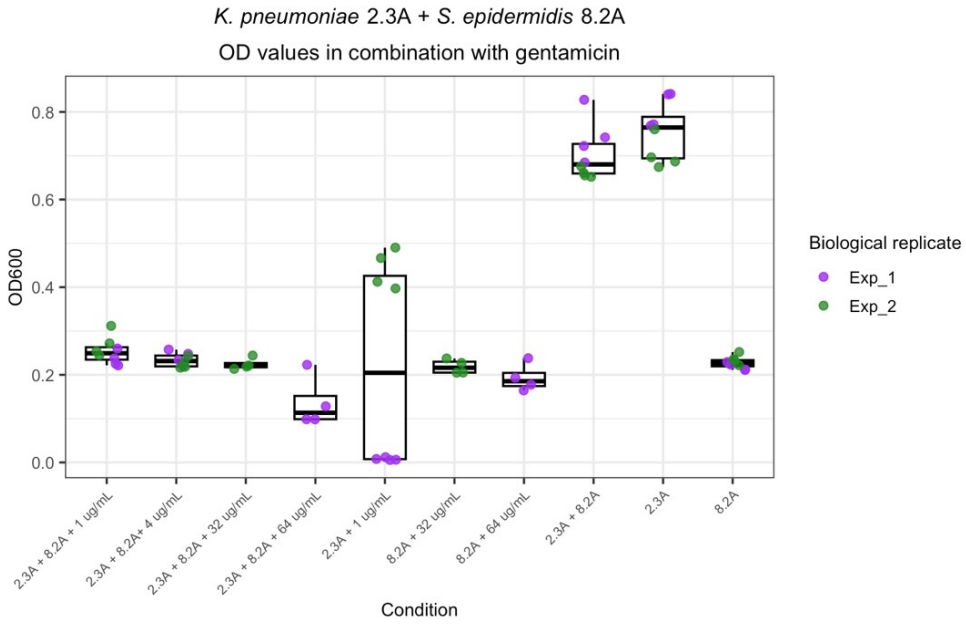

Fig. 73. Optical density of co-cultivation experiments of combination S. epidermidis 8.2A and K. pneumoniae 2.3A with gentamicin. The x-axis shows different samples of mono- and co-cultures with different gentamicin concentrations. The y-axis shows OD_{600} values of the samples. The figure demonstrates limited growth of the susceptible K. pneumoniae 2.3A strain in monoculture with gentamicin concentrations of 1 µg/mL in one biological replicate.

In the combination *S. epidermidis 8.2A* + *K. michiganensis 8.3A* the susceptible strain also survived at gentamicin concentration of 2 µg/mL (MIC value) in co-culture, while growth of *S. epidermidis 8.2A* was inhibited (at least not detected by dPCR) (Fig. 74). However, weak growth of *K. michiganensis 8.3A* was observed in monoculture at the same gentamicin concentration based on optical density measurements (Fig. 75), limiting the interpretation of the result as cross-protection.

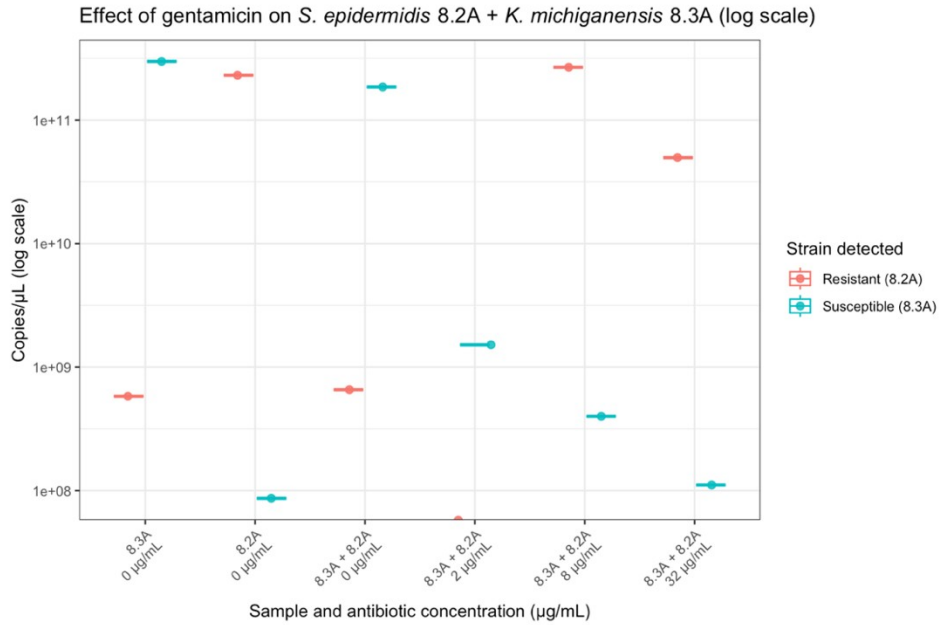

Fig. 74. Co-culture of S. epidermidis 8.2A and K. michiganensis 8.3A with and without gentamicin plotted on logarithmic scale. The x-axis shows different samples of mono- and co-cultures with different gentamicin concentrations. On the logarithmic y-axis number of gene copies per µL of sample detected by dPCR are marked. Individual data points represent one biological replicate. Positive signals of the susceptible strain (blue) were detected in co-cultures at antibiotic concentrations of 1 µg/mL. Further weak positive signals were detected in co-cultures with all other antibiotic concentrations, however they remained lower than the background signal observed in monoculture control and were therefore not considered significant.

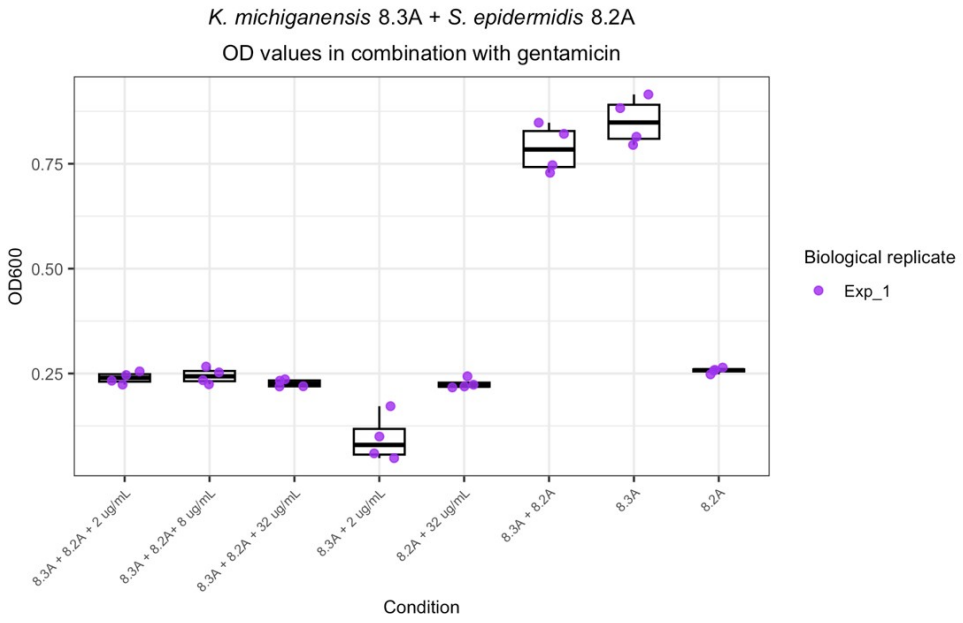

Fig. 75. Optical density of co-cultivation experiments of combination S. epidermidis 8.2A and K. michiganensis 8.3A with gentamicin. The x-axis shows different samples of mono- and co-cultures with different gentamicin concentrations. The y-axis shows OD_{600} values of the samples. The figure demonstrates limited growth of the susceptible K. michiganensis 8.3A strain in monoculture with gentamicin concentrations of 2 μg/mL (MIC value).

The dPCR data obtained from monocultures and co-cultures are presented in Tables 19-23. While these measurements should not be interpreted quantitatively, they provide additional

support for the qualitative interpretation of strain survival and growth under different gentamicin concentrations.

Gentamicin concentration [μg/mL]	Strain	Growth in monoculture (Copies per μL)	Growth in co-culture (Copies per μL)	Change in growth between mono- and co-culture	Relative abundance in co-culture
0	*S. epidermidis 8.2A* Resistant	$6.41 * 10^{10} \pm 1.14 * 10^{10}$	$3.25 * 10^{8} \pm 4.6 * 10^{8}$	-99.49%	0.16%
	E. coli 13.3C Susceptible	$3.39 * 10^{11} \pm 1.51 * 10^{11}$	$1.99 * 10^{11} \pm 1.9 * 10^{11}$	-41.39%	99.84%
4	*S. epidermidis 8.2A* Resistant		$6.86 * 10^{10} \pm 1.99 * 10^{10}$	7.09%	99.98%
	E. coli 13.3C Susceptible		$1.45 * 10^{7} \pm 2.06 * 10^{7}$	-99.99%	0.02%
16	*S. epidermidis 8.2A* Resistant		$4.81 * 10^{10} \pm 2.35 * 10^{7}$	-24.9%	99.98%
	E. coli 13.3C Susceptible		$1.08 * 10^{8} \pm 4.6 * 10^{7}$	-99.99%	0.02%
32	*S. epidermidis 8.2A* Resistant		0	-100%	0%
	E. coli 13.3C Susceptible		$4.03 * 10^{7}$	-99.99%	100%
64	*S. epidermidis 8.2A* Resistant		$6.27 * 10^{9}$	-90.21%	98.82%
	E. coli 13.3C Susceptible		$7.48 * 10^{7}$	-99.98%	1.18%

Table 19. dPCR analysis of resistant S. epidermidis 8.2A and susceptible E. coli 13.3C during co-cultivation under different gentamicin concentrations. Growth is expressed as DNA copy number per μL (mean ± SD, where applicable). Relative abundance indicates the contribution of each strain to the total bacterial population in co-culture. Percentage changes in growth were calculated relative to the corresponding monoculture grown without antibiotic treatment.

Gentamicin concentration	Strain	Growth in monoculture	Growth in co-culture	Change in growth	Relative abundance

[μg/mL]		(Copies per μL)	(Copies per μL)	between mono- and co-culture	in co-culture
0	*S. epidermidis 8.2A* Resistant	$8.08 * 10^{10} \pm 4.56 * 10^{10}$	$2.78 * 10^{8} \pm 3.94 * 10^{8}$	-99.66%	0.08%
	E. coli 14.3B Susceptible	$3.72 * 10^{11} \pm 4.27 * 10^{11}$	$3.39 * 10^{11} \pm 3.50 * 10^{11}$	-9.13%	99.92%
4	*S. epidermidis 8.2A* Resistant		$4.60 * 10^{10} \pm 1.64 * 10^{10}$	-43.03%	92.44%
	E. coli 14.3B Susceptible		$3.77 * 10^{9} \pm 3.11 * 10^{9}$	-98.99%	7.56%
16	*S. epidermidis 8.2A* Resistant		$6.28 * 10^{10} \pm 2.25 * 10^{10}$	-22.31%	99.65%
	E. coli 14.3B Susceptible		$2.18 * 10^{8} \pm 1.3 * 10^{8}$	-99.94%	0.35%
32	*S. epidermidis 8.2A* Resistant		$2.36 * 10^{10}$	-70.83%	97.92%
	E. coli 14.3B Susceptible		$5.01 * 10^{8}$	-99.87%	2.08%
64	*S. epidermidis 8.2A* Resistant		$1.21 * 10^{10}$	-84.91%	98.51%
	E. coli 14.3B Susceptible		$1.84 * 10^{8}$	-99.95%	1.49%

Table 20. dPCR analysis of resistant S. epidermidis 8.2A and susceptible E. coli 14.3B during co-cultivation under different gentamicin concentrations. Growth is expressed as DNA copy number per μL (mean ± SD, where applicable). Relative abundance indicates the contribution of each strain to the total bacterial population in co-culture. Percentage changes in growth were calculated relative to the corresponding monoculture grown without antibiotic treatment.

Gentamicin concentration [μg/mL]	Strain	Growth in monoculture (Copies per μL)	Growth in co-culture (Copies per μL)	Change in growth between mono- and	Relative abundance in co-culture

				co-culture	
0	*S. epidermidis 8.2A* Resistant	$1.13 * 10^{11} \pm 1.53 * 10^{10}$	$3.11 * 10^{8} \pm 4.4 * 10^{8}$	-99.73%	0.55%
	K. pneumoniae 2.3A Susceptible	$4.28 * 10^{11} \pm 7.93 * 10^{10}$	$5.59 * 10^{10} \pm 7.91 * 10^{10}$	-86.93%	99.45%
1	*S. epidermidis 8.2A* Resistant		$4.48 * 10^{10} \pm 3.11 * 10^{9}$	-60.48%	81.61%
	K. pneumoniae 2.3A Susceptible		$1.01 * 10^{10} \pm 1.4 * 10^{10}$	-97.64%	18.39%
4	*S. epidermidis 8.2A* Resistant		$1.05 * 10^{11} \pm 7.8 * 10^{9}$	-7.76%	99.9%
	K. pneumoniae 2.3A Susceptible		$1.08 * 10^{8} \pm 1.5 * 10^{8}$	-99.97%	0.1%
32	*S. epidermidis 8.2A* Resistant		$2.53 * 10^{10}$	-77.71%	99.75%
	K. pneumoniae 2.3A Susceptible		$6.38 * 10^{7}$	-99.99%	0.25%
64	*S. epidermidis 8.2A* Resistant		$2.68 * 10^{9}$	-97.63%	100%
	K. pneumoniae 2.3A Susceptible		0	-100%	0%

Table 21. dPCR analysis of resistant S. epidermidis 8.2A and susceptible K. pneumoniae 2.3A during co-cultivation under different gentamicin concentrations. Growth is expressed as DNA copy number per µL (mean ± SD, where applicable). Relative abundance indicates the contribution of each strain to the total bacterial population in co-culture. Percentage changes in growth were calculated relative to the corresponding monoculture grown without antibiotic treatment.

Gentamicin concentration [µg/mL]	**Strain**	**Growth in monoculture (Copies per µL)**	**Growth in co-culture (Copies per µL)**	**Change in growth between mono- and co-culture**	**Relative abundance in co-culture**
0	*S. epidermidis 8.2A*	$3.12 * 10^{11}$	$3.06 * 10^{8}$	-99.9%	0.11%

	Resistant				
	K. pneumoniae 40.9B Susceptible	3.65 * 10^{11}	2.9 * 10^{11}	-20.4%	99.89%
1	*S. epidermidis 8.2A* Resistant		8.19 * 10^{10}	-73.79%	71.88%
	K. pneumoniae 40.9B Susceptible		3.2 * 10^{10}	-91.22%	28.12%
4	*S. epidermidis 8.2A* Resistant		1.25 * 10^{11}	-59.99%	99.85%
	K. pneumoniae 40.9B Susceptible		1.92 * 10^{8}	-99.94%	0.15%
32	*S. epidermidis 8.2A* Resistant		2.4 * 10^{10}	-92.29%	99.62%
	K. pneumoniae 40.9B Susceptible		9.2 * 10^{7}	-99.97%	0.38%

Table 22. dPCR analysis of resistant S. epidermidis 8.2A and susceptible K. pneumoniae 40.9B during co-cultivation under different gentamicin concentrations. Growth is expressed as DNA copy number per μL (mean ± SD, where applicable). Relative abundance indicates the contribution of each strain to the total bacterial population in co-culture. Percentage changes in growth were calculated relative to the corresponding monoculture grown without antibiotic treatment.

Gentamicin concentration [μg/mL]	**Strain**	**Growth in monoculture (Copies per μL)**	**Growth in co-culture (Copies per μL)**	**Change in growth between mono- and co-culture**	**Relative abundance in co-culture**
0	*S. epidermidis 8.2A* Resistant	2.3 * 10^{11}	6.56 * 10^{8}	-99.71%	0.35%
	K. michiganensis 8.3A	2.98 * 10^{11}	1.85 * 10^{11}	-37.82%	99.65%

	Susceptible				
2	*S. epidermidis 8.2A* Resistant		0	-100%	0%
	K. michiganensis 8.3A Susceptible		$1.52 * 10^9$	-99.49%	100%
8	*S. epidermidis 8.2A* Resistant		$2.67 * 10^{11}$	16.11%	99.85%
	K. michiganensis 8.3A Susceptible		$3.99 * 10^8$	-99.87%	0.15%
32	*S. epidermidis 8.2A* Resistant		$4.96 * 10^{10}$	-78.45%	99.78%
	K. michiganensis 8.3A Susceptible		$1.11 * 10^8$	-99.96%	0.22%

Table 23. dPCR analysis of resistant S. epidermidis 8.2A and susceptible K. michiganensis 8.3A during co-cultivation under different gentamicin concentrations. Growth is expressed as DNA copy number per μL (mean ± SD, where applicable). Relative abundance indicates the contribution of each strain to the total bacterial population in co-culture. Percentage changes in growth were calculated relative to the corresponding monoculture grown without antibiotic treatment.

Discussion

The obtained results show that genomic predictions of antibiotic resistance in general correlate with phenotypic data from MIC assays, however the presence or absence of ARGs did not always directly reflect the observed susceptibility profile. For β-lactam antibiotics, the correlation between *in silico* analysis and MIC results was most evident: strains encoding β-lactamases were, in most cases, resistant to ampicillin and/or piperacillin, whereas strains lacking the relevant genes remained susceptible. Notably, all *Bifidobacterium* and *Lactobacillus* strains included in this study were susceptible to β-lactams, which is consistent with the absence of β-lactam resistance determinants in their genomes. This finding is

particularly relevant, as ampicillin is one of the most frequently administered antibiotics in NICUs and is routinely used in treatment regimens for preterm infants (Butranova, O., et al., 2023; Simeoli, R., et al., 2022). Consequently, exposure to ampicillin may not only affect potential pathogens, but also beneficial members of the developing gut microbiome. The addition of tazobactam decreased resistance in all but one strain, confirming the central role of β-lactamases in the resistant phenotype. Nevertheless, certain deviations, e.g. *S. epidermidis LH_NM_637*, demonstrated that the presence of a gene or an operon does not necessary indicate its functional activity.

Results for gentamicin resistance demonstrated a weaker genotype - phenotype correlation. An increase in MIC values for several strains confirmed the limited effectiveness of gentamicin under anaerobic conditions. Furthermore, *Lactobacillus* spp. were found to be resistant to gentamicin in the absence of aminoglycoside-specific ARGs, which is consistent with the intrinsic resistance of *lactobacilli* described in the literature. This resistance might be associated with specific mechanisms of antibiotic transport across the cell membrane (Dec, M., et al., 2017; Abriouel, H. et al., 2015). The results of MIC assays confirm that phenotypic resistance may be determined not only by specific resistance genes, but also by bacterial physiology, environmental conditions, and mechanisms that are not always clearly identified by standard genomic screening.

An important limitation in the interpretation of MIC data is the lack of EUCAST reference values for some of the species studied, including *Lactobacillus, Bifidobacterium,* and *Klebsiella*. This complicates the formal classification of strains into susceptible and resistant groups and makes interpretation dependent on phenotypic observations and comparisons with closely related species. An additional problem is the lack of a universal protocol, equally applicable to all bacterial strains studied. Different groups of microorganisms have specific requirements regarding culture media and conditions, for example, *Bifidobacterium* and *Lactobacillus* spp. did not show consistent growth in MHB, whereas members of the *Enterobacteriaceae* family grew well in all tested media. This is particularly important, as the composition of the culture medium itself can influence bacterial growth and the development of antibiotic resistance, as well as antibiotics themselves.

Growth analysis confirmed the need to optimize proper cultivation conditions for each bacterial group. MHB proved to be suitable for the *Enterobacteriaceae* family but did not support stable growth of more demanding or strictly anaerobic bacteria, even after the addition of essential components (L-cysteine). The use of alternative media, such as BHI or an MHB/MRS mixture, enabled us to identify more suitable conditions for further experiments. However, their effects

on antibiotic stability should also be tested in advance. These data are important not only technically, but also conceptually. If the growth of a strain in the selected medium is unstable, then further interpretation of its antibiotic susceptibility or interactions in co-culture becomes less reliable. Moreover, nutrient availability and medium composition can alter bacterial metabolic activity and gene expression, potentially influencing resistance patterns and interspecies interactions (Bottery, M., et al., 2020; Adamowicz, E., et al., 2018; De Vos, M., et al., 2017).

Co-cultivation experiments showed that potential cross-protection may occur only in certain combinations of strains and antibiotics. The most convincing evidence of such an effect was observed in experiments involving piperacillin/tazobactam and gentamicin, where a susceptible strain survived in co-culture at antibiotic concentrations at which it did not grow in monoculture. However, these results should be interpreted carefully, because in some cases susceptible bacteria demonstrated growth even in monoculture at previously inhibitory antibiotic concentrations, indicating variability within the same strain and even single colony. This made it difficult to reliably determine the MIC at which a susceptible strain is unable to survive on its own and consequently complicated the demonstration of cross-protection. For future experiments, if cross-protection is detected again, additional experiments should be performed to exclude horizontal gene transfer between resistant and susceptible strains and to confirm that the observed effect results from interspecies interactions.

Interestingly, in several co-culture experiments no measurable fitness cost associated with antibiotic resistance was observed in the absence of antibiotics, as resistant strains did not show reduced growth compared to susceptible strains. At the same time, both strains generally exhibited slightly lower growth in co-culture than in monoculture, suggesting competition for available nutrients without complete competitive exclusion. In the absence of gentamicin, all susceptible strains tested (*Escherichia* and *Klebsiella* spp.) appeared to outcompete the resistant *Staphylococcus* strain, indicating a competitive advantage under antibiotic-free conditions. However, this pattern changed in the presence of antibiotic. While *E. coli* showed strongly reduced growth even at low antibiotic concentrations, *Klebsiella* spp. largely lost their competitive advantage and became more comparable to the resistant *Staphylococcus*. This observation suggests that antibiotics may alter interspecies competition even at subinhibitory concentrations, thereby influencing community structure before complete growth inhibition occurs.

An additional limiting factor was the detection of weak positive dPCR signals in monocultures where the relevant strains were absent. As the specificity of the primers had been verified and

contamination had been ruled out by conventional PCR, such signals were interpreted as either technical background noise in dPCR or low-level contamination undetectable by PCR. However, this made it difficult to establish a reliable threshold above which the signal could be considered indicative of bacterial growth in co-cultures. For further experiments, it will be necessary to optimize the overall experimental protocol to improve the sensitivity and specificity of detecting each strain in the combined culture.

Despite these limitations, the data suggest that interbacterial interactions may influence the response of microorganisms to antibiotics. Possible cross-protection could be linked to the degradation of the antibiotic by the resistant strain, the activation of non-specific resistance mechanisms, such as multidrug efflux pump systems, or other types of interactions between bacteria. Additionally, the role of cross-feeding should not be excluded, where metabolic interactions between strains may alter their resistance or tolerance to antibiotics (Semenec, L., et al., 2022; Adamowicz, E., et al., 2018). These effects are especially important in the context of the gut microbiome, where bacteria live in a complex community.

For further experiments, it would be reasonable to increase the number of biological replicates and optimize co-cultivation parameters. In particular, the initial inoculum and the ratio between strains should be tested, because the relative abundance of community members could significantly influence interspecies interactions (Ruelens, P., et al., 2025; Denk-Lobnig, M., et al., 2023). Another promising approach involves performing antibiotic susceptibility testing and co-cultivation on agar, which would demonstrate how the spatial distribution of bacteria influences cross-protection, particularly given that such effects may be more pronounced in biofilms and dense bacterial communities (Liu, H., et al., 2024).

In the future beneficial bacteria such as *Bifidobacterium* and *Lactobacillus* spp. also should be included in the analysis. Particularly interesting is the question of whether Lactobacillus strains that are resistant to gentamicin under aerobic conditions can protect opportunistic bacteria. This may have clinical significance, as probiotic bacteria can be administered to preterm infants to support the development of a healthy gut microbiome (Panwar, R., et al., 2021). Therefore, testing probiotic strains of *Lactobacillus* for antibiotic resistance and cross-protection could be an important area for further research.

The β-lactamase activity of the studied strains deserves special attention. Since β-lactamases can reduce the concentration of the antibiotic in the environment and thereby protect susceptible bacteria, direct measurement of β-lactamase activity would help to better explain the effects observed in co-cultures. Furthermore, unpublished data on the presence of ampicillin and its derivatives in stool samples from the study cohort confirm this antibiotic to

be present in the intestinal lumen and potentially undergoes bacterial degradation. This makes the study of β-lactamase activity and cross-protection particularly relevant for this cohort.
In summary, this study confirms that *in silico* analysis of ARGs is a helpful tool for the initial prediction of antibiotic resistance; however, it cannot completely replace phenotypic analysis. MIC assays remain an essential step for confirming functional resistance. Despite technical limitations, co-cultivation experiments demonstrated the significance of interspecies interactions for bacterial survival in the presence of antibiotics. This highlights the need to study antibiotic resistance not only at the level of individual isolates, but also in more complex models that better reflect the real-world conditions of the gut microbiome.

Conclusion

Extremely preterm neonates often remain hospitalized in NICUs for prolonged periods and are routinely administered broad-spectrum antibiotic therapy and subjected to invasive medical interventions (Thänert, R., et al., 2024). These conditions strongly affect the development of the gut microbiome and contribute to dysbiosis characterized by reduced microbial diversity and the predominance of opportunistic and antibiotic-resistant bacteria, including *Enterobacteriaceae, Staphylococcus,* and *Enterococcus* species (Mulinge, M., et al., 2023; Gibson, M., et al., 2016). Such microbiome changes have been associated not only with neonatal sepsis and necrotizing enterocolitis, but also with long-term neurodevelopmental complications, including white matter damage (Baranowski, J., et al., 2019; Wang, Y., et al.,

2023; Seki, D., et al., 2024). Therefore, understanding how gut-associated bacteria respond to antibiotics and interact within microbial communities is important for improving neonatal care and reducing microbiome disruption in vulnerable preterm infants.

This study demonstrated that genomic prediction of antibiotic resistance generally correlates with phenotypic resistance observed in MIC assays, although the presence or absence of ARGs did not always directly reflect the susceptibility profile of the bacteria. For β-lactam antibiotics, the correlation between *in silico* analysis and phenotypic testing was most clear, while gentamicin resistance appeared to be strongly affected by environmental conditions, especially oxygen availability. In addition, intrinsic resistance mechanisms were observed in *Lactobacillus* spp., highlighting that phenotypic resistance depends not only on ARGs, but also on bacterial physiology and growth conditions.

The results also showed that cultivation conditions play an important role in influencing both bacterial growth and antibiotic susceptibility testing. Different bacterial groups required different media and environmental conditions, demonstrating the absence of a universal cultivation protocol suitable for all gut-associated microorganisms. This is particularly relevant for beneficial gut-associated bacteria, as they are often more demanding with regards to cultivation media and environmental conditions.

Co-cultivation experiments suggested that interspecies interactions may influence bacterial survival in the presence of antibiotics. A potential cross-protection effect was observed in several combinations, particularly with piperacillin/tazobactam and gentamicin, where susceptible strains survived in co-culture at antibiotic concentrations, at which they would be inhibited in monoculture. However, interpretation of these results was limited by variable response of susceptible strains and background dPCR signals, indicating the need for further optimization of the experimental setup.

Taken together, the findings of this study demonstrate that genomic predictions alone are not sufficient for the accurate characterization of antibiotic resistance, and phenotypic testing should be performed to confirm functional resistance. The results also indicate that bacterial behaviour in microbial communities may differ from that in monoculture, as interactions between strains can lead to cross-protection of susceptible ones. Therefore, investigating antibiotic resistance in complex communities is important for a better understanding of resistance dynamics within the preterm infant gut microbiome and may help to improve future antimicrobial and healthy microbiome-supportive strategies in NICUs.

Supplemental Materials

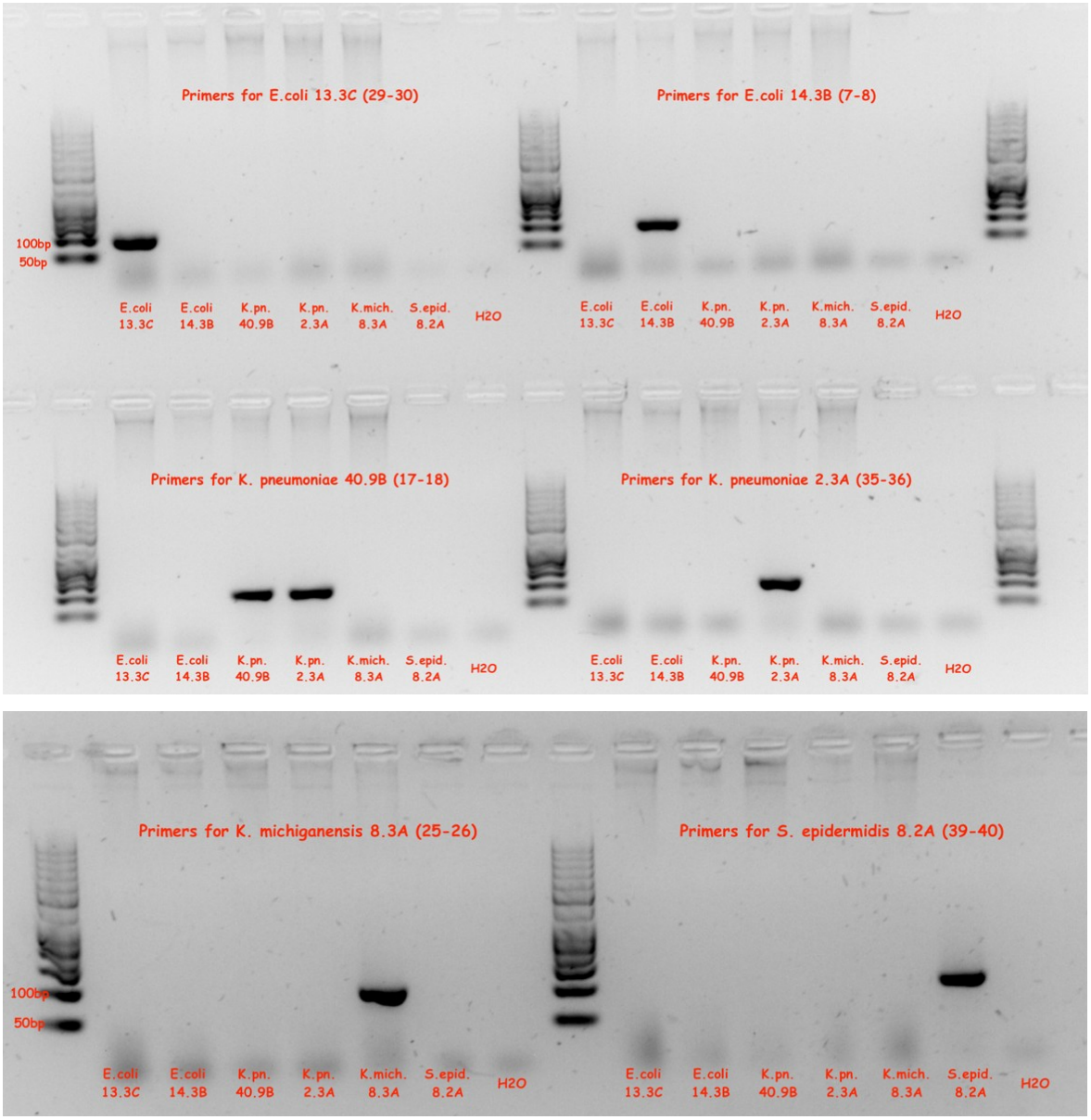

Fig. S1. Conventional PCR analysis for primers specificity testing.

Each primer set was tested against all bacterial strains included in this study. All primer pairs demonstrated strains specificity except for the primer set targeting K. pneumoniae 40.9B, which also amplified K. pneumoniae 2.3A. This was considered acceptable for this study, as co-cultivation experiments involving both K. pneumoniae strains were not performed.

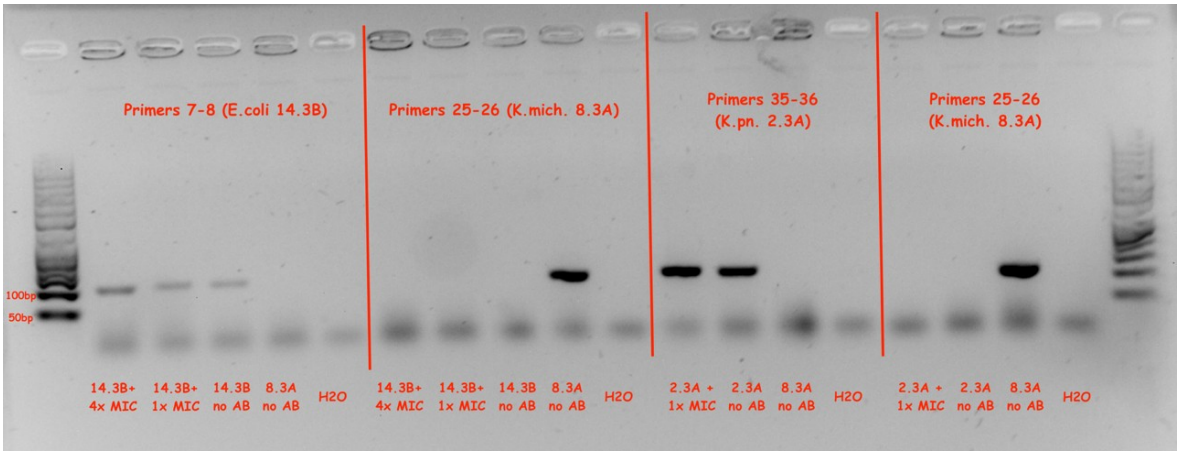

Fig. S2. Conventional PCR for contamination testing in co-cultivation experiment.

In co-cultures of E. coli 14.3B + K. michiganensis 8.3A and K. pneumoniae 2.3A + K. michiganensis 8.3A, unexpected growth of susceptible strains was observed in the presence of piperacillin/tazobactam at MIC concentrations (and additionally at 4x MIC for E. coli 14.3B). Conventional PCR analysis confirmed the absence of contamination by resistant strain (K. michiganensis 8.3A). This may suggest activation of antibiotic-unspecific ARGs expression in tested strains.

Disclaimer

During the writing process of this thesis, I have used OpenAI ChatGPT-5.5 and DeepL Translator on a limited basis to translate and harmonize text passages, and to support for using R Studio in data analysis (e.g., for correcting code). After using AI tools, I have reviewed and edited the content as needed and therefore, I take full responsibility for the final content of this thesis.

References

Abriouel, H., Del Carmen Casado Muñoz, M., Lerma, L., Montoro, B., Bockelmann, W., Pichner, R., Kabisch, J., Cho, G., Franz, C., Gálvez, A., & Benomar, N. (2015). New insights in antibiotic resistance of Lactobacillus species from fermented foods.. *Food research international*. https://doi.org/10.1016/j.foodres.2015.09.016.

Adamowicz, E., Flynn, J., Hunter, R., & Harcombe, W. (2018). Cross-feeding modulates antibiotic tolerance in bacterial communities. *The ISME Journal, 12*, 2723 - 2735. https://doi.org/10.1038/s41396-018-0212-z.

Adams-Chapman, I., Heyne, R., Demauro, S., Duncan, A., Hintz, S., Pappas, A., Vohr, B., McDonald, S., Das, A., Newman, J., & Higgins, R. (2018). Neurodevelopmental Impairment Among Extremely Preterm Infants in the Neonatal Research Network. *Pediatrics, 141*. https://doi.org/10.1542/peds.2017-3091.

Ahmed, A., Grandi, S., Pullenayegum, E., McDonald, S., Beltempo, M., Premji, S., Pole, J., Bacchini, F., Shah, P., & Pechlivanoglou, P. (2024). Short-Term and Long-Term Mortality Risk After Preterm Birth. *JAMA Network Open, 7*. https://doi.org/10.1001/jamanetworkopen.2024.45871.

Alcock *et al*. 2023. CARD 2023: Expanded Curation, Support for Machine Learning, and Resistome Prediction at the Comprehensive Antibiotic Resistance Database. *Nucleic Acids Research*, **51**, D690-D699.

Arboleya, S., Sánchez, B., Milani, C., Duranti, S., Solís, G., Fernández, N., De Los Reyes-Gavilán, C., Ventura, M., Margolles, A., & Gueimonde, M. (2015). Intestinal Microbiota Development in Preterm Neonates and Effect of Perinatal Antibiotics. *The Journal of Pediatrics*. https://doi.org/10.1016/j.jpeds.2014.09.041.

Arboleya, S., Binetti, A., Salazar, N., Fernández, N., Solís, G., Hernández-Barranco, A., Margolles, A., De Los Reyes-Gavilán, C., & Gueimonde, M. (2012). Establishment and

development of intestinal microbiota in preterm neonates.. *FEMS microbiology ecology, 79 3*, 763-72 . https://doi.org/10.1111/j.1574-6941.2011.01261.x.

Arrieta, M., Stiemsma, L., Amenyogbe, N., Brown, E., & Finlay, B. (2014). The Intestinal Microbiome in Early Life: Health and Disease. *Frontiers in Immunology, 5*. https://doi.org/10.3389/fimmu.2014.00427.

Baranowski, J., & Claud, E. (2019). Necrotizing Enterocolitis and the Preterm Infant Microbiome.. *Advances in experimental medicine and biology, 1125*, 25-36 . https://doi.org/10.1007/5584_2018_313.

Beghetti, I., Barone, M., Brigidi, P., Sansavini, A., Corvaglia, L., Aceti, A., & Turroni, S. (2023). Early-life gut microbiota and neurodevelopment in preterm infants: a narrative review. *Frontiers in Nutrition, 10*. https://doi.org/10.3389/fnut.2023.1241303.

Bernier, S., Létoffé, S., Delepierre, M., & Ghigo, J. (2011). Biogenic ammonia modifies antibiotic resistance at a distance in physically separated bacteria. *Molecular Microbiology, 81*. https://doi.org/10.1111/j.1365-2958.2011.07724.x.

Bhattarai, S., Du, M., Zeamer, A., Morzfeld, B., Kellogg, T., Firat, K., Benjamin, A., Bean, J., Zimmerman, M., Mardi, G., Vilbrun, S., Walsh, K., Fitzgerald, D., Glickman, M., & Bucci, V. (2024). Commensal antimicrobial resistance mediates microbiome resilience to antibiotic disruption. *Science Translational Medicine, 16*. https://doi.org/10.1126/scitranslmed.adi9711.

Bixby, M., Daley, E., Collins, L., Salay, J., Bryson, A., & Hirsch, E. (2024). Skipped wells and scientific error during fosfomycin agar dilution and broth microdilution lead to inconsistent minimal inhibitory concentrations and may be cause for reevaluating testing methods for Klebsiella pneumoniae. *Microbiology Spectrum*. https://doi.org/10.1128/spectrum.04205-23.

Bottery, M., Pitchford, J., & Friman, V. (2020). Ecology and evolution of antimicrobial resistance in bacterial communities. *The ISME Journal, 15*, 939 - 948. https://doi.org/10.1038/s41396-020-00832-7.

Butranova, O., Ushkalova, E., Zyryanov, S., & Chenkurov, M. (2023). Developmental Pharmacokinetics of Antibiotics Used in Neonatal ICU: Focus on Preterm Infants. *Biomedicines*. https://doi.org/10.3390/biomedicines11030940.

Campedelli, I., Mathur, H., Salvetti, E., Clarke, S., Rea, M., Torriani, S., Ross, P., Hill, C., & O'Toole, P. (2019). Genus-Wide Assessment of Antibiotic Resistance in Lactobacillus spp.. *Applied and Environmental Microbiology*. https://doi.org/10.1128/AEM.01738-18.

Campos-Madueno, E., Moser, A., Keller, P., Perreten, V., Poirel, L., Nordmann, P., & Endimiani, A. (2023). Evaluation of Phenotypic Tests to Detect Extended-Spectrum β-Lactamase (ESBL)-Producing Klebsiella oxytoca Complex Strains. *Journal of Clinical Microbiology, 61*. https://doi.org/10.1128/jcm.01706-22.

Cao, G., Liu, J., & Liu, M. (2022). Global, Regional, and National Incidence and Mortality of Neonatal Preterm Birth, 1990-2019. *JAMA Pediatrics, 176*, 787 - 796. https://doi.org/10.1001/jamapediatrics.2022.1622.

Chaves, B., Tadi., P., Gentamicin. [Updated 2023 Apr 10]. In: StatPearls [Internet]. Treasure Island (FL): StatPearls Publishing; 2026 Jan-. Available from: https://www.ncbi.nlm.nih.gov/books/NBK557550/

Chen, Y., Brook, T., Soe, C., O'Neill, I., Alcon-Giner, C., Leelastwattanagul, O., Phillips, S., Caim, S., Clarke, P., Hall, L., & Hoyles, L. (2020). Preterm infants harbour diverse Klebsiella populations, including atypical species that encode and produce an array of antimicrobial resistance- and virulence- associated factors. *Microbial Genomics*. https://doi.org/10.1099/mgen.0.000377.

Chong, C., Bloomfield, F., & O'Sullivan, J. (2018). Factors Affecting Gastrointestinal Microbiome Development in Neonates. *Nutrients, 10*. https://doi.org/10.3390/nu10030274.

Daruka, L., Czikkely, M., Szili, P., Farkas, Z., Balogh, D., Grézal, G., Maharramov, E., Vu, T., Sipos, L., Juhász, S., Dunai, A., Daraba, A., Számel, M., Sári, T., Stirling, T., Vásárhelyi, B., Ari, E., Christodoulou, C., Manczinger, M., Enyedi, M., Jaksa, G., Kovács, K., Van

Houte, S., Pursey, E., Pintér, L., Haracska, L., Kintses, B., Papp, B., & Pál, C. (2025). ESKAPE pathogens rapidly develop resistance against antibiotics in development in vitro. *Nature Microbiology*. https://doi.org/10.1038/s41564-024-01891-8.

De Vos, M., Zagórski, M., McNally, A., & Bollenbach, T. (2017). Interaction networks, ecological stability, and collective antibiotic tolerance in polymicrobial infections. *Proceedings of the National Academy of Sciences, 114*, 10666 - 10671. https://doi.org/10.1073/pnas.1713372114.

Dec, M., Urban-Chmiel, R., Stępień-Pyśniak, D., & Wernicki, A. (2017). Assessment of antibiotic susceptibility in Lactobacillus isolates from chickens. *Gut Pathogens*. https://doi.org/10.1186/s13099-017-0203-z.

Denk-Lobnig, M., & Wood, K. (2023). Antibiotic resistance in bacterial communities.. *Current opinion in microbiology*. https://doi.org/10.1016/j.mib.2023.102306.

El-Halfawy, O., & Valvano, M. (2012). Non-genetic mechanisms communicating antibiotic resistance: rethinking strategies for antimicrobial drug design. *Expert Opinion on Drug Discovery, 7*, 923 - 933. https://doi.org/10.1517/17460441.2012.712512.

Estrela, S., & Brown, S. (2018). Community interactions and spatial structure shape selection on antibiotic resistant lineages. *PLoS Computational Biology, 14*. https://doi.org/10.1371/journal.pcbi.1006179.

European Committee on Antimicrobial Susceptibility Testing. MIC distributions and epidemiological cut-off value (ECOFF) setting, EUCAST SOP 10.2, 2021. http://www.eucast.org [online accessed on 24.06.2025]

European Committee on Antimicrobial Susceptibility Testing. Data from the EUCAST MIC distribution website. https://www.eucast.org [online accessed on 24.06.2025]

European Committee on Antimicrobial Susceptibility Testing. Search database. Antimicrobial wild type distributions of microorganisms. https://mic.eucast.org/search/ [online accessed on 24.06.2025]

European Committee on Antimicrobial Susceptibility Testing. Media preparation for EUCAST disk diffusion testing and for determination of MIC values by the broth microdilution method, EUCAST Ver. 7.0, 2022, http://www.eucast.org [online accessed on 24.06.2025]

Feldgarden, M., Brover, V., Gonzalez-Escalona, N., Frye, J. G., Haendiges, J., Haft, D. H., Hoffmann, M., Pettengill, J. B., Prasad, A. B., Tillman, G. E., Tyson, G. H., & Klimke, W. (2021). AMRFinderPlus and the Reference Gene Catalog facilitate examination of the genomic links among antimicrobial resistance, stress response, and virulence. *Scientific reports*, *11*(1), 12728. https://doi.org/10.1038/s41598-021-91456-0

Flannery, D., Edwards, E., Puopolo, K., & Horbar, J. (2021). Early-Onset Sepsis Among Very Preterm Infants. *Pediatrics, 148*. https://doi.org/10.1542/peds.2021-052456.

Gajdács, M., Spengler, G., & Urbán, E. (2017). Identification and Antimicrobial Susceptibility Testing of Anaerobic Bacteria: Rubik's Cube of Clinical Microbiology?. *Antibiotics, 6*. https://doi.org/10.3390/antibiotics6040025.

García-Santamarina, S., Kuhn, M., Devendran, S., Maier, L., Driessen, M., Mateus, A., Mastrorilli, E., Brochado, A., Savitski, M., Patil, K., Zimmermann, M., Bork, P., & Typas, A. (2024). Emergence of community behaviors in the gut microbiota upon drug treatment.. *Cell*. https://doi.org/10.1016/j.cell.2024.08.037.

Gibson, M., Wang, B., Ahmadi, S., Burnham, C., Tarr, P., Warner, B., & Dantas, G. (2016). Developmental dynamics of the preterm infant gut microbiota and antibiotic resistome. *Nature Microbiology, 1*. https://doi.org/10.1038/nmicrobiol.2016.24.

Han, M., Park, K., Jeon, J., Lee, J., Lee, J., Choi, E., & Lee, S. (2020). SHV Hyperproduction as a Mechanism for Piperacillin–Tazobactam Resistance in Extended-Spectrum Cephalosporin-Susceptible Klebsiella pneumoniae. *Microbial Drug Resistance, 26*, 334 - 340. https://doi.org/10.1089/mdr.2019.0079.

Healy, D., Ryan, C., Ross, R., Stanton, C., & Dempsey, E. (2021). Clinical implications of preterm infant gut microbiome development. *Nature Microbiology, 7*, 22 - 33. https://doi.org/10.1038/s41564-021-01025-4.

Kilani, A., Alabi, E., & Adeleke, O. (2024). Coexistence of the blaZ gene and selected virulence determinants in multidrug-resistant Staphylococcus aureus: insights from three Nigerian tertiary hospitals. *BMC Infectious Diseases*. https://doi.org/10.1186/s12879-024-10171-z.

Klare, I., Konstabel, C., Müller-Bertling, S., Reissbrodt, R., Huys, G., Vancanneyt, M., Swings, J., Goossens, H., & Witte, W. (2005). Evaluation of New Broth Media for Microdilution Antibiotic Susceptibility Testing of Lactobacilli, Pediococci, Lactococci, and Bifidobacteria. *Applied and Environmental Microbiology*. https://doi.org/10.1128/AEM.71.12.8982-8986.2005.

Korpela, K., Blakstad, E., Moltu, S., Strømmen, K., Nakstad, B., Rønnestad, A., Brække, K., Iversen, P., Drevon, C., & De Vos, W. (2018). Intestinal microbiota development and gestational age in preterm neonates. *Scientific Reports, 8*. https://doi.org/10.1038/s41598-018-20827-x.

Kovács, R., Erdélyi, L., Fenyvesi, F., Balla, N., Kovács, F., Vámosi, G., Klusóczki, Á., Gyöngyösi, A., Bacskay, I., Vecsernyés, M., & Váradi, J. (2022). Concentration-Dependent Antibacterial Activity of Chitosan on Lactobacillus plantarum. *Pharmaceutics, 15*. https://doi.org/10.3390/pharmaceutics15010018.

Kowalska-Krochmal, B., & Dudek-Wicher, R. (2021). The Minimum Inhibitory Concentration of Antibiotics: Methods, Interpretation, Clinical Relevance. *Pathogens, 10*. https://doi.org/10.3390/pathogens10020165.

Lee, Y. (2017). White Matter Injury of Prematurity: Its Mechanisms and Clinical Features. *Journal of Pathology and Translational Medicine, 51*, 449 - 455. https://doi.org/10.4132/jptm.2017.07.25.

Li, Y., Wu, Y., Li, D., Du, L., Zhao, L., Wang, R., Chen, X., Jia, X., , R., Wang, T., Li, J., Zhang, G., Wang, X., Hu, M., Chen, X., Wang, X., Kang, W., Sun, H., Xu, Y., & Liu, Y.

(2023). Multicenter comparative genomic study of Klebsiella oxytoca complex reveals a highly antibiotic-resistant subspecies of Klebsiellamichiganensis.. *Journal of microbiology, immunology, and infection = Wei mian yu gan ran za zhi*. https://doi.org/10.1016/j.jmii.2023.10.014.

Liu, H., Prentice, E., & Webber, M. (2024). Mechanisms of antimicrobial resistance in biofilms. *npj Antimicrobials and Resistance*. https://doi.org/10.1038/s44259-024-00046-3.

Mitrea, L., Nemeș, S., Szabó, K., Teleky, B., & Vodnar, D. (2022). Guts Imbalance Imbalances the Brain: A Review of Gut Microbiota Association With Neurological and Psychiatric Disorders. *Frontiers in Medicine, 9*. https://doi.org/10.3389/fmed.2022.813204.

Molina-Santiago, C., Daddaoua, A., Fillet, S., Duque, E., & Ramos, J. (2014). Interspecies signalling: Pseudomonas putida efflux pump TtgGHI is activated by indole to increase antibiotic resistance.. *Environmental microbiology, 16 5*, 1267-81 . https://doi.org/10.1111/1462-2920.12368.

Moriel, N., Jones, L., Harpanes, E., Rakow, N., Shmorak, S., Friedman, S., Shlomai, N., & Yassour, M. (2025). Development of the preterm infant gut and gastric residuals microbiome. *Nature Communications, 16*. https://doi.org/10.1038/s41467-025-64819-8.

Morreale, C., Giaroni, C., Baj, A., Folgori, L., Barcellini, L., Dhami, A., Agosti, M., & Bresesti, I. (2023). Effects of Perinatal Antibiotic Exposure and Neonatal Gut Microbiota. *Antibiotics*. https://doi.org/10.3390/antibiotics12020258.

Mulinge, M., Mwanza, S., Kabahweza, H., Wamalwa, D., & Nduati, R. (2023). The impact of neonatal intensive care unit antibiotics on gut bacterial microbiota of preterm infants: a systematic review. *Frontiers in Microbiomes*. https://doi.org/10.3389/frmbi.2023.1180565.

Nøhr-Meldgaard, K., Struve, C., Ingmer, H., Koza, A., Al-Nakeeb, K., & Agersø, Y. (2023). Antimicrobial susceptibility testing and tentative epidemiological cut-off values for Lactobacillaceae family species intended for ingestion. *Frontiers in Antibiotics*. https://doi.org/10.3389/frabi.2023.1162636.

Panwar, R., Sequeira, R., & Clarke, T. (2021). Microbiota-mediated protection against antibiotic-resistant pathogens. *Genes and Immunity, 22*, 255 - 267. https://doi.org/10.1038/s41435-021-00129-5.

Payne, D., Cramp, R., Winstanley, D., & Knowles, D. (1994). Comparative activities of clavulanic acid, sulbactam, and tazobactam against clinically important beta-lactamases. *Antimicrobial Agents and Chemotherapy, 38*, 767 - 772. https://doi.org/10.1128/aac.38.4.767.

Perlin, M., Clark, D., McKenzie, C., Patel, H., Jackson, N., Kormanik, C., Powell, C., Bajorek, A., Myers, D., Dugatkin, L., & Atlas, R. (2009). Protection of Salmonella by ampicillin-resistant Escherichia coli in the presence of otherwise lethal drug concentrations. *Proceedings of the Royal Society B: Biological Sciences, 276*, 3759 - 3768. https://doi.org/10.1098/rspb.2009.0997.

Pineda, L., & Watt, K. (2015). New antibiotic dosing in infants.. *Clinics in perinatology*. https://doi.org/10.1016/j.clp.2014.10.009.

Quan, P., Sauzade, M., & Brouzes, E. (2018). dPCR: A Technology Review. *Sensors (Basel, Switzerland), 18*. https://doi.org/10.3390/s18041271.

Ramasethu, J. (2017). Prevention and treatment of neonatal nosocomial infections. *Maternal Health, Neonatology and Perinatology, 3*. https://doi.org/10.1186/s40748-017-0043-3.

Rao, C., Coyte, K., Bainter, W., Geha, R., Martin, C., & Rakoff-Nahoum, S. (2021). Multi-kingdom ecological drivers of microbiota assembly in preterm infants. *Nature, 591*, 633 - 638. https://doi.org/10.1038/s41586-021-03241-8.

Rocha, G., Nogueira, J., Santos, M., Boaventura, J., Soares, R., De Simoni Gouveia, J., Da Costa, M., & Gouveia, G. (2022). Impact of polymorphisms in blaZ, blaR1 and blaI genes and their relationship with β-lactam resistance in S. aureus strains isolated from bovine mastitis.. *Microbial pathogenesis*, 105453 . https://doi.org/10.1016/j.micpath.2022.105453.

Ruelens, P., De Ridder, E., De Visser, A., & Wortel, M. (2025). Density-dependent feedback limits the spread of beta-lactamase mutants: experimental observations and population dynamic model. *mBio*. https://doi.org/10.1128/mbio.01500-25.

Samarra, A., Renwick, S., Arzamasov, A., Rodionov, D., Spann, K., Cabrera-Rubio, R., Acuna-Gonzalez, A., Martínez-Costa, C., Hall, L., Segata, N., Osterman, A., Bode, L., & Collado, M. (2025). Human milk oligosaccharide metabolism and antibiotic resistance in early gut colonizers: insights from bifidobacteria and lactobacilli in the maternal-infant microbiome. *Gut Microbes*. https://doi.org/10.1080/19490976.2025.2501192.

Samarra, A., Alcañiz, A., Martínez-Costa, C., Marina, A., Comas, I., Segata, N., Quijada, N., & Collado, M. (2025). Breastfeeding and early Bifidobacterium-driven microbial colonization shape the infant gut resistome. *Nature Communications*. https://doi.org/10.1038/s41467-025-61154-w.

Sanidad, K., & Zeng, M. (2020). Neonatal gut microbiome and immunity.. *Current opinion in microbiology, 56*, 30-37 . https://doi.org/10.1016/j.mib.2020.05.011.

Saturio, S., Nogacka, A., Alvarado-Jasso, G., Salazar, N., De Los Reyes-Gavilán, C., Gueimonde, M., & Arboleya, S. (2021). Role of Bifidobacteria on Infant Health. Microorganisms, 9. https://doi.org/10.3390/microorganisms9122415.

Schwendener, S., & Perreten, V. (2022). The bla and mec families of β-lactam resistance genes in the genera Macrococcus, Mammaliicoccus and Staphylococcus: an in-depth analysis with emphasis on Macrococcus.. *The Journal of antimicrobial chemotherapy*. https://doi.org/10.1093/jac/dkac107.

Seemann, T., Abricate, Github https://github.com/tseemann/abricate

Seki, D., Mayer, M., Hausmann, B., Pjevac, P., Giordano, V., Goeral, K., Unterasinger, L., Klebermass-Schrehof, K., De Paepe, K., Van De Wiele, T., Spittler, A., Kasprian, G., Warth, B., Berger, A., Berry, D., & Wisgrill, L. (2021). Aberrant gut-microbiota-

immune-brain axis development in premature neonates with brain damage. *Cell Host & Microbe, 29*, 1558 - 1572.e6. https://doi.org/10.1016/j.chom.2021.08.004.

Seki, D., Kirkegaard, R., Osvatic, J., Hausmann, B., Séneca, J., Pjevac, P., Berger, A., Hall, L., Wisgrill, L., & Berry, D. (2024). Gut microbiota genome features associated with brain injury in extremely premature infants. *Gut Microbes, 16*. https://doi.org/10.1080/19490976.2024.2410479.

Semenec, L., Cain, A., Dawson, C., Liu, Q., Dinh, H., Lott, H., Penesyan, A., Maharjan, R., Short, F., Hassan, K., & Paulsen, I. (2022). Cross-protection and cross-feeding between Klebsiella pneumoniae and Acinetobacter baumannii promotes their co-existence. *Nature Communications, 14*. https://doi.org/10.1038/s41467-023-36252-2.

Simeoli, R., Cairoli, S., Decembrino, N., Campi, F., Vici, D., Corona, A., & Goffredo, B. (2022). Use of Antibiotics in Preterm Newborns. *Antibiotics, 11*. https://doi.org/10.3390/antibiotics11091142.

Sorg, R., Lin, L., Doorn, G., Sorg, M., Olson, J., Nizet, V., & Veening, J. (2016). Collective Resistance in Microbial Communities by Intracellular Antibiotic Deactivation. *PLoS Biology, 14*. https://doi.org/10.1371/journal.pbio.2000631.

Sparo, M., Urbizu, L., Solana, M., Pourcel, G., Delpech, G., Confalonieri, A., Ceci, M., & Bruni, S. (2011). High-level resistance to gentamicin: genetic transfer between Enterococcus faecalis isolated from food of animal origin and human microbiota. *Letters in Applied Microbiology*. https://doi.org/10.1111/j.1472-765X.2011.03182.x.

Stentz, R., Horn, N., Cross, K., Salt, L., Brearley, C., Livermore, D., & Carding, S. (2014). Cephalosporinases associated with outer membrane vesicles released by Bacteroides spp. protect gut pathogens and commensals against β-lactam antibiotics. *Journal of Antimicrobial Chemotherapy, 70*, 701 - 709. https://doi.org/10.1093/jac/dku466.

Stiefel, U., Tima, M., & Nerandzic, M. (2015). Metallo-β-Lactamase-Producing Bacteroides Species Can Shield Other Members of the Gut Microbiota from Antibiotics. *Antimicrobial Agents and Chemotherapy*. https://doi.org/10.1128/AAC.03719-14.

Thänert, R., Schwartz, D., Keen, E., Hall-Moore, C., Wang, B., Shaikh, N., Ning, J., Rouggly-Nickless, L., Thänert, A., Ferreiro, A., Fishbein, S., Sullivan, J., Radmacher, P., Escobedo, M., Warner, B., Tarr, P., & Dantas, G. (2024). Clinical sequelae of gut microbiome development and disruption in hospitalized preterm infants.. *Cell host & microbe*. https://doi.org/10.1016/j.chom.2024.07.027.

Türkyılmaz, O., & Darcan, C. (2026). Molecular basis of ampicillin resistance: combinatorial mechanisms and future strategies. *World Journal of Microbiology & Biotechnology, 42*. https://doi.org/10.1007/s11274-026-04826-z.

Wang, Y., Zhu, J., Zou, N., Zhang, L., Wang, Y., Zhang, M., Wang, C., & Yang, L. (2023). Pathogenesis from the microbial-gut-brain axis in white matter injury in preterm infants: A review. *Frontiers in Integrative Neuroscience, 17*. https://doi.org/10.3389/fnint.2023.1051689.

Wang, Y., Florez, I., Morgan, R., Foroutan, F., Chang, Y., Crandon, H., Zeraatkar, D., Bała, M., Mao, R., Tao, B., Shahid, S., Wang, X., Beyene, J., Offringa, M., Sherman, P., Gouhary, E., Guyatt, G., & Sadeghirad, B. (2023). Probiotics, Prebiotics, Lactoferrin, and Combination Products for Prevention of Mortality and Morbidity in Preterm Infants: A Systematic Review and Network Meta-Analysis.. *JAMA pediatrics*. https://doi.org/10.1001/jamapediatrics.2023.3849.

Weiss, G., & Hennet, T. (2017). Mechanisms and consequences of intestinal dysbiosis. *Cellular and Molecular Life Sciences, 74*, 2959-2977. https://doi.org/10.1007/s00018-017-2509-x.

Xu, F., Jiang, M., Li, D., Yu, P., , H., & Lu, H. (2024). Protective effects of antibiotic resistant bacteria on susceptibles in biofilm: Influential factors, mechanism, and modeling.. *The Science of the total environment*, 172668 . https://doi.org/10.1016/j.scitotenv.2024.172668.

Yang, F., Zhao, Q., Wang, L., Wu, J., Jiang, L., Sheng, L., Zhang, L., Xue, Z., & Yi, M. (2022). Diminished Susceptibility to Cefoperazone/Sulbactam and Piperacillin/Tazobactam in Enterobacteriaceae Due to Narrow-Spectrum β-Lactamases as Well as Omp Mutation. *Polish Journal of Microbiology*. https://doi.org/10.33073/pjm-2022-023.

Yassara, S., Zeouk, I., Jaouhar, S., Sbiti, M., & Bekhti, K. (2025). Extended-spectrum beta-lactamases: definition, history, an update on their genetic environment and detection methods. *Journal of Medical Microbiology*. https://doi.org/10.1099/jmm.0.002033.

Zárate, S., Claure, M., Benito-Arenas, R., Revuelta, J., Santana, A., & Bastida, Á. (2018). Overcoming Aminoglycoside Enzymatic Resistance: Design of Novel Antibiotics and Inhibitors. *Molecules : A Journal of Synthetic Chemistry and Natural Product Chemistry, 23*. https://doi.org/10.3390/molecules23020284.

Zhao, X., Ruelens, P., Farr, A., De Visser, J., & Baraban, L. (2023). Population dynamics of cross-protection against β-lactam antibiotics in droplet microreactors. *Frontiers in Microbiology, 14*. https://doi.org/10.3389/fmicb.2023.1294790.